LIPOTOXIC ENDOPLASMIC RETICULUM STRESS-ASSOCIATED INFLAMMATION: MOLECULAR MECHANISMS AND MODIFICATION BY A BIOACTIVE LIPOKINE

A THESIS
SUBMITTED TO THE DEPARTMENT OF MOLECULAR BIOLOGY AND GENETICS AND THE GRADUATE SCHOOL OF ENGINEERING AND SCIENCE OF BILKENT UNIVERSITY IN PARTIAL FULFILLMENT OF THE REQUIREMENTS FOR THE DEGREE OF MASTER OF SCIENCE

BY

ŞEYMA DEMIRSOY

SEPTEMBER 2012

I certify that I have read this thesis and that in my opinion it is fully adequate,

in scope and in quality, as a thesis for the degree of Master of Science.

_____

Assist.Prof.Dr. Ebru ERBAY

I certify that I have read this thesis and that in my opinion it is fully adequate,

in scope and in quality, as a thesis for the degree of Master of Science.

_____

Assist. Prof. Dr. Uygar TAZEBAY

I certify that I have read this thesis and that in my opinion it is fully adequate,

in scope and in quality, as a thesis for the degree of Master of Science.

_____

Assist. Prof. Dr. Çağdaş D. SON

Approved for the Graduate School of Engineering and Science

_____

Prof. Dr. Levent Onural

Director of the Graduate School

ABSTRACT

Lipotoxic endoplasmic reticulum stress-associated inflammation: molecular mechanisms and modification by a bioactive lipokine

Şeyma Demirsoy

M.Sc.in Molecular Biology and Genetics

Supervisor Assist. Prof. Dr. Ebru Erbay

September 2012, 127 Pages

Physiologic or pathologic processes that disturb protein folding in the endoplasmic reticulum (ER) activate a signaling pathway named the unfolded protein response (UPR). UPR promotes cell survival by reducing misfolded protein levels. The three proximal stress sensors of the UPR are known as PKR-resemble like ER kinase (PERK), inositol-requiring enzyme-1 (IRE1) and activating transcription factor 6 (ATF6), which monitor the quality of protein folding in the ER membrane and relay that information to the rest of the cell. If ER homeostasis can not be restored, prolonged UPR signaling can lead to cell death.

Recent studies have shown metabolic overload, particularly high levels of fatty acids and cholesterol can induce ER stress and activate UPR signaling. These studies also demonstrated ER stress is a central mechanism that underlies the pathogenesis of metabolic diseases including obesity, type 2 diabetes, insulin resistance, atherosclerosis and hepatosteatosis. Understanding how nutrient excess activates the UPR and its novel molecular mechanisms of operation during metabolic stress could facilitate the development of novel and effective future therapeutics aiming to restore ER homeostasis.

The molecular mechanisms of lipid induced activation of UPR and how the three proximal UPR stress sensors are linked to lipid metabolism and inflammation is not well understood. One of the UPR stress sensors, PERK, is a trans-membrane serine/threonine kinase with only two known downstream substrates, the eukaryotic translation initiation factor (eIF2α) that controls translation initiation, and an anti-oxidant transcription factor, Nuclear factor eryhthroid-2-related factor-2 (Nrf2), that keeps redox homeostasis. One of the existing road blocks in studying PERK signaling has been the lack of molecular or chemical tools to regulate its activity. For my thesis studies, I developed a chemical-genetic approach to specifically modify PERK's kinase activity. In this approach, the ATP binding pocket of a particular kinase is altered via site-directed mutagenesis in order to accommodate a bulky ATP analog that is not an effective substrate for the wild type kinase. Thus, only the mutated kinase can be targeted by the activatory or inhibitory bulky ATP analogs and this form of the kinase is referred to as ATP analog sensitive kinase (ASKA). Furthermore, I identified specific siRNA sequences that can be efficiently delivered to mouse macrophages and significantly reduce PERK expression. Both of these methods can be applied to study the direct impact of PERK activity on lipotoxic ER stress- associated inflammation. The results of the siRNA mediated PERK expression silencing experiments showed that PERK has a direct contribution to lipid-induced pro-inflammatory response in macrophages.

Finally, I examined whether palmitoleate, a bioactive monounsaturated fatty acid previously shown to reduce lipid-induced ER stress and death, could also modify lipotoxic ER stress-associated inflammation. Based on the results from my experiments,

palmitoleate is highly effective in preventing lipid induce inflammation. Unexpectedly, I also observed that palmitoleate could significantly block LPS-induced inflammation, too.

In summary, during my thesis study I generated several useful tools including siRNA mediated knock-down of PERK and a novel chemical-genetic tool to directly and specifically modify PERK kinase activity. The findings from my studies demonstrate that PERK plays a significant role in lipid-induced inflammation, suggesting modification of PERK activity or its direct pro-inflammatory substrates could become desirable approaches to inhibit obesity-induced inflammation that contributes to the pathogenesis of diabetes and atherosclerosis. The outcome of my studies also showed that palmitoleate can significantly reduce lipotoxic-ER stress associated inflammation, which may explain its beneficial impact on both insulin resistance and atherosclerosis. Furthermore, the ATP-analog sensitive PERK mutant developed in my thesis can be coupled with proteomics to identify the full repertoire of PERK substrates during metabolic stress. In conclusion, the findings and tools developed in my thesis studies can form the basis of future studies to identify the molecular details of PERK's involvement in lipid induced inflammation, the identification of novel PERK substrates during metabolic stress and the development of new therapeutic strategies against metabolically induced inflammation in obesity, diabetes and atherosclerosis.

Key words: UPR, ER stress, PERK, Palmitate, Palmitoleate

ÖZET

Lipotoksik endoplazmik retikulum stresine bağlı inflamasyon: Bir biyoaktif lipokine tarafından gerçekleştirilen moleküler mekanizmalar ve modifikasyonlar

Şeyma Demirsoy
Moleküler Biyoloji ve Genetik Yüksek Lisansı
Tez Yöneticisi: Yrd.Doç. Dr. Ebru Erbay
Eylül 2012, 127 Sayfa

Endoplazmik retikulumdaki (ER) protein katlanmasını bozan fizyolojik ya da patolojik süreçler katlanmamış protein yanıtı (KPY) adı verilen bir sinyal yolağını aktifleştirir. KPY yanlış katlanmış protein seviyelerini düşürerek hücre kurtuluşunu sağlar. KPY'nin 3 yakınsal sensörü PKR'yi anımsatan ER kinazı (PERK), inositol-gerektiren enzim-1 (IRE1) ve aktifleştiren transkripsiyon faktör 6'dır. Bunlar ER zarındaki protein katlanmasının kalitesini gözlemler ve bu bilgiyi hücrenin geri kalanına yayar. Eğer ER dengesi yeniden sağlanamazsa, uzun süre devam eden KPY hücre ölümüne neden olabilir.

Son zamanlarda yapılan çalışmalar göstermiştir ki metabolik aşırı yüklenme, özellikle yüksek seviyede bulunan yağ asitleri ve kolesterol, ER stresi tetikleyebilir ve KPY sinyal yolağını aktifleştirebilir. Bu çalışmalar aynı zamanda ER stresinin obezite, tip 2 diyabet, insülin direnci, aterozkleroz ve karaciğer yağlanması da dâhil olmak üzere metabolik hastalıkların patolojilerinin temelinde yatan merkezi bir mekanizma olduğunu da göstermiştir. Besin maddelerinin fazlasının KPY'yi nasıl aktifleştirdiğini ve buna

bağlı özgün stres mekanizmalarının metabolik stres sürecinde nasıl çalıştığını anlamak, gelecekte ER dengesini yeniden sağlamaya yönelik özgün ve etkili tedavi yöntemlerinin gelişimini kolaylaştıracaktır. Yağ fazlasının, bu stres sensörlerini nasıl aktive ettiği ve özellikle de yağ metabolizması ve inflamasyon olmak üzere değişmiş hücresel yanıtlarla nasıl ilişkilendirileceği konusu halen araştırılmayı gerektirmektedir.

KPY'nin yağlarla aktifleştirilen moleküler mekanizması, ve KPY'nin üç yakınsal sensörünün yağ metabolizması ve inflamasyonla olan bağlantısı henüz anlaşılamamıştır. KPY'nin sensörlerinden biri olan PERK, translasyon mekanizmasının başlayışını kontrol eden ökaryotik translasyon başlatan faktör α (eIF2α) ve redoks dengesini sağlayan bir antioksidan transkripsiyon faktörü olan çekirdeksel faktör eritroid-2-ilgili faktör-2 (Nrf2) olmak üzere yalnızca iki bilinen substrata sahip hücre zarına gömülü serine/threonin kinazdır. PERK'den kaynaklanan sinyal yolağını çalışmadaki var olan en büyük engellerden biri onun aktivitesini düzenleyen kimyasal ve moleküler bir tekniğin eksikliği olmuştur. Bu çalışmada PERK'ün özellikle kinaz aktivitesini modifiye eden kimyasal-genetik bir yaklaşım geliştirdim. Bu yaklaşıma göre belirli bir kinazın ATP bağlayan paketi, mutasyona uğratılmamış doğal kinaz için etkin bir substrat olmayan iri hacimli ATP analoğuna uyum sağlayabilmesi için mutasyona uğratılır. Böylece sadece mutasyona uğramış kinaz, aktive edici veya engelleyici özelliğe sahip iri hacimli ATP analogları tarafından hedeflenebilir ve buna da ATP analoğuna duyarlı kinaz (AZKA) denilmektedir. Bunun dışında fare makrofajlarına etkili bir şekilde ulaştırılabilecek ve PERK ifadesini önemli ölçüde azaltabilecek özel siRNA dizileri tespit ettim. Bu iki metot da PERK aktivitesinin, lipotoksik ER stresine-bağlı inflamasyon üzerindeki doğrudan etkisinin araştırılması için kullanılabilir. PERK

ifadesini azaltmaya yönelik siRNA deney sonuçları, makrofajlarda palmitat uyarısına bağlı pro-inflamatuvar yanıta PERK'ün doğrudan bir katkısının olduğunu göstermiştir.

Son olarak yağlara bağlı ER stresi ve ölümünü azaltmak için daha önceden de gösterilen bir biyoaktif tekli doymamış yağ asidi olan palmitoleatın, lipotoksik ER stresine-bağlı inflamasyonu modifiye edip edemeyeceğini de inceledim. Yapmış olduğum deneylerin sonuçlarına göre palmitoleat, yağa bağlı inflamasyonun engellenmesinde oldukça etkilidir. Beklenmeyen bir şekilde palmitoleatın LPS'e bağlı inflamasyonu da önemli ölçüde engellediği gözlemlenmiştir.

Özet olarak tez çalışmam boyunca PERK kinaz aktivitesini doğrudan ve özel olarak modifiye etmek için etkin bir kimyasal-genetik mekanizması ve PERK ifadesini azaltabilen siRNA dizileri gibi yararlı araçlar geliştirdim. Yapmış olduğum çalışmanın sonuçları PERK'ün yağa bağlı inflamasyonda önemli bir rol oynadığını göstermiştir. Bu da PERK aktivitesinde veya PERK'ün doğrudan pro-inflamatuvar hedeflerinde yapılacak modifikasyonun, diyabet ve aterozkleroz patogenezine katkıda bulunan obeziteye bağlı inflamasyonun engellenmesinde arzu edilen yaklaşımlardan biri olabileceği anlamına gelmektedir. Bu sonuçlar aynı zamanda palmitoleatın lipotoksik ER stresine bağlı inflamasyonu azaltabileceğini göstermiştir ve bu da hem insülin direncini hem de aterozkleroz üzerinde yarattığı yararlı etkiyi açıklayabilir. Ayrıca, geliştirmiş olduğum bu ATP-analoglarına duyarlı PERK mutantı, metabolik stres sırasında PERK'ün hedeflerinin tümünü tespit etmek için proteomik çalışmaları ile birleştirilebilir. Sonuç olarak, tez çalışmamda geliştirdiğim bulgular ve araçlar, yağa bağlı inflamasyonda PERK'ün rolünün moleküler mekanizmasının tanımlanması, metabolik stress sırasında PERK'e özgün hedeflerinin tespiti ve obezite, diyabet ve

aterozkleroz hastalıklarında metabolik inflamasyona karşı yeni tedavi yöntemlerinin geliştirilmesi yönünde yapılacak olan çalışmalara temel oluşturabilir.

Anahtar sözcükler: KPY, ER stresi, PERK, Palmitat, Palmitoleat

ACKNOWLEDGEMENT

I am deeply indebted to my supervisor Assit.Prof.Dr.Ebru Erbay whose help, stimulating suggestions and encouragement helped me during my research and writing of this thesis. I learned a lot from her and it felt proud for working with her.

I want to thank Assist.Prof.Dr.Uygar Tazebay and Assist.Prof.Dr.Çağdaş D.Son for being members of my thesis committee and helpful suggestions.

I would like to give my special thanks to the former members of our group, Aylin Göke, Gülhan Saraçaydın and Arda Mızrak for helping the first step of this master thesis. Additionally, I can not find words to express my gratitude to the current members of our group, Özlem Tufanlı and Büşra Yağabasan and our new member and a former senior student, İnci Şimşek for their friendships, patience and support during my studies. I have furthermore to thank to Elif Senem Kayalı and Hakan Köksal for assisting me during my experiments.

I would like to express my deepest appreciation to Bilkent MBG doctoral program student, Verda Bitirim who was always willing to help me as a valuable friend during my experiments and writing of thesis. Many thanks to Defne Bayık, Gözde Güçlüer, Aysegül Örs and Gülesin Eren for their friendships and moral support. It would be a lonely lab without them.

This thesis would not have been possible without Assoc.Prof. İhsan Gürsel, Assist.Prof.Uygar Tazebay and Prof.Dr.Mehmet Öztürk and their groups allowing me to

use their instruments and materials. I would like to express my gratitude to all those who gave me the possibility to complete this thesis.

I would like to thank all past and present MBG family for providing me an enjoyable work place. Without them the journey in my study would be challenge to me.

I want to give my special thanks to TUBITAK for supporting me with a scholarship during my thesis study.

I wish to thank my very close friends Esra Yalçın, Reyhan Mutlu, İlke Ilgaz, Tuğçe Başer, Özge Kalman and Nihan Dilşat Dağtaş for their friendships and moral support. Furthermore, I would like to thank to my very close friend Emrah Ataş for friendship as well as helping me with grammar corrections for my thesis. All helped me to be who I am.

I would like to express my special thanks to Seda Yağabasan and Mehmet Yağabasan for cheering me up and standing by me through the good times and bad during my thesis study.

Last but not the least, many thanks and gratitude to my family for giving me the strength to plod on despite my constitution wanting to give up and throw in the towel.

TABLE OF CONTENTS

LIST OF FIGURES

LIST OF TABLES

1. Introduction

1.1 Endoplasmic Reticulum Function and Biogenesis

The endoplasmic reticulum (ER), an extended membrane network, is the main organelle for protein folding and secretion, lipid synthesis and lipid droplet formation and a major store for calcium (Ca^{++}). The ER controls a wide range of cellular process such as organogenesis, transcriptional activity, stress responses and apoptosis due to its many homeostatic functions[9].

Secreted and transmembranes proteins are folded and reach maturation in the ER, which is the major gateway for the secretory pathway. The translation of proteins occurs in the ribosomes located on the cytosolic surface of the rough ER[1]. The proteins in the ER lumen or the newly synthesized, unfolded proteins being translocated into ER by Sec61 complex[118] are covered with chaperones and associate with folding enzymes in the oxidizing and Ca^{++} rich environment of the ER. These nascent chains become N-glycosylated and assume their secondary and tertiary structures with the assistance of stabilizing protein disulfide isomerase (PDI). Endoplasmic reticulum oxidoreductin 1α and β (Ero1α and Ero1β) are responsible for the oxidation of PDI[19, 113]. In the first step, a disulfide is introduced into the substrate protein with the concomitant reduction of a disulfide within the active site in PDI[79]. Then Ero1α or Ero1β catalyzes the reoxidation of the PDI active site in a reaction involving the reduction of oxygen to liberate hydrogen peroxide[132, 43]. In addition to these, the amino acid cis-trans isomerases, the chaperones such as the glucose regulated protein (GRP) 94 and immunoglobulin (Ig) heavy chain binding protein (BiP), N-glycosylation enzymes and the lectins, calnexin

and calreticulin; all reside in the ER and function in protein maturation. Mature proteins that pass quality control are transferred to Golgi, while the unqualified proteins become targets ER-associated degradation (ERAD). ER-associated degradation (ERAD) includes a translocation into cytosol by a translocon channel for proteosomal degradation. Recent studies show that the mammalian translocon associated proteins, with the help of Sec 61, can bind to improperly folded proteins and accelerate their degradation[103]. The other proteins as a translocon channel are derlins [86, 87, 168, and 155]. Taken together, ER is an important organelle for cell homeostasis and protein metabolism.

ER is also a major store for Ca^{++}; the concentration of Ca^{++} in rested ER can reach to three to four times higher than that in the cytosol. This difference is generated by the sarco (endo) plasmic reticulum Ca^{++} ATPase (SERCA) proteins that pump the Ca^{++} into ER lumen. The latter release of Ca^{++} is controlled by the signaling molecule, Ins (1, 4, 5) $P_{3,}$ and the ryanodine receptors[9].

Furthermore, it was recently suggested that lipid droplet formation from ER membrane is mediated by ER resident proteins such as calnexin and the immunoglobulin heavy chain binding protein BiP[117]. Lipid droplets are the main intracellular storage sites for esterified fatty acids and neutral lipids such as triglycerides (TG) and cholesterol esters (CE). While the outer layer involves amphipathic lipids such as phospholipids (PL) and cholesterol (CL), the core is made of only neutral lipids[93]. The lipid droplets provide building blocks for biological membranes through hormone-dependent and independent-pathways[33]. The biogenesis mechanism of lipid droplets is not clear, but data shows it is mainly derived from the ER. The ER may assume a central role in lipid

droplet biogenesis through its enzymes like the diacylglycerol acyltransferase 1(DGAT) or 1-acylglycerol-3-phosphate acyltransferase (AGAT), which synthesize neutral lipids residing on the ER membrane. Additionally, Robenek and colleagues observed that a large portion of lipid droplets are covered by ER membranes [127]. When fatty acids accumulate in the cell, TG is formed as a form of storing these fatty acids for future energy and neutralization. For this purpose, three fatty acids and one glycerol molecule are joined by enzymes resident in the ER membrane such as acyltransferases. The newly formed TG molecules are stored in lipid droplets that are surrounded by a single PL membrane layer and associated proteins. One hypothesis is that the lipid droplet originates from between two membranes of the ER and moves toward the outer cytoplasmic layer of the ER membrane via bud formation. This hypothesis could explain why the lipid droplet is surrounded by a PL monolayer [15]. A contrasting second theory explains that the lipid droplet occurs outside of the ER but with the ER facilitating synthesis of the surrounding PL monolayer[127]. Regardless of the model, ER membranes and associated proteins are found to be integral components of lipid droplets.

Another crucial function of the ER is in lipid biosynthesis; ER is a major site for the production of phospholipids, cholesterol and ceramides[96]. For example, low intracellular cholesterol levels activate the ER resident sterol regulatory element-binding protein (SREBP 1 and 2), a transcriptional regulator of the fatty acid and cholesterol synthesis pathway, respectively, which works to upregulate the expression of enzymes responsible for cholesterol synthesis. Stearoyl coenzyme A (CoA) desaturase (SCD), which catalyzes the delta-9 desaturation of saturated free fatty acids (FFAs) is another enzyme located on the ER membranes. Furthermore, serine

palmitoyltransferase, which is rate –limiting enzyme of de novo ceramide production, is found on the ER membrane. Fatty acid elongation beyond the 16-Carbons (length of the palmitate) produced by the cytoplasmic Fatty acid synthase (FAS) is mainly catalyzed by enzymes such as DGATs [DAG (diacylglycerol) acyltransferases] for triacyl-glycerols) and/or ASATs (acyl-CoA: sterol acyltransferases) for SEs (steryl esters) associated with the ER[48]. These ER enzymes lengthen not only fatty acids produced by FAS but also the dietary polyunsaturated fatty acids. Formation of a double bond in a fatty acid involves the following endoplasmic reticulum membrane proteins such as desaturases, NADH-cyt b5 Reductase and Cytochrome b_5.

The expansion of ER based on the increased demands on the exocytic pathway was documented in some specialized cells including the β cells of the pancreas and antibody-secreting plasma cells. However, the molecular mechanisms coordinating the protein and lipid components of the ER during this process remain unclear[48]. A study conducted by Sriburi and colleagues showed that spliced XBP-1 (X box binding protein-1) activated by UPR was enough to stimulate synthesis of phosphatidylcholine, the primary PL of the ER membrane[138]. Overexpression of the spliced XBP-1 in cells resulted in increased membrane PLs, surface area and volume of the rough ER, and enhanced activity of the cytidine diphosphocholine pathway of phosphatidylcholine biosynthesis[138]. This data showed that coordinating induction of phospholipid biosynthesis with up-regulated expression of ER resident proteins allows the mammalian UPR to both build and equip the ER, at least via XBP-1 activity. These findings demonstrate ER plays an important role in the maintenance of its own biogenesis.

The ER plays a role on insulin biosynthesis from pre-pro-insulin to pro-insulin[90]. The newly synthesized and signal tagged pre-pro-insulin in the cytoplasm is translocated into the lumen of the ER[124, 125]. After the signal peptide is cleaved in the ER by the endopeptidase called proprotein convertase 1, pro-insulin undergoes folding process in the ER lumen and the newly formed disulfide bonds lead to its stabilization and bioactivity[124, 125]. Then, this processed pro-insulin passes into secretory granules through Golgi apparatus. In final step, it gets native structure and then is secreted.

1.2 Endoplasmic Reticulum Stress

1.2.1 Endoplasmic Reticulum Stress : The Causes and Consequences

The ER participates in wide range of cellular activity from protein folding, lipid synthesis, calcium homeostasis to its own biogenesis. That's why many factors that negatively impact cellular homeostasis leads to ER dysfunction and stress. Protein overload, accumulation of unfolded proteins, protein trafficking defects, chaperones deficiency, environmental toxins, viral infections, aging and chemicals such as tunicamycin, thapsigargin, and DTT destroy the balanced environment of the ER leading to a unique signaling cascade emanating from the ER and known as the accumulation of unfolded protein response (UPR) [30, 35]. Physiological and pathological processes including aging[105], glucose deprivation, aberrant calcium regulation, viral infection and hypoxia may alter the protein folding and cause ER stress[70, 128]. In the stressed ER, the misfolded or unfolded proteins are targeted for destruction through the ER-associated degradation (ERAD) pathway, which leads to their translocation to the cytosol for proteasomal degradation where they are degraded by ubiquitin-proteasome machinery[70]. Such proteins become subject to the ER quality system (ERQC), in which molecular chaperones are the main players aiding in proper folding and evaluation of

protein damage[30]. If the screened substrates fail to pass this quality test, they are marked as substrates for ERAD with the help of 76 amino acid peptide- specific E3 ubiquitin near or in ER membrane and then targeted to the proteasome, which is a multi-catalytic protease that resides in cytoplasm. If the ER stress can not be relieved, a specific stress response pathway, the UPR, is activated. A major function of the UPR is to combat with the accumulation of unfolded proteins through three complementary signaling pathways activated depending on the duration and the degree of the cellular insult. These functions of the UPR include reducing the protein load, increasing the capacity of the ER to handle the unfolded proteins and the decision to commit the cell to apoptotic death. This response is made of three signaling arms each governed by a proximal stress sensor: Inositol requiring enzyme 1 (IRE1), PKR resemble ER kinase (PERK) and activating transcription factor 6 (ATF6).

Recent studies showed that metabolic stress during obesity leads to ER stress and activation of the UPR especially in metabolically active sites such as liver, adipose tissues and pancreatic cells[57]. Nutrient or energy deprivation, in addition to its excess in obesity, can lead to ER stress. How obesity leads to ER stress remains a question of great interest. The maintenance of ER membrane function is supported by lipid metabolism, so one possibility is that obesity-driven perturbations in lipid metabolism can cause stress in the ER and lead to its metabolic dysfunction[37]. ER stress is a marker of early consequences of nutrient excess and a causally linked to the development of inflammation and insulin resistance in metabolic tissues including hepatocytes, cardiomyoblasts, pancreatic β cells and macrophages[17, 18, 75, 158]. Based on its duration, ER stress can be categorized as acute, periodic and chronic. The acute form of ER stress can be induced experimentally through treatments of chemicals such as tunicamycin,

DTT, calcium ionophores, thapsigargin and high levels of lipids such as saturated fatty acids or free cholesterol. An example of periodic ER stress is related to the rhythmic and transient physiological changes that occur during feeding and fasting cycles[17, 116]. After each cycle, the activation of the UPR is completely restored back to the basal levels. On the other hand, chronic ER stress indicates that the stress cannot be resolved and is continuous due to the presence of an ER stress inducer or as part of a vicious cycle, such as that created during obesity[38].

1.2.2 **The Unfolded Protein Response**

Kozutsumi and colleagues suggested for the first time that unfolded proteins can activate a signal transduction pathway emanating from the ER[78]. This study observed that the expression of mutant influenza hemagglutinin lead to the induction of both unfolded proteins and the expression of ER resident proteins[78]. The delineation of this signaling pathway was first depicted in yeast, Saccharomyces cerevisiae, in which a 22-bp cis-acting element termed the UPR element was identified in the promoter of most genes up-regulated by UPR[98, 99]. The screening of the yeast mutants that induced this UPR element helped identify an ER trans-membrane protein, IRE1p. IRE1p turned out to be a bifunctional enzyme with both Ser/Thr kinase and endoribonuclease activities, which cleaves a transcriptional factor HAC1, in its C terminal domain[26, 98]. Originally, the IRE1p was identified as a gene required for inositol prototrophy in *S. cerevisiae* and hinting to its mammalian counterpart's diverse functions in lipid metabolism[107]. In eukaryotic cells, ER homeostasis is controlled and communicated through the unfolded protein response (UPR) initiated by three ER membrane associated proteins, PERK (PKR-like eukaryotic initiation factor 2 α kinase), IRE1 (Inositol requiring enzyme 1), and ATF 6 (activating transcriptional factor 6) (Figure 1.1). To maintain ER

homeostasis, these proteins keep a dynamic control over the ER chaperones-BiP/GRP78[10, 134]. However, when ER homeostasis cannot be maintained, IRE1 and PERK are oligomerized and become fully activated to engage the downstream adaptive or destructive signaling pathways[129]. Furthermore, the ER resident transcription factor, ATF6, translocates to the Golgi where it is cleaved by a serine protease site -1 protease (S1P) and the metalloprotase site-2 protease (S2P) for full activation[23] (Figure 1.1).

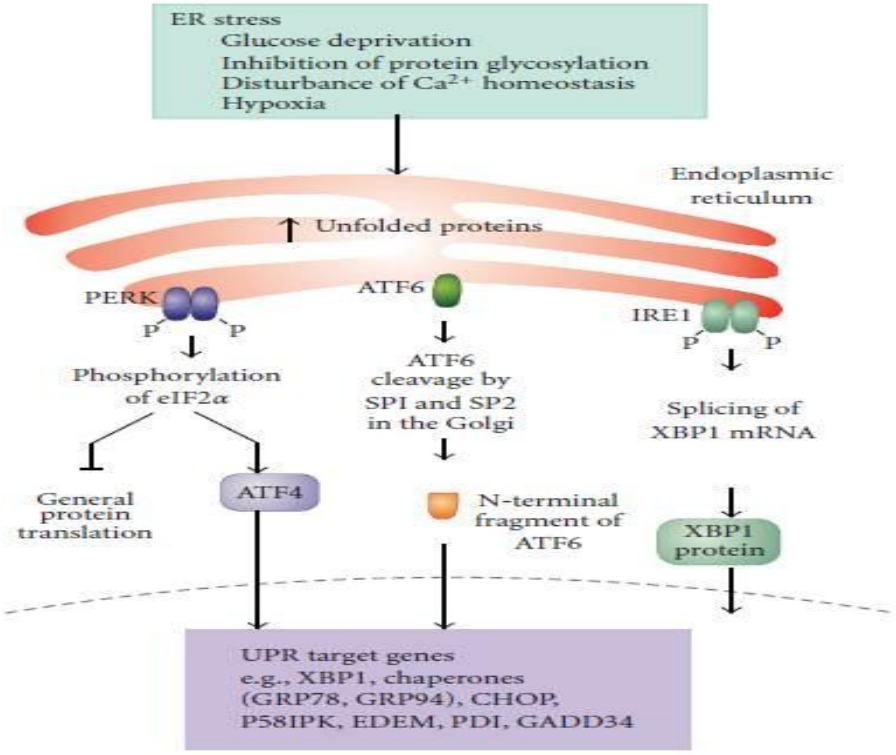

Figure 1. 1 ER stress and Unfolded Protein Response (reprinted with permission from Simone F., Gorman AM., Hori O., and Samali A. (2010). Cellular Stress Responses: Cell Survival and Cell Death. *International Journal of Cell Biology*, vol. 2010, Article ID 214074, 23 pages.)

ER stress caused by various disturbances leads to the activation of the three arms of unfolded protein response regulated by PERK (PKR resemble ER kinase), activating transcription factor 6 (ATF 6) and Inositol requiring enyzme 1 (IRE1). PERK phosphorylates eukaryotic initiation factor 2 alpha (eIF2α) followed by global translation silencing and activation of activating transcription factor 4 (ATF 4) resulting in the expression of UPR target genes such as protein chaperones. ATF 6 goes to Golgi and is cleaved into the mature form, followed by transportation of nucleus where it regulates the expression of

UPR related genes. IRE1 phosphorylates itself and also catalyzes splicing of XBP-1 (X-box binding protein 1) mRNA through its RNAase activity.

Historically, the first discovered and conserved branch of the UPR is regulated by IRE1, which regulates the production of key ER chaperons through processing and activating the XBP1 mRNA[20, 15]. IRE1 has two homologs: IRE1α is expressed in a variety of tissues including placenta, liver, skeletal muscle, lung and especially pancreas[145], but IRE1β is expressed only in the intestinal epithelia[145, 156]. IRE1 is activated by homo-oligomerization followed by auto-phosphorylation of the C-terminal kinase domain at serine 724[114, 133, 159,161]. The kinase activity of IRE1 has only one known substrate, itself. Although poorly understood, IRE1 has a unique effector function which leads to the endonucleolytic cleavage of its main substrate: mRNA encoding a transcription factor called HAC1 in yeast and XBP1 (X-box binding protein 1) in metazoans. IRE1's endonucleolytic activity cleaves 26 nucleotides from the intron of XBP1-mRNA[81, 135, 171], resulting in a 41 kDA frameshift variant (sXBP1) that is an active transcription factor. XBP-1 regulates the expression of ER chaperones and the components of ERAD machinery[92, 123]. Furthemore, XBP1 upregulates the phospholipid synthesis enzymes leading to ER expansion, a hallmark of UPR. IRE1 also has a nonspesific RNAse activity that degrades mRNAs localized on ER membrane, reducing the synthesis and import of the corresponding proteins into the ER lumen[53]. Additionally, XBP-1 can upregulate the expression of $P58^{IPK}$; a member of the Hsp40 (heat shock protein 40 kD) known as DNAJ in short name that is responsible of proper protein folding, acts as a co-chaperones and also negatively regulates PERK activity forming one of the many intersections between the three UPR braches[167]. The IRE1 dimers also interact with adaptor proteins such as TNF receptor-associated factor 2 (TRAF2) to induce the

apoptosis signal regulating kinase (ASK1) and subsequently activate the pro-apoptotic cJUN NH2-terminal Kinase (JNK) and p38 mitogen activated kinase (p38MAPK) [149] and caspase 12 Pro-caspase 12 forms a complex with TRAF2, but with activation of ER stress these two proteins dissociate leading to the activation of caspase 12 and resulting in cell death[169]. IRE1 can also modulate the activation of extracellular signal regulated kinases (ERKs) and nuclear factor $_{\kappa}$B (NF-κB) pathways[62, 106] via JNK-AP1 pathways (Figure 1.2).

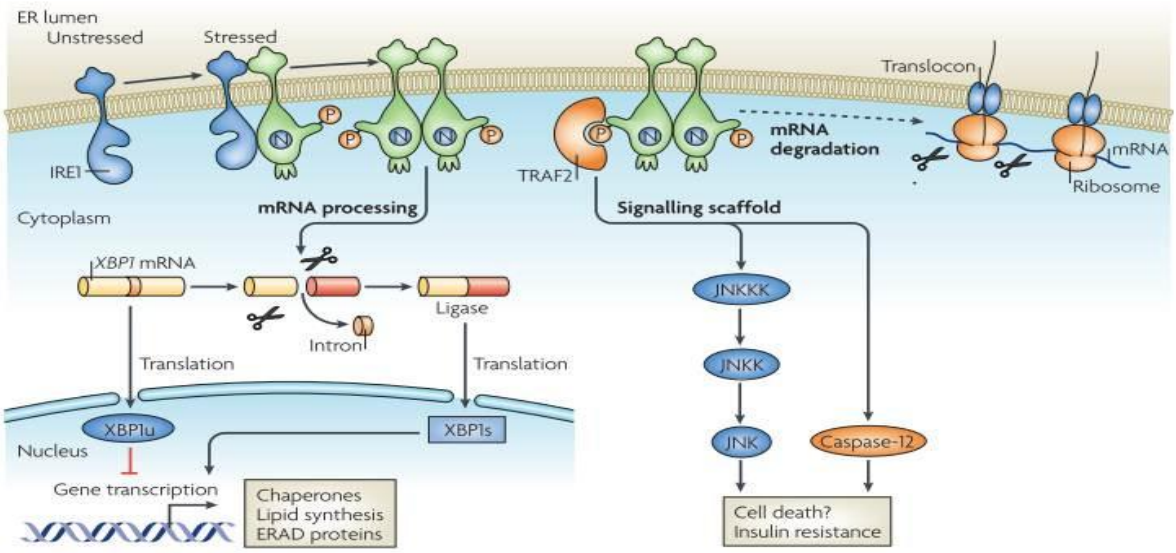

Figure 1. 2 IRE1 signaling (reprinted with permission from Ron, D., and Walter, P. (2007). Signal integration in the endoplasmic reticulum unfolded protein response. Nat. Rev. Mol. Cell Biol. 8, 519–529. © Nature publishing Group, 2007)

While inositol requiring enzyme 1 (IRE1) is in nonoligomerization state in unstressed conditions, IRE1 oligomerizes and autophosphorylates itself in stressed conditions. Upon stress induced activation, the RNAse activity of IRE1 cleaves X-box binding protein (XBP-1) in higher eukaryotes (HAC1 (homologous to ATF/CREB1) in yeast) into small RNA fragment encoding the active form of XBP-1 transcription factor, while unspliced XBP-1 encodes XBP1u, an inhibitor of UPR[171]. This is followed by the transcriptional upregulation of unfolded protein response (UPR) related genes. XBP-1 is also controls ER biogenesis. Alternatively, phosphorylated IRE1 recruits TRAF2 (tumour necrosis factor receptor (TNFR)-associated factor-2 resulting in activation of Jun N-terminal kinase (JNK) [149] and change

intracellular signaling such as insulin resistance[109]. Additionally, the IRE1-TRAF2 complex acts on caspase 12 activation and cell death[171]. ER stress can also lead to an ER-associated degradation (ERAD) of misfolded proteins.

Another arm of the UPR is initiated by the stress sensor known as the activating transcription factor 6 (ATF6), which is a 90kDA bZIP protein that becomes active after specific post-translational modifications. The disulfide and glycosylation bound luminal domain of ATF6 participates in sensing ER stress[54, 102]. Activation of ATF6 leads to its translocation to the Golgi, where it gets processed by site-1 and site-2 protease (S1P and S2P), which sequentially remove the luminal domain and the trans-membrane anchor of ATF6, respectively. After cleavage, now a 50 kDA protein, ATF6 translocates into the nucleus, where it binds to ER stress response element (ERSE; CCAAT(N)9CCACG)[171] found in genes especially involved in the ERAD pathway, as well as some involved in lipid biosynthesis, ER expansion and protein folding[45]. A regulatory step for ATF6 activity involves the Wolfram Syndrome 1 (WSF1) protein, which marks ATF6 as a target for ubiquitination and proteasomal degradation by E3 ubiquitin ligase, HMG-CoA reductase degradation protein 1 (HRD1)[36]. Recent studies identified some homologs of ATF6 such as OASIS, CREBH, LUMAN, CREB4 and BBF2H7 can undergo similar processing at the Golgi and may have a role at tissue-specific cellular stress responses[129] (Figure 1.3).

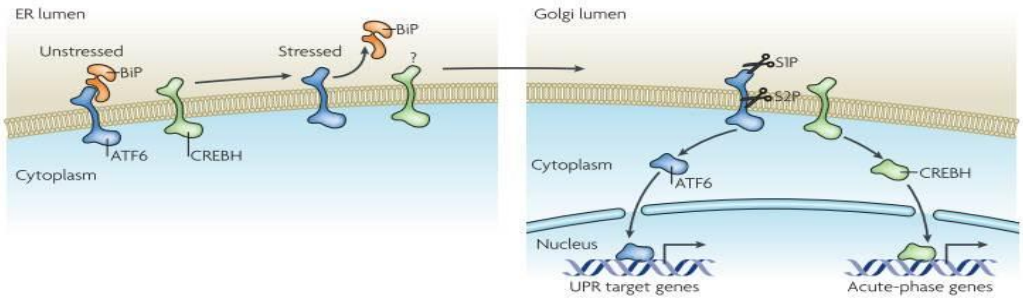

Figure 1. 3 ATF6 signaling (reprinted with permission from Ron, D., and Walter, P. (2007). Signal integration in the endoplasmic reticulum unfolded protein response. Nat. Rev. Mol. Cell Biol. 8, 519–529. © Nature publishing Group, 2007).

In unstressed conditions, activating transcription factor 6 (ATF6) and cylic AMP response element binding protein hepatocyte (CREBH) are located in the ER. Also, ATF6 is tethered to the ER by an ER chaperone immunoglobulin –binding protein (BiP) found in the lumenal domain of ER membrane. In stressed conditions, both ATF6 and CREBH translocate to the Golgi apparatus with the help of unknown vesicular transport system and are cleaved by first the lumenal site-1 protease and then the intra-membrane site 2 protease. After this activating cleavage, both proteins move to the nucleus, where ATF 6 activates UPR target genes and CREBH activates acute phase genes.

The third UPR arm is governed by the PKR-like eukaryotic initiation factor 2 α kinase (PERK), also known as pancreatic eIF2-alpha kinase (PEK). This is a type-1 trans membrane protein with ER luminal stress sensor and a cytosolic protein kinase domain. Under stress conditions, BiP dissociates from the N terminal of PERK, leading to its dimerization and autophosphorylation at the Threonine 981 on its kinase domain[73]. The C terminal kinase domain PERK shares similarities with other eukaryotic initiation factor 2 α a kinase such as double stranded RNA-dependent protein kinase R (PKR), activated by double stranded RNAs derived from viral infections, the general control non-depressible kinase 2 (GCN2), activated by uncharged tRNAs during amino acid deprivation, and the heme regulated inhibitor kinase (HRI), activated by heme limitation[51, 136, 137]. Under stress conditions, PERK phosphorylates α subunit of eIF2 at

serine 51[52]. The eIF2α is a heterodimer protein that is required for the transport of the initiating protein methoinyl-transfer RNA (met-tRNA) to the ribosome. Under stress conditions, PERK phosphorylates eIF2α, which inhibits translation initiation[70, 52]. PERK activity also stimulates some stress induced genes including the activating transcription factor-4 (ATF-4), the nuclear erythroid 2 p45-related factor 2 (Nrf-2)[27] and nuclear factor kappa β (NF-κB) [28]. ATF-4 regulates the expression of genes involved in amino acid import, glutathione biosynthesis, resistance to oxidative stress[50] as well as the pro-apoptotic genes such as the CCAAT/enhancer binding protein (C/EBP) homologous protein (CHOP) and activating transcription factor-3 (ATF 3) [90, 65, 119]. PERK dependent phosphorylation of the Nuclear factor eryhthroid-2-related factor-2) Nrf2/Keap1 (Kelch-like ECH-associated Protein 1) complexes leads to dissociation of this complex followed by Nrf2's import into the nucleus[27]. The dephosphorylation of eIF2α is mediated by the growth arrest and DNA damage inducible gene (GADD34) interacting with catalytic subunit of protein phosphatase (PP) 1[108] (Figure 1.4). Additionally, $P58^{IPK}$ that is induced by the activation of ATF6 binds to the cytosolic kinase domain of PERK and represses its activity[151, 167]. Interestingly, $P58^{PIK}$ expression occurs several hours after PERK activation and eIF2α phosphorylation. Thus, $P58^{IPK}$ induction may be thought as a marking the end of UPR and the beginning of the alarm/apoptosis phase of response[140] since at this point, if the ER stress can be handled, ER returns to normal function and the cell survives; but if the stress keeps going on, the blocking of the translational suppression by $P58_{IPK}$ might lead to apoptosis[140]

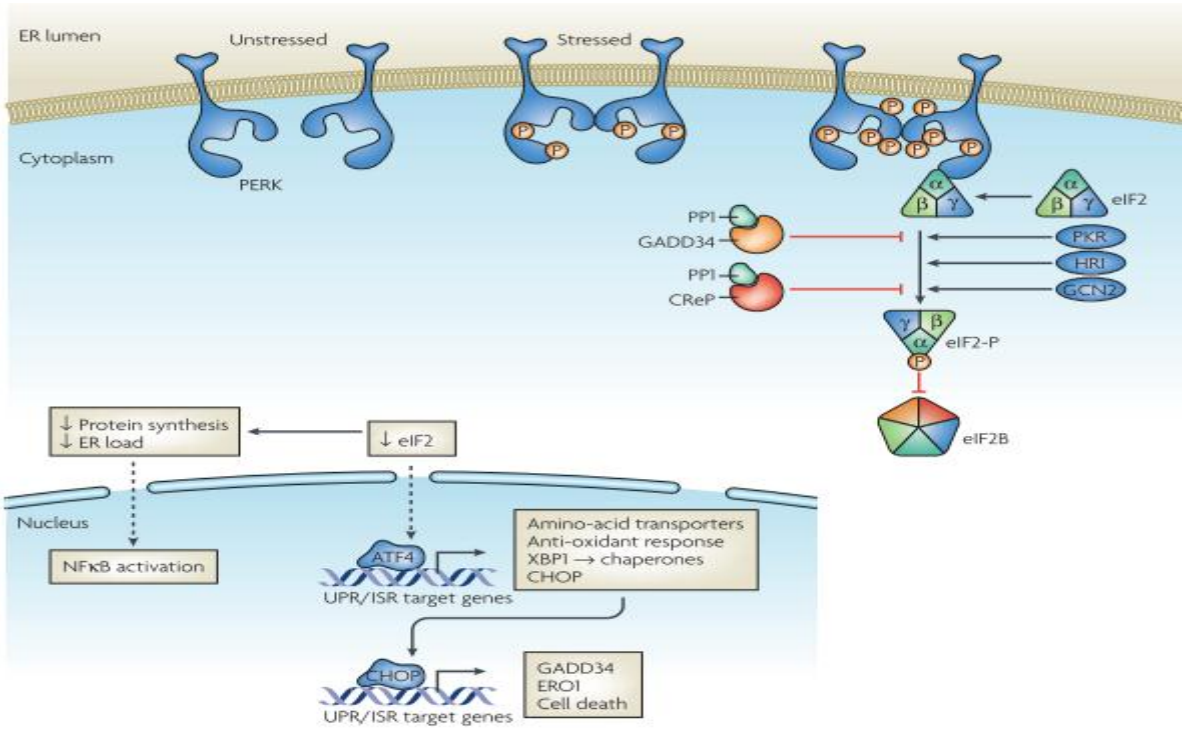

Figure 1. 4 PERK signaling pathway (reprinted with permission from Ron, D., and Walter, P. (2007). Signal integration in the endoplasmic reticulum unfolded protein response. Nat. Rev. Mol. Cell Biol. 8, 519–529. © Nature publishing Group, 2007)

Under stress conditions, protein kinase RNA (PKR) - like ER kinase (PERK) is activated, resulting in the phosphorylation of eukaryotic initiation factor 2 alpha (eIF2alpha) followed by general translation inhibition but selective translational activation of several UPR related genes. eIF2alpha can also be phosphorylated by other kinases including protein kine RNA (PKR), heme regulated inhibitor kinase (HRI) and general control non-derepressible-2 (GCN2) in an independent manner from ER stress. Hence, the larger stress response to a multitude of cellular insults and that includes the UPR is known as the integrated stress response (ISR).

1.2.3 **The Adaptive and Destructive Outcomes of the Unfolded Protein Response**

UPR response involves three phases: adaptation, alarm and apoptosis (Figure 1.5). In the adaptation phase, UPR tries to re-establish homeostasis in cells by upregulating the expression of chaperone proteins that aid in protein folding. While the unfolded proteins degradation increases, global translation is attenuated in order to reduce the build up of further misfolded proteins in the ER. If this stage fails, UPR stimulates an alarm phase,

followed by the execution of the apoptosis program[122]. The alarm phase includes several signal transduction events, leading to the suppression of the expression and activity of pro-survival factors such as the B-cell lymphoma (Bcl2) protein. Beyond this stage, the stressed cell will undergo apoptosis. In addition ER stress can induce autophagy[8, 39, 61, 69, 77, 111, and 170]. This fate decision from survival to death can be due to unresolved stress and incomplete recovery from the accumulation of misfolded proteins in the ER, ER Ca^{++} depletion, hampered disulfide formation and perturbed in redox state. All these stressors result in ER dysfunction and when prolonged, in apoptosis through the up regulation of the pro-apoptototic CCAAT/enhancer binding protein (CHOP), activation of JNK kinase and caspase 12 and via the interaction of IRE1 with other ER-localized pro-apoptotic B-cell lymphoma 2 (Bcl-2) family proteins[141]. However, the decision from survival to death in UPR may change from cell to cell since UPR is cell autonomous and context-dependent[47]. As an example, salubrinal, an inhibitor of eIF2α de-phosphorylation, protects pheochromocytoma cells from ER stress whereas it induces apoptosis in pancreatic β cells and renders them sensitive to free fatty acids[25, 80].

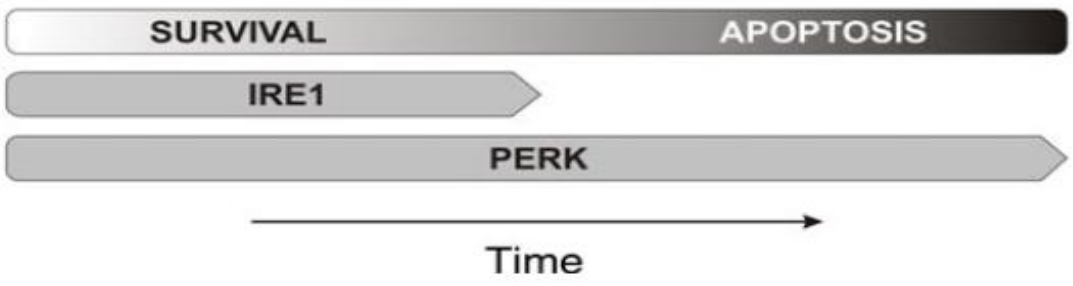

Figure 1. 5 The switch from survival to apoptosis during ER stress (reprinted with permission from Jäger R., Mathieu J.M., Bertran, Gorman A.M., Vandenabeele P., and Samali A. (2012). The unfolded Protein Response at the crossroads of cellular life and death during endoplasmic reticulum stress. *Biol. Cell*; 104, 259–270. © John Wiley and Sons, 2012

In early steps of ER stress, Both IRE1 and PERK favour cell survival, but in prolonged ER stress, adaptive signaling of IRE1 attenuates whereas PERK begins to engage pro-apoptotic pathways.

1.3 The Interface Between ER Stress And Inflammation

Recent studies have shown that the UPR may be linked to inflammatory signaling cascades and stress signaling pathways through multiple scenarios including activation of JNK and NF-κB pathways[28, 62], the production of ROS and the generation of nitric oxide resulting in both ER stress and inflammation[27, 42]. These pathways also have a central role in obesity-induced inflammation and metabolic abnormalities, especially in abnormal insulin action[56].

IRE1 is required for the ER stress induced activation of JNK, which regulates many inflammatory genes[149]. Earlier studies showed that pro-inflammatory cytokines such as TNF-alpha, IL6 and MCP-1 are suppressed in the absence of JNK in cells and tissues, and that chronic JNK activation contributes to insulin resistance and type 2 diabetes[55, 146 and 150].

Other mechanism that leads to inflammation involves NF-κB-IKK activation by both IRE1α, through the interaction of TRAF2 (TNF receptor-associated factor 2) and apoptosis signal-regulating kinase 1 (ASK1), which, in turn, causes the phosphorylation and activation of JNK. This active JNK phosphorylates and induces the activity of transcription factor activator protein 1 (AP-1), which leads to the expression of inflammatory genes. Additionally, AP-1 recruits IκB kinase (IKK) causing release of NFκB and so promotes NFκB mediated inflammation. Moreover, PERK via PERK eIF2α mediated translation suppression of IκB can directly stimulate NFκB (negatively regulating nuclear factor-κB) activation. This activation results in increase in the ratio of NFκB to IκB, thereby allowing the excess NFκB to enter the nucleus to trigger

expression of inflammatory cytokines[28, 62, and 138]. Furthermore, recent studies also link the ATF6-regulated branch of UPR to NF-κB-IKK signaling, suggesting specific inflammatory signals may be induced through all three branches of the UPR[166]. Some studies in cellular systems report that experimental induction of UPR via free cholesterol or high amounts of free fatty acids[68] may cause increased expression of pro-inflammatory molecules such as IL-8, IL-6, MCP-1 and TNFalpha[82].

Another mechanism that ER stress may be linked to inflammation involves the transcription factor cyclic-AMP-responsive-element-binding protein H (CREBH), which also resides on the ER membrane and stimulates the production of acute phase response genes in the liver such as C reactive protein (CRP) and serum amyloid P-component (SAP) [174]. CREBH and CHOP also may play an important role in the regulation of peptide hormone hepcidin, which may present a link between iron metabolism and inflammatory output via ER[152]. However, these interactions between ER stress and inflammation are not unidirectional, because recent studies in the brain provided proof that both ER stress and inflammation can activate each other, while inhibiting normal cellular metabolism[174]. In this particular study, activation of IKK-β led to ER stress and the activation of ER stress induced IKK-β.

More recently it was discovered that double stranded RNA-dependent protein kinase (PKR), which is another eIF2α kinase that is homologous to PERK, plays a unique role in linking over-nutrition to ER stress and inflammation in metabolic diseases[104]. Here, PKR was activated by lipids and was shown to have a central role in the activation of JNK and inflammatory responses during obesity. Moreover, PKR directly blocked insulin action via phosphorylating insulin receptor substrate-1 (IRS1). It is speculated

that PKR could assemble a putative metabolically-activated inflammatory complex called metabolic inflammasome or "metaflammasome" that integrates insulin action, pathogen responses and nutrient sensing. This scaffold may explain the functional overlap and between multiple signaling pathways, metabolic, stress and inflammatory, in modulating metabolism. Moreover, Baltzis et al. observed that PERK deficient mouse embryonic fibroblasts (MEF), which display much higher levels of vesicular stomatitis virus replication than that in the wild type MEFs, also exhibited partial PKR activation, suggesting a cross talk may occur between PKR and PERK[5].

The interactions between ER stress and inflammation also involves oxidative stress caused by a toxic accumulation of ROS in the cells[27]. This can be due to protein chaperones uplegulated by UPR involving in disulfide bond formation in ER. Ero1p an essential for respiration and vegetative growth 2 (Erv2p), two enzymes responsible for disulfide bond formation, utilize oxidation/reduction reactions for reducing molecular oxygen. This reduced molecular oxygen also accumulates during increased improper protein folding in ER stress and is toxic to cells[49]. This increase in ROS levels due to UPR occurs through PERK mediated activation of antioxidant program with the help of transcriptional factor Nrf2 to neutralize the toxic effects of ROS. Hence, PERK to Nrf2 signaling may be another potential link between inflammation and ER stress.

Moreover, nitric oxide (NO) generation may be related to ER stress such that NO-induced S-nitrosylation of PDI, which catalyzes the thiol-disulphide exchange by facilitating disulphide bond formation and rearrangement reactions, inhibits its enzymatic activity and leads to the accumulation of polyubiquitinated proteins and activation of the UPR[147]. ER stress also can induce iNOS via activation of pro-

inflammatory responses through NKκβ activation[165]. However, the ER molecules that have direct effect on iNOS activation still remain unknown.

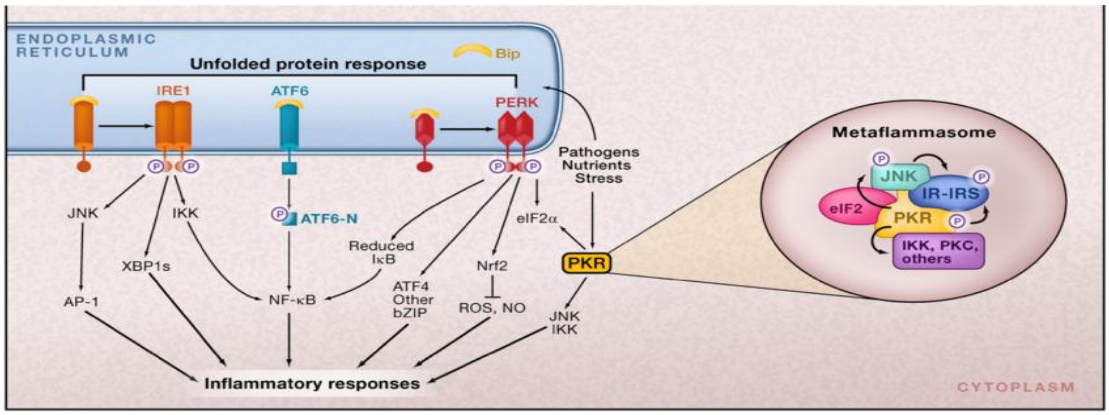

Figure 1. 6 ER stress and Inflammation (reprinted with permission from Hotamisligil GS. (2008b) Endoplasmic Reticulum stress and inflammatory basis of metabolic disease. *Cell* 140, 900–917. © Elsevier, 2010.

There are several potential pathways by which ER stress may be linked to inflammatory responses. Protein attenuation mediated by PERK activity can cause the release of NF-κB from its inhibitor IκB. This results in the transport of NF-κB to nucleus followed by changes in some genes involved in inflammatory pathways such as cytokines IL-1 and TNFalpha. Also, IRE1 recruits tumor necrosis factor 2 (TRAF2) and this complex causes activation of IκB and JNK resulting in activation of some inflammatory genes in downstream. The eIF2α kinase protein kinase RNA (PKR), induced upon ER stress, can form the core of a putative metabolic inflammasome called metaflammasome and has a direct interaction with some inflammatory kinases such as JNK and IKK, insulin receptor signaling components such as IRS1 and the translational machinery via eIF2α.

The UPR may play a role in the dysfunction and death of macrophages under lipotoxic stress[95]. Also, it has been reported that lipid chaperones such as the adipocyte and macrophage fatty acid binding protein 2 (aP2) that can bind long chain fatty acids could be a link between toxic lipids and ER stress[32]. In the study by Erbay and colleagues, $aP2^{-/-}$ macrophages were found to be resistant to ER stress induced by high amounts of

saturated fatty acids and the lipid-induced toxicity was mediated by the aP2 protein. Lipotoxicity of immune cells such as macrophages is one of the critical features of obesity and atherosclerosis suggesting that the action of the lipid chaperones in controlling lipid-induced ER stress could be therapeutically targeted to treat these diseases and their complications[32, 91]. To this date, the precise molecular links between ER stress and inflammation and how ER stress in immune cells alters the progress of chronic metabolic diseases is not fully understood (Figure 1.6).

1.4 ER Stress And Inflammation In Cardiometabolic Syndrome

Myocardial infarction and stroke are two consequences of the atherosclerotic disease and the leading cause of mortality and morbidity worldwide. Even though there have been important advances to understanding the pathogenic mechanisms underlying these metabolic diseases, due to very limited preventive and therapeutic strategies they still account for one third of all deaths annually. The signaling pathways that lie at the interface of chronic inflammation and nutrient metabolism strongly influence these chronic diseases as well as obesity, insulin resistance and type 2 diabetes[59].

Atherogenesis is triggered with the subendothelial retention of apolipoprotein (apo) B-containing lipoproteins in focal areas of the arterial subendothelium[162, 142]. A series of maladaptive inflammatory responses are triggered against oxidized or alternatively modified lipoproteins[162, 142, 89, 84 and 40]. Blood-borne monocytes are attracted to focal sites of activated endothelial cells (ECs) overlying areas of lipoprotein retention, followed by monocyte differentiation into macrophages. The recruited macrophages ingest these modified lipoproteins, convert to foam cells, and are of pro-inflammatory nature[89, 40, 41 and 84].

In most lesions, the detrimental clinical results of atherosclerosis are prevented by several adaptive processes: The remodeling of the vessel wall maintains the patency of the arterial lumen. The phagocytic clearance ("efferocytosis") of dead cells, mostly apoptotic macrophages, prevents plaque necrosis. The scar formation by collagen-producing intimal smooth muscle cells (myofibroblasts) helps to defend against matrix protease–mediated erosion or rupture of the intima into the lumen. Despite all these measures, a minority of these lesions progress due to increased lesional macrophage apoptosis, defective efferocytosis, and death of collagen producing intimal smooth muscle cells. These plaques erode or rupture, leading to the exposure of the blood to coagulation and thrombotic factors released from the necrotic lesions and acute lumenal thrombosis [7, 83, 143 and 154]. Studies conducted in animal models of atherosclerosis and, most importantly, through the analysis of human atherosclerotic lesions, support ER stress occurs in atherosclerotic plaques, particularly in the advanced stages of the disease leading to acute thrombosis[101]. ER stress occurs in lipid-laden macrophages at all stages of the disease[34, 101 and 175]. In Miyoishi and colleagues' study human coronary artery lesions from autopsy samples and fresh human carotid endarterectomy specimens were examined in terms of lesion stage, UPR markers, and apoptosis, revealing a striking relationship among advanced lesion stage, CHOP expression, and lesional apoptosis[101].

The possible connection between endoplasmic reticulum stress and metabolic disorders such as obesity, diabetes and atherosclerosis may occur through several ways. First, there is a direct relation between lipid metabolism and ER stress, including the existence of lipogenic enzymes in ER domains. Furthermore, XBP1 plays a role in ER phosphatidylcholine synthesis and ER membrane expansion[139]. Multiple studies also

show that ER stress promotes lipogenesis and hepatic lipid accumulation, but how the individual UPR branches plays a role in this remains unclear[59]. Second, ER stress leads to abnormal insulin action and hyperglycemia by causing insulin resistance, stimulation of hepatic glucose production and suppression of glucose disposal. Studies show ER stress is a potential link between obesity, type 2 diabetes and atherosclerosis[121]. Moreover, ER stress may lead to the production of inflammatory mediators and reactive oxygen species, which are destructive for insulin action, lipid metabolism and glucose homeostasis[60].

It is known that primary macrophages play an important role in the progress of atherosclerosis[97]. Hence, the studies on the role of ER stress in macrophages may provide clues to ER stress contribution to atherosclerosis. ER stress can be induced by excess accumulation of free cholesterol, resulting with cell death in macrophages. The overload of fatty acid leads to their accumulation and stiffening of ER membranes, which are known to be poor in cholesterol content. Consequently, the stiffening of ER membranes activates the UPR and the PERK-mediated CHOP activation leads to apoptosis[34].

Recently, it has been reported that obesity and insulin resistance may stimulate ER stress in lesion macrophages due to elevations of saturated fatty acids (SFAs) [32, 131]. SFAs cause the loss of fluidity of the ER membrane bilayer, which is a known inducer of the UPR. However, the exact mechanism of SFA-induced ER stress is not fully understood. Erbay and colleagues demonstrated that intracellular lipid chaperones (or macrophage/adipoctye fatty acid-binding protein-4, aP2) mediates SFA- induced ER stress and apoptosis in macrophages. In this study, $ApoE^{-/-}$ (apolipoprotein E) mouse

model fed by Western diet, when genetically deficient for aP2 were found to be protected against lipid induced PERK activation, XBP-1 splicing and apoptosis in macrophage-rich regions of atherosclerotic lesions. These results implicated aP2 as a central mediator of lipotoxic ER stress in macrophages during atherogenesis. Furthermore, reduction of ER stress by chemical chaperons reduced atherosclerosis in mice[32]. Collectively; the described findings show the important contribution of lipid-induced ER stress to atherosclerosis progression and offer new insights into metabolic disease pathogenesis.

1.5 Restoring ER Stress

Restoring ER function may become a promising future therapeutic strategy against metabolic diseases including insulin resistance, diabetes, fatty liver disease, obesity and atherosclerosis. For example, Qi et al. (2004) [120] and Vilatabo et al. (2005) [153] observed that 4-phenylbutyric acid (PBA), which is known as a chemical chaperon, has protective effects against cerebral ischemia and liver ischemia reperfusion injury by inhibiting ER-stress- related apoptosis. Another reagent tauroursodeoxycholic acid (TUDCA), a hydrophilic endogenous bile acid, also prevented diet-induced ER stress and ER-stress associated apoptosis in human liver cells through unknown mechanisms[31]. Additional studies in obese and diabetic mouse models showed that the administration of TUDCA and PBA can reduce ER stress, normalize hyperglycemia, increase systemic insulin sensitivity, resolve the fatty liver disease and enhanced insulin action in liver, muscle and adipose tissues[110]. Furthermore, administration of PBA to Apolipoprotein E null (ApoE−/−) mice with atherosclerosis exhibit ER stress and UPR activation in the lesions[175] resulted in a dose-dependent reduction ER stress in macrophages and atherosclerotic lesions[32]. In this study, the ER stress markers phosphorylated-eIF2α,

phosphorylated-PERK and ATF3 expression were significantly reduced in the atherosclerotic lesions of mice treated with PBA, suggesting restoring ER function with chemical chaperone and reducing ER stress and death of macrophages in lesions can protect against the deleterious effects of toxic lipids and prevent atherosclerosis[32]. Additionally, it was also observed that gastric bypass induced weight loss results in the reduction of the ER stress markers, GRP78, sXBP1, phosphorylated-eIF2α and JNK-1 in the liver samples of these patients[43]. These observations indicate reduction in nutrient intake and in adipose tissue size may reduce the ER stress levels in metabolically active tissues in humans. Furthermore, a study conducted by Diakogiannaki showed that the administration of a monounsaturated fatty acid palmitoleate for 18 hrs., reduced ER stress induced by both a saturated fatty acid palmitate and also tunicamycin (a chemical stressor of the ER by blocking N glycosylation) in β cells[29]. When the two species of fatty acid palmitate and palmitoleate were given in combination, the extent of cell damage was less than that when palmitate was applied alone. In fact, examination of multiple images showed that the overall ER membrane area was reduced in palmitate and palmitoleate administration compared with in only palmitate administration; suggesting that mono unsaturated fatty acids entering membrane lipids is less destructive to membrane architecture than when saturated molecules exist[29].

The possibility of applying these chemical chaperones to restore ER function and reduce ER stress in human metabolic diseases still remains to be fully explored. However, new studies are appearing with promising results. For instance, a study conducted by Kars et al. in 2010 displays TUDCA-stimulated increase in the muscle and hepatic insulin sensitivity of obese and insulin resistant patients[71].

1.6 Chemical Genetics And Its Applications

Advances in high throughput chemistry and genetics have created a new field dubbed "chemical genetics", which generates tools that can help elucidate and validate novel drug targets. This approach can also be successfully applied to deciphering signal transduction cascades, particularly, in discovering novel substrates of kinases[74].

The traditional genetics approach can examine the function of a single protein at the level of the organism, a major reason why knock out mice have become popular tools for target analyses. However, this approach has some disadvantages. For example, genetic approach knocks out a specific gene without discriminate against the other proteins that associated with the targeted protein or in other words, leading to the disassembly of associating proteins in a protein complex (for instance, the targeted gene may be an important scaffold in a complex) or abolish an enzymatic function of the targeted protein. This unwanted effect renders it difficult to determine the direct and indirect effects of the gene knock-out approach. Second, the genetic approach lacks temporal control over the targeted protein. While, inducible knock outs and RNA based approaches (such as antisense and RNAi) have been devised, these lead to a slow change in protein activity compared to quick signaling responses that normally take place in cells. In addition, Causton et al. in 2001 showed that a temporal shift in yeast (from 25 ^{o}C and 37^{o}C) leads to significant differences in genome expression[22]. This study indicates that conditional or inducible systems such as temperature sensitive alleles may cause secondary perturbations with unwanted side effects. Finally, some genes, which play significant roles in embryonic development result in lethal phenotype making these genetic models inapplicable, particularly valid for knockout mice[63].

Because of these and other reasons, genetic approach can fall short in analyzing processes such as signal transduction.

In addition to these, purely chemical approaches for studying protein function have their own shortcomings. Even though chemicals are useful tools for analyzing functions of a protein in a temporal manner, they can lack target specificity. Therefore, with this approach, determination of individual target's direct actions and biological role can be difficult. In addition, these "off targets" can be the major cause for toxicity.

In summary, the genetics approach provides target specificity while chemistry allows for temporal control over the function of the targeted protein. The chemical genetics approach combines the specificity of genetics with pharmacologically relevance and control of small molecule chemistry[2]. Therefore, combining these two experimental approaches into one by means of chemical genetics offers great advantages in validating targets and in drug discovery in the post genomic area.

Protein kinases represent approximately 2% of all human genes and play important roles in cellular process and consequently, in many diseases processes. Therefore, they offer a rich source of drug targets. The recent application of the chemical genetics approach to protein kinases involves the discovery of analog sensitive alleles (ASKAs) and corresponding small molecule analog compounds that can specifically modulate ASKA's activity[13]. The main feature of this approach is the creation of unique structural distinction between the catalytic domains of one kinase. This distinction is achieved by making a mutation in ATP binding pocket of the kinase that enlarges it: All proteins contain bulky amino acid residues at conserved positions in ATP-binding pocket called

"gatekeeper residue". When this gatekeeper residue is converted into small side-chain amino acids such as alanine or glycine, a gateway to the deep hydrophobic 'specificity pocket" is created. This kind of a mutation in the gatekeeper residue is silent, in other words, almost never disrupts the kinase's activity[163], enzymatic activity[88] and cellular function[11, 12, 21 and 159]. This gatekeeper mutation can be determined by simply comparing amino acid sequence alignments even if there's no 3D structural knowledge about the kinase since the gatekeeper residue is highly conserved among all ATP binding pockets of kinases[12].

The ASKA technology can be applied to discover the unknown substrates of potentially interesting kinases. With the help of bulky ATP analogs that are uniquely accepted by the ASKA, direct substrates of mutated kinases can be labeled during in vivo or in vitro kinase assays and then coupled to mass spectrometry for identification of potential substrates. In this strategy, ASKA is incubated with the bulky ATP analogy, N6-alkylated ATPγS and thiophosphorylates its substrates. Following, alkylation with PNBM (p-nitro benzyl mesylate) thiophosphate esters are formed on the modified substrates. These groups can be specifically recognized by a monoclonal antibody called anti-thiophoshate antibody and pulled down by immunoprecipitation method. After the separation of the phosphorylated substrates from the immunoprecipitates by one or two dimensional gel electrophoresis, each band can be excised and identified by mass spectrophotometry[74] (Figure 1.7). An example of a successful study using this approach identified 28 new substrates of the energy-sensing AMP-activated protein kinase (AMPK) discovered[6]. Moreover, Allen and colleagues showed that in cells isolated from a mouse that express endogenously levels of ASKA allele of the extracellular-signal-related kinase (Erk2) identified several direct and previously unknown substrates

of Erk2[2]. Furthermore, Ultanir et al. in 2012 used this method and found 5 putative substrates of the nuclear Dbf2-related kinase (NDR1) that plays an important role in polarized growth and control of dentrite growth and morphology[148].

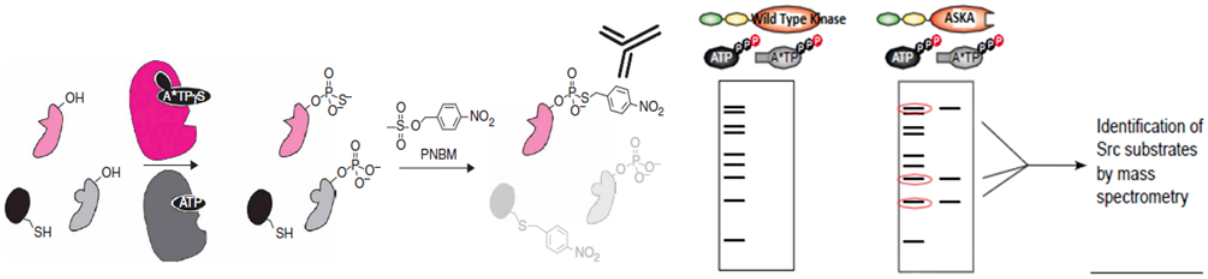

Figure 1. 7 Strategy for labeling individual kinase substrates and identification of direct substrates via ASKA approach. (reprinted with permission from Allen JJ., Li M., Brinkworth CS., Paulson JL., Wang D., Hübner A., Chou WH., Davis RJ., Burlingame AL., Messing RO, Katayama CD., Hedrick SM, Shokat K.M. (2007). A semisynthetic epitope for kinase substrates. *Nat Methods*.Jun;4(6):511-6.© Nature Publishing Group, 2007.

In first step analog sensitive kinase uses N6-alkylated ATPγS (A*TPγS) to form thiophosphorylates on its substrates. Next, PNBM alkylates these substrates resulting in thiophosphate esters or thioesters that is recognized by a specific antibody, α-hapten-IgG and pulled down by immunoprecipitation technique. After these steps, the potential substrates from the immunoprecipitates can be analyzed by mass spectrophotometry.

The ASKA strategy can be applied to in cells or in vivo mouse models for pharmacologically relevant target validation. In this strategy, wild type kinase is replaced by its ASKA counterpart with the help of gene targeting in embryonic stem cells. The resultant transgenic mice can be used either directly in various chemically induced disease models or by mating to suitable disease model strains. Potent, specific kinase inhibition can be achieved by the intraperitoneal injection of orthoganal inhibitor that inhibits only the ASKA and not the wild type kinases[74] (Figure 1.8). In 2005, Chen

and colleagues[23] used this approach to study neurotrophin signaling, where they reported in vivo administration of an ATP analog inhibitor, 1NM-PP1, (by intraperiotenal injection or in the drinking water) only inhibited the ASKA allele of the kinase of interest, leading to the elimination of specific populations of neurons in the chemical-genetic mouse model but not in their wild type littermates. Wang et al. in 2003[157] also used this approach to control CaMKII-mediated synaptic plasticity in the forebrain during distinct stages of memory processes[157].

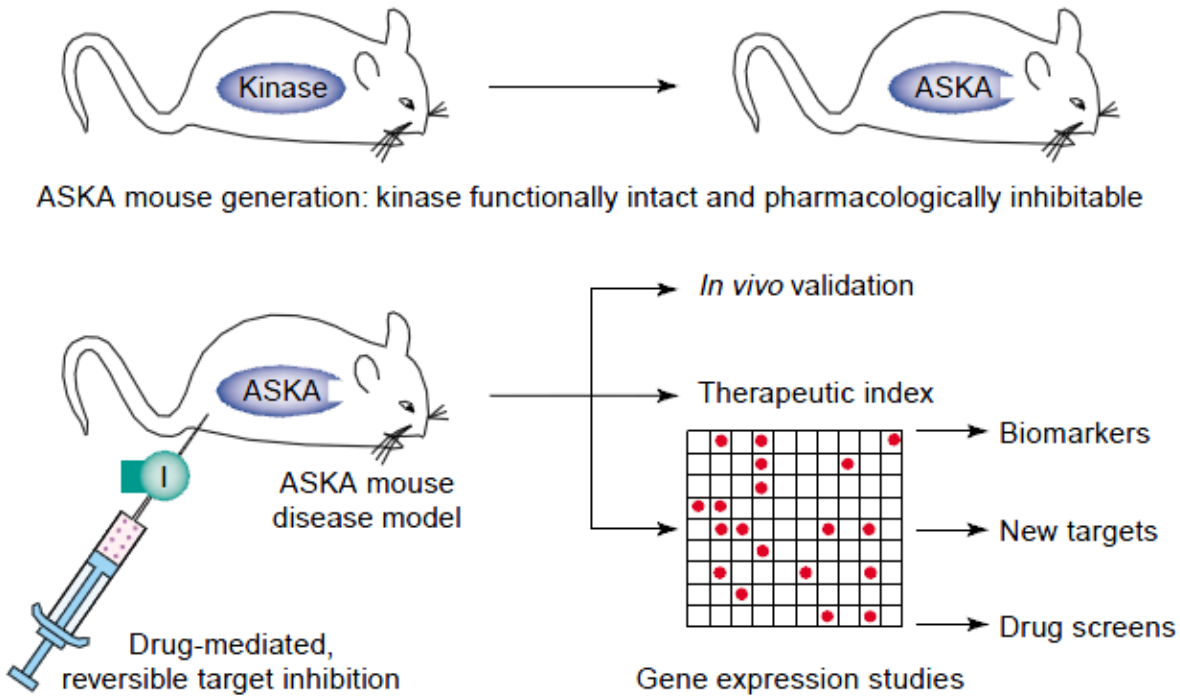

Figure 1. 8 ASKA mouse studies: target validation, therapeutic index and biomarkers (reprinted with permission from Kevan Shokat and Mark Velleca (2002). Novel chemical genetics approaches to the discovery of signal gtransduction inhibitors. *Drug Discov Today*.Aug 15; 7(16):872-9. © Elsevier, 2002.

Analog sensitive kinase alleles (ASKA) mouse studies for drug screens, the discovery of biomarkers and new targets. Wild type kinase mouse strains can be changed by ASKA counterpart by use of transgenic approaches or gene targeting in embryonic stem cells. These mouse strains can be useful in direct use or

in the mate of disease model strains. The bulky ATP analog inhibitors specific to ASKA may be applied to mouse models by intra-peritoneal injection.

The other applications of chemical-genetics include genomic profiling using microarrays to define the impact of this kind of highly specific drug-mediated kinase inhibition on gene expression. Importantly, two studies[12, 21] demonstrated the blueprints of their targeted kinases differed significantly from those generated by knockdown or knockout technologies against the same kinase. For example, the study conducted by Carroll and colleagues showed that a novel role for Pho85 cyclin dependent kinase in a metabolic pathway, that could only be revealed by acute chemical inhibition of ASKA and has been missed in studies using the knock out approach against the same kinase[21].

A final application of chemical genetics involves the carrying out genomic profiling in high throughput and high content drug screens in preclinical in vivo models using the chemical-genetic inhibition as a reference to establish a therapeutic index and generate new biomarkers[74]

2. OBJECTIVES AND RATIONALES

Endoplasmic reticulum stress has been linked to inflammation through several ways. One of these links involves PERK-mediated translation attenuation that causes a reduction in IκB protein levels and the release of NF-κB, which can then translocate to nucleus and activate the transcription of inflammatory genes such as interleukin 1 (IL1) and tumor necrosis factor alpha (TNFα). Additionally, activated PERK can phosphorylate nuclear erythroid 2 p45-related factor 2 (Nrf2) followed by its release from the Nrf2/Keap1 complex and subsequent transportation into the nucleus[27], where it regulates the expression of antioxidant response element-dependent genes encoding heme oxygenase-1 (HO-1), thioredoxin reductase 1 (TXNRD1) and the glutathione S-transferases GSTP1, GSTM1, and GSTm2[27]. Furthermore, chronic ER stress can lead to oxidative stress due to increased ROS production from the ER. The ER ROS production is the result of UPR-stimulated up regulation of protein chaperones mediating disulfide bond formation in the ER lumen, which is a process which involves the activities of Ero1p and Erv2p enzymes that use oxidation/reduction reactions, with molecular oxygen as the final electron recipient[27]. ROS accumulation can result in inflammation through engaging kinases such as JNK and NFκB and some proteins such as COX2, an important mediator of inflammation and iNOS activity[67]. Hence, ROS produced from the ER can be another link between chronic ER stress and inflammation.

The IRE-1 branch also connects ER stress with inflammation. The activation of IRE1 causes the recruitment of tumor necrosis factor-a (TNF-a)-receptor-associated factor 2 (TRAF2) and the activating IκB/ NF-κB (IKK) complex[62] or JNK, leading to the

activation of NF- κB or activating transcription factor 1 (AP1) pro-inflammatory transcriptional targets such as TNFalpha, interleukin 6 and INOS, in the nucleus[149].

Elevated lipids in obesity or dyslipidemia such as saturated and oxidized lipids are known to cause ER stress and inflammation[37]. For example, saturated fatty acids such as palmitate and stearate induce ER stress in various cell types such as liver, 3T3-L1 fibroblasts, preadipocytes, pancreatic Beta cells and macrophages[4, 46 and 158]. However, it's not clear which branch of UPR and to what extent mediates the lipid-induced inflammation since all three arms of the UPR are activated by metabolic stress during obesity.

In this thesis study, I developed an experimental approach, which can address the direct impact of one specific arm of the UPR, initiated by PERK, on inflammation during lipid stress. I used specific siRNA-based silencing of PERK activity to study the loss of function for PERK during lipid-induced inflammation. In addition, I developed a molecular tools based on chemical genetics that can be used to identify the full spectrum of PERK's substrates. In the chemical genetics approach, the interested kinase can be mutated as an ATP analog sensitive kinase allele, whose kinase activity can be inhibited by cell permeable bulky ATP analogs. When coupled to proteomics, the ATP-analog sensitized mutant of PERK can be valuable tool for future studies intending to identify the full spectrum of PERK's substrates. In this thesis study, I used the siRNA based silencing of PERK activity for initial characterization of PERK's role on lipid induced inflammation in macrophages.

Finally, I analyzed the impact of ER stress reduction on lipid-induced inflammation by simultaneously treating macrophages with palmitoleate, known to block lipid-induced ER stress. Taken together, the findings presented in this thesis demonstrates the direct role of PERK in lipid induced ER stress and inflammation, an important pathogenic mechanisms underlying metabolic diseases including insulin resistance, fatty liver diseases, diabetes, atherosclerosis and obesity. Furthermore, the outcome of my studies suggests reduction of lipid induced inflammation by palmitoleate may explain its protective effects in metabolic diseases.

3. MATERIALS AND METHODS

3.1 MATERIALS

3.1.1 General Laboratory Reagents

The reagents utilized during this research were purchased from major companies such as Sigma-Aldrich (St Louis, MO, USA), AppliChem (Darmstadt, Germany) and Merck (NJ, USA). DMSO was purchased from AppliChem (Darmstadt, Germany). Ethanol, Methanol, Isopropanol was from Sigma-Aldrich (St.Louis, MO). Plasmid mini- and midi-prep kits for plasmid extraction were bought from Qiagen (Hilden, Germany), Promega (Wisconsin, USA) and Invitrogen (CA, USA). Gel DNA Recovery kit used in DNA purification was from Zymo Research Corporation (CA, USA). PCR Purification kit was bought from MO-BIO Company (CarlsbadCA, USA) Agarose was purchased from PRONA (The European Economic Community). Yeast extract, tryptone, NaCl , Bacto Peptone and agar were purchased from CONDA (Madrid, Spain), Sigma ALDRICH (St. Louis,MO,USA) ,BD (MD,USA); respectively. ECL Plus western blot detection kit was from Amersham Pharmacia Biotech Company (Amersham, UK). Bradford Reagent was bought from Sigma-ALDRICH (St.Lous, MO, USA). Poly-ethylamine was from PolySciences (Warrington, PA, USA). High Grade pure water and Phospho Saline Buffer (PBS) were purchased from HyClone (Rockford, USA)

3.1.2 Tissue Culture Materials And Reagents

All plastic materials utilized in cell culture such as petri dishes, plates, flask were purchased from Greiner Bio One (Monroe, NC, USA). Serological Pipettes were from Sarstedt Inc. (Newton, NC, USA). Dulbecco's modified Eagle's Medium was purchased

from Thermo Scientific HyClone (Rockford, USA) and Lonza (Basel, Switzerland). NEON Transfection System was bought from Invitrogen (Carlsbad, CA, USA). Other reagents such as Trypsin-EDTA, Fetal Bovine Serum and L-Glutamine were bought from HyClone (Rockford, USA) and GIBCO (Invitrogen, Carlsbad, CA, USA), respectively.

3.1.3 Bacterial Strains

Escherichia coli E.coli DH5α strain was used.

3.1.4 Enzymes

EcoR1 and Xho1 purchased from New England BioLabs (Ipswich, MA, UK) were used in restriction digestion during this research. T4 Ligase for ligation is bought from Fermentas Molecular Biology Tools (Thermo Scientific, Rockford, USA). The enzyme "Phusion Hot Start II High Fidelity DNA polymerase used in site-directed mutagenesis PCR and Phire Hot Start used in other PCR types such and conventional PCR, colony PCR were bought from FINNZYMES (Thermo Scientific, Vantaa, Finland).

3.1.5 Nucleic acids

DNA molecular weight markers were bought from Fermentas (Thermo Scientific, Rockford, USA). The plasmids used during this research such as pcDNA5F-FLAG (Invitrogen) and pBABE-Puro were kindly provided by Batu ERMAN (Sabanci University, Turkey).

3.1.6 Oligonucleotides

Primer	Sequence	Tm
mPERK M888A Fwd	5'GTATCTGTACATTCAGGCGCAGCTGTGCAGGAA GG 3'	63°C
mPERK M888A Rev	5'CCTTCCTGCACAGCTGCGCCTGAATGTACAGATA C 3'	63°C
mPERK M888G Fwd	5'GTATCTGTACATTCAGGGGCAGCTGTGCAGGAA GG 3'	63°C
mPERK M888G Rev	5'CCTTCCTGCACAGCTGCCCCTGAATGTACAGATA C 3'	63°C
mPERK Seq-1 Fwd	TCGGAGACAGTGTTTGGCTTAG	NA
mPERK Seq-2 Rev	CGTCCATCTAAAGTGCTGATGATTAC	NA
mPERK Seq-3 Fwd	CCTCTTCCAGTGGGACCG	NA
mPERK Seq-4 Fwd	GGGAGTACCAGTTTTGTACTCC	NA
mPERK Seq-5 Fwd	CGCAGATCACAGTCAGGTTC	NA
mPERK Seq-6 Fwd	CCACCAGAGAAGTGGCAAG	NA
mPERK Seq-7 Fwd	CACTCCTTTGAACTTTGTCC	NA
mPERK Seq-8 Fwd	CATCTTCCTGCAGATCGCAG	NA
mPERK Seq-9 Fwd	GATGGTTCAAGACATGCTCTCTC	NA

Table 3. 1 The list of used primer; sequences and melting temperatures (Tm)

The name of siRNA	Company Name	Catalog number
Mm_Eif2ak3_1 FlexiTube siRNA (NM_010121, XM_988416)	Qiagen	SI00991319
Mm_Eif2ak3_3 FlexiTube siRNA (NM_010121, XM_988416)	Qiagen	SI00991333
Mm_Eif2ak3_5 FlexiTube siRNA (NM_010121, XM_988416)	Qiagen	SI02689981
Mm_Eif2ak3_6 FlexiTube siRNA (NM_010121, XM_988416)	Qiagen	SI02736615

Table 3. 2 The list of siRNAs used: company and catalog information

3.1.7 Electrophoresis, photography and spectrophotometry

In gel electrophoresis, Agarose Basica Lee was bought from PRONA. The apparatus and power supply PS300-B for electrophoresis was purchased from Hoefer, Inc. (Holliston, MA). The concentration of nucleic acids determined by NanoDrop from Thermo Scientific (Wilmington, USA).Protein concentration with Bradford Reagent, which is purchased from Sigma(Taufkirchen, Germany), were measured by using spectrophotometer Beckman Du640 (Beckman Instruments Inc., Ca, USA).

3.1.8 Electroporation

Electroporation apparatus, Transfection Systems Pipette Station & Pipette and Transfection System 10 ul and 100 ul Kit were bought from NEON Transfection System of Invitrogen (Carlsbad, CA, USA).

3.1.9 Antibodies

The antibodies used in this study and their catalog numbers, working dilutions and conditions are listed in the table 3.3.

Antibody	Company and catalog number	Working Dilution	Incubation time
p-PERK (Thr 980) (16F8) Rabbit mAB	Cell Signaling,3179	1:500	Over-night at 4^{o}C , followed by 1 hour exposure at room temperature
c-myc (9E10)	Santa Cruz,sc-40	1:1000	1 hour at room temperature
B Tubulin (H-235)	Santa Cruz,sc-9104	1:1000	1 hour at room temperature
B actin	Santa Cruz	1:1000	1 hour at room temperature
Goat Anti-mouse IgG-HRP	Santa Cruz,sc2005	1:5000	1 hour at room temperature
Goat Anti-rabbit IgG-HRP	Santa Cruz,sc2004	1:5000	1 hour at room temperature
p-IRE	Epitomics,3881-1	1:1000	1 hour at room temperature
Total-IRE	Cell signaling, 3294	1:1000	Overnight at 4^{o} C
SAPK/JNK	Cell signaling, 9252	1:300	2 hours at room temperature
SAPK/JNK phospho-p54 phosphor-p46	Cell signaling, 9255	1:200	2 hours at room temperature

Table 3. 3 A list of antibodies used; catalog numbers, working dilutions and incubation times.

3.2 SOLUTIONS AND MEDIA

3.2.1 General Solutions

50X Tris-Acetate-EDTA (TAE)	242 gr Tris-Trizma Base, 37.2 gr EDTA (Tritiplex 3) and 57.1 ml Glacial Acetic Acid is dissolved in 1 liter ddH2O and autoclaved.
Ethidium Bromide	1X is used as a working solution in ddH2O from 10 mg/ml stock solution. 3 uL for 50 ml % 1 Agarose gel is used.

3.2.2 Bacteria Solutions:

Luria_bertani Medium (LB Medium)	10 g NaCl, 10 g Bacto-Tryptone, 5 gr Bacto-yeast exract are dissolved in 1 liter ddH2O and then autoclaved. 20 g/L Bacto-agar is used for agar plates.
Amphicilin (1000X)	100 mg/ml stock solution in ddH_2O (1000X) Working solution was 100 ug/ml (1X)
Glycerol Stock Solution	Final concentration was %25 in LB

3.2.3 Tissue Culture Solutions

DMEM/RPMI media	Complete medium contains %10 fetal bovine serum, %1 L-glutamine, stored at 4^{o} C.
1X Phosphate Buffered Saline (PBS)	This was bought from Invitrogen Gibco.
Thapsigargin	300 μM of Tg was prepared as a stock solution in DMSO. Working solution is 300 nM.
NaPP1	40 μM of NaPP1 were dissolved in DMSO as a stock solution. Working solution is 20 μM.

Palmitic acid (palmitate)	500 mM of palmitate were dissolved in high pure absolute EtOH.Working solution is 500 µM dissolved in filtered complete media containing % 5 fatty acid free BSA. It is incubated and vortexed until completely dissolving.
Palmitoleic acid (palmitolate)	500 mM of palmitolate were dissolved in high pure absolute EtOH.Working solution is 500 µM dissolved in filtered complete media containing % 5 fatty acid free BSA.
Phospho Lysis Buffer	50 mM HPES pH:7.9, 100 mM NaCl, 4mM Na Pyruvate,10 mM EDTA,10 mM NaF, % 1 Triton , 2 mM NA Vanadate , 1mM PMSF , 1X phosphatase inhibitor cocktail 3 (Sigma, P0044) and 1 X (10 µM / ml) protease inhibitor cocktail.

3.2.4 Competent Cell Solutions

<u>$CaCL_2$ sln</u>:

Solutions:

PIPEs (Mw= 307.37 g/mol)	pH: 6.4	0.1 M	stored at room temperature
$CaCl_2$ (Mw= 147.g/ mol)		2 M	stored at room temperature
Glycerol		% 87	stored at room temperature

The preparation of Mixture for 500 ml from stock solutions:

Stock solutions	Final concentration:
2 M Cacl2	**60 mM**
0.1 M PIPEs	**10 mM**
% 87 Glycerol	**%15**
ddH_2O	up to final volume

**Autoclave or filter the solution before use and store at 4 degrees.

3.2.5 Sodium Deodecyl Sulphate (SDS)-Polyacrylamide Gel Electrophoresis (PAGE) And Immunoblotting Solution

In this study, Mini PROTEAN Tetra Cell western blotting system (Bio Rad, CA, and USA) was used for the westernblot experiments. The gels used were prepared as % 10 resolving gels and % 5 stacking gels.

% 10 Resolving Gel	%30 Acyrlamide mix, 1.5 mM Tris HCl (pH: 8.8) %10 SDS and amonium persulfate, %0.08 TEMED with suitable volume of ddH_2O to complete desired volume.
% 5 Stacking Gel	%30 Acyrlamide mix, 1.5 mM Tris HCl (pH: 6.8) %10 SDS and ammonium persulfate, %0.1 TEMED with suitable volume of ddH2O to complete total desired volume.
5 X Running Buffer	124 mM Tris Base, 960 mM Glycine, 17.4 mM SDS were dissolved in ddH2O as a stock solution. Working solution is 1 X.
5 X Transfer Buffer	64.4 mM Glycine, 80 mM Trisma Base and 2.14 mM SDS was dissolved in ddH2O. Working solution is 1X while working.

10 X Tris Buffered Saline (TBS)	100 mM Trisma Base, 1.5 M NaCl in ddH_2O and is adjusted to pH: 8 with 1 N HCl.
1 X TBS-Tween 20	0.2 % Tween in 1 X TBS
Blocking Solution	% 5 (w/ v) BSA (Bovine Serum Albumin) was dissolved in % 0.2 TBS-Tween 20.

3.3 METHODS

3.3.1 The use of Software Programs

3.3.1.1 Pymol

The hypothetical 3D model of PERK was created using SwissModel Tools program and then aligned with the other kinases ATP binding pockets (whose crystal structures were solved previously) in a complex with ATP or 1NM-PP1 using PyMOL15 according to manufacturer's recommendations (PyMOL, http://pymol.org/educational/).

The proteins used for comparison was GCN2 (ID number: 1YZ5; Padyane et al., 2005; http://www.pdb.org/pdb/explore/explore.do?structureId=1ZY5) and TgCDPKI (ID number:3I7B, Kayode et al.,2010; http://www.pdb.org/pdb/explore/explore.do?structureId=3I7B)

3.3.1.2 BioLign

The sequence information for PERK in the AB1 format or a DNA sequence chromatogram from the sequencing machine was visualized in BioLign 4.0.6 Tool according to the manufacturer's recommendations (http://en.bio-soft.net/dna/BioLign.html).

3.3.1.3 ClustalW2

Homosapiens PERK sequence (NM_004836.5, December 2010) and mus musculus PERK sequence (NM_010121.2, December,2010) was aligned with other kinases with known crystal structures for their ATP binding domains using the ClustalW2 program as per se the manufacturer's recommendations (Clustal W2, EMBL-EBI;

http://www.ebi.ac.uk/Tools/msa/clustalw2/).

3.3.2 Molecular Cloning Methods

3.3.2.1 Chemical Competent Cell Preparation

For the preparation of competent cells, firstly, a BIOLABS NeB-5-alpha High efficiency competent E.coli cell was inoculated into 50 ml Luria-Bertani media (LB media) without any antibiotics for 12 hours. Then, 200 µl of this culture was diluted into 100 ml LB. After one hour, the optical density (OD) of culture was checked using a spectrometer until it reached 0.345 OD, demonstrating a logarithmic growth in culture. The culture was divided into 2x50 ml falcon tubes on ice and incubated for 10 minutes. After centrifugation at 1600g (4^oC) for 20 minutes, the bacterial pellet was resuspended in 10 ml of ice cold $CaCl_2$ solution. This suspension was centrifuged in 1100 g (4^oC) for 10 minutes before resuspending in 10 ml of ice-cold $CACl_2$ solution again. Then, it was incubated on ice for another 30 minutes, followed by centrifugation at 1100g (4^oC) for 10 minutes. The obtained pellet was dissolved in 2 ml of ice cold $CaCl_2$ solution and dispensed into pre-chilled sterilized eppendorf tubes on ice (50µl/tubes). These aliquots were frozen immediately in liquid nitrogen and stored away in -80^oC freezer. The competency of the cells was tested each time by transforming a previously confirmed plasmid.

3.3.2.2 Transformation

First, 50 µl competent cells were thawed on ice and 2 µl (≤100 pg) of plasmid of interest was added and gently tapped couple times. Then, this was incubated on ice for 30 minutes, followed by heat shock at 42^{o}C for 45 seconds. After this, it was incubated on ice for another 10 minutes until it was diluted into 200 µl of room temperature LB. Following this, the transformation mix was incubated in a shaker at 37^{o}C for 60 minutes at 250 rpm. Meanwhile, the agar plates were put on the 37^{o}C incubator for warming up. One hour later, the transformation mixture was seeded on two agar plates at 150 µl and 50 µl volumes. These were incubated at 37^{o}C incubator for 16 to 18 hours until single colonies were apparent. These colonies were selected for further growth in larger cultures of LB.

3.3.2.3 Glycerol Stock Preparation

A single colony from plate was picked with a sterile tip and cultured in ~ 5 ml LB with the selectable antibiotics in 50 ml falcon tubes (without exceeding %10 of total volume for proper airing) for 14 to 15 hours at 37^{o}C and 225 rpm. Next day, 500 µl of the culture was inoculated into 500 ml of sterile %50 glycerol solution (at the final ratio of 1:4, Glycerol to LB culture). Finally, the glycerol stocks were frozen and stored at -80^{o}C .

3.3.2.4 Restriction Enzyme Digestion

The plasmid exposed to any kind of experiments methods such as ligation, mutation is digested by corresponding suitable enzyme to confirm to be accuracy of that our interested gene was still inside the interested vector. In this case, our interested gene,

PERK was between EcoR1 and Xho1 restriction site. Approximately, 1000ng of PERK plasmid was digested with EcoR1 and Xho1 restriction enzyme with the corresponding amount of manufacturer's recommendation and then waited for 4 hrs. After that, the samples were run on the variable agarose gel concentration depending on the purpose of the experiment. If it was only for confirmation, % 1 basica agarose gel was used due to our insert and backbone size; 3577 bp and 5400 bp or 5169 bp respectively. However, if it was needed for further process like gel DNA extraction, % 0.5 reducta agarose gel was used to make extraction more purified.

3.3.2.5 Agarose Gel Electrophoresis

DNA samples and PCR products were detected on agarose gel using Hoefer SUB10 Mini Plus submarine electrophoresis system (Holliston, MA, USA) with the help of Hoefer PS300B 300 Volt Power Supply. Gels dissolved and run in 1X TAE buffer were in different agarose concentrations between %0.5-%1 depending on the size of the DNA fragment and the aim of experiment .For DNA gel recovery; DNA products were run on % 0.5 or 0.8 agarose gels. % 1 agarose gels were used in the detection of DNA fragments for molecular cloning. During the preparation of the gel, corresponding amount of agarose was dissolved in 1X TAE buffer and boiled in microwave for couple minutes. After that, the solution put under the hood to cool it down for a while and EtBr was added on with the final concentration of 30 ug/ml before pouring the gel. DNA samples were mixed with 10X bromophenol blue loading dyes before loading into gel. Agarose gels were run at room temperature under around 100-80V voltage for 40 min or 60 min., respectively. Fermentas #SM0241 Gene ruler 100 bp or #SM0311 Gene Ruler 1 kb ladders used as reference point on the gels when the gels were visualized under UV Light.

3.3.2.6 Site Directed Mutagenesis

This method was used in the creation defined mutagen site in DNA molecule described before by PyMOL: M888A and M888G mPERK.Firstly, the completely complementary primer pairs were designed by using http://bioinformatics.org/primerx working very well for single amino acid changes. The desired mutation site in mPERK was put in the middle. The parameters of designed primer pairs condition was like below:

PERK Mouse:

Mutagen Site	Sequence of Primer		T_m	% GC	Length
M888A	F	5'GTATCTGTACATTCAGGCGCAGCT GTGCAGGAAGG 3'	63	54.29	35
	R	5'CCTTCCTGCACAGCTGCGCCTGAA TGTACAGATAC 3'			
M888G	F	5'GTATCTGTACATTCAGGGGCAGCT GTGCAGGAAGG3'	73	54.29	35
	R	5'CCTTCCTGCACAGCTGCCCCTGAA TGTACAGATAC 3'			

Table 3. 3 A list of primers used for site-directed mutagenesis

Site Directed mutagenesis reactions were prepared in 50 µl total volume containing 50 ng DNA. The final volume of primers were 0.4 uM. It was optional was % 3 of DMSO was added into each samples. Phusion Hot Start II, high fidelity DNA polymerase with

proofreading activity (Finnzymes, Finland) was used as reaction enzymes. Reactions started with initial denaturation step at 98^0C for 5 minutes. Then, 25 cycles of amplification reaction was performed at 98^0C 35 seconds, at 63^0C 30 seconds, at 72^0C 5 min (~30 s/kb).After that, ~5 µl of the reaction was run on the gel to see band corresponding to the expected product. After seeing of the band, the rest of reactions was proceed to next step.

3.3.2.7 Dpn1 Digestion

As soon as the confirmation of succession in Site directed mutagenesis, 1 µl of Dpn1 (20 U/ µl) bought from NEB (Ipswich, MA) was added into 50 µl of reaction to get rid of the template DNA since it cut methylated DNA. Then it was incubated at 37^oC for overnight and the reaction was inactivated at 80^oC for 20 minutes. After that, 2 µl of the sample was transformed into competent cells.

3.3.2.8 Gel DNA Extraction

Zymoclean Gel DNA recovery kit was used for pure DNA purification from agarose gel. 50 µl of sample loaded into %0.5 agarose gels and run at 100 volts for 40 minutes. Then, it was cut under UV light and then followed by manufacturer's recommendations. In the end; DNA was dissolved at 10 µl of DNA/RNAase free ddH_2O.

3.3.2.9 Ligation

The plasmids were ligated to the insert (DNA) at 1:7 ratios with the help of T4 ligase enzyme (Fermentas). The amount of buffer and enzyme were determined depending on manufacturer's recommendations.

3.3.2.10 Colony PCR

Single colonies swiped with the tip of pipets from the plates were placed in PCR tubes. .A PCR mixture was prepared including 1 µl of the 5X Phire enzyme buffer, 0.2 µl forward and reverse primers, 0.3 µl DMSO, 0.8 µl $MgCl_2$, 0.2 µl dNTP, 0.2 µl Phire Hot Start Enzyme (Finnzymes) in ddH_2O (total reaction volume was 10 µl). The PCR program used was the same as the molecular cloning PCR since the same primers and enzyme were used here as well.

3.3.2.11 Mini Prep

Invitrogen PureLink Quick Plasmid Miniprep Kit (Carlsbad, CA, USA) and Promega Pure Yield Miniprep System (Fitchburg, Wisconsin, USA) protocols were used according to the manufacturer's recommendations. At the end, the obtained DNA samples were dissolved in 50 µl DNA/RNAase free sterilized water and measured with spectroscopy.

3.3.2.12 Midi Prep

For midiprep cultures, the initial culture was prepared in 1mL of LB and grown for a few hours at 37 ^{o}C and 225 rpm. This initial culture was transferred into 100 ml LB for overnight incubation (the amount of LB was not exceeding %10 of total volume of flask). The QIAGEN Plasmid Midiprep Kit (Hilden, Germany) or Invitrogen (Carlsbad, CA, USA) protocols were followed according to the manufacturer's recommendations. At the end of the protocol the DNA samples were dissolved in 200 µl DNA/RNAase free sterilized water.

3.3.3 Tissue Culture Methods

3.3.3.1 Cell Lines And Growth Conditions Of Cells

The cell lines used in this research were grown in either RPMI or DMEM. 293HEK, $PERK^{-/-}$. Mouse fibroblast was cultured in DMEM. RAW 264.7 (mouse murine macrophage cell lines) were grown in RPMI. DMEM and RPMI mediums for cell culture were complete medium including % 10 fetal bovine serums, %1 L-Glutamine. All cells were placed in incubators at 37^{o} C with % 5 CO_2 concentrations in air. All cells in incubators were regularly checked and changed into a new dishes or plates before they reached to high confluency.

3.3.3.2 Passage Of The Cell Lines

After the medium was sucked out with the help of vacuum, trypsin-EDTA was added into plate or dishes with the variable concentrations. The concentration was determined depending on the surface area of the dish or plate but not exceeding % 10 of total volume. Trypsinized cells were kept in the incubators for few minutes. After that, detached cells were collected in complete medium in 15 ml or 50 ml falcon tubes with serological pipettes. Cells were pipetted up and down. With the determined dilution of collected cells were re-seeded on plates or dishes.

The passage of macrophages was different from other types of cell lines. Instead of trypsinization, they were scraped by a scrapper and then collected with a complete medium in the 15 or 50 ml falcon tubes. Then, they were distributed by pipetting up and down. They were reseeded into plates.

All mediums used in cell passage were pre-warmed by incubating in the water bath at 37^{o}C prior to usage.

3.3.3.3 Thawing The Cells

Stock cell lines in cryovial tubes were transferred from -80^{o}C freezer or liquid nitrogen tank to ice immediately. The vials were incubated in the water bath at 37^{o}C for a couple minutes until completely thawed. 1 ml of pre-heated complete medium was mixed into the vial by pipetting up and down for few times. Meanwhile, 6 ml of pre-heated complete medium was added into t25 flasks. The mixture in the vial was collected by serological pipettes and placed inside the flask. Cells were distributed in the flask by moving the flask back and forth or right and left (but never swirling). After growing for a day, the cells were refreshed with a new medium. The 80% confluent plates were split again.

3.3.3.4 Freezing Of The Cells

Cell stocks were prepared from cells that have reached %70 to 80 confluency in growth plates. First, the medium was sucked out and washed with PBS for 2 twice. The cells were collected after detachment with trypsin-EDTA treatment for 5 minutes a room temperature. For macrophages, detachment was possible through scraping. The collected cells were next centrifuged for 5 minutes at 1000 rpm. In the meantime, the freezing medium was prepared containing % 10 DMSO, % 40 FBS and % 50 medium (DMEM or RPMI, depending on the cell type). The pellet was then resuspended with this freezing medium. For each cell type, 1 ml of the freezing medium was transferred into a single cyrotubes and frozen at -80^{o}C freezer covered by tissue paper in foam boxes. One day later, they were transferred into liquid nitrogen tanks.

3.3.3.5 Transient Transfection Of Cells

The type of transient transfection method was determined depending on the types of cell lines.

The Type of Cell Lines	Method used
HEK293	PEI (Polyethylenimine)
$PERK^{-/-}$ MEFs	NEON Electroporation System http://www.invitrogen.com/site/us/en/home/Products-and-Services/Applications/Cell-Culture/Transfection/Transfection___Selection-Misc/Neon-Transfection-System.html?CID=fl-neon
RAW 264.7	NEON Electroporation System http://www.invitrogen.com/site/us/en/home/Products-and-Services/Applications/Cell-Culture/Transfection/Transfection___Selection-Misc/Neon-Transfection-System.html?CID=fl-neon

Table 3. 4 The various transfection methods used for different cell lines

3.3.3.5.1 Transfection By Using Polyethylenimine

Transfection of plasmids into HEK cell lines was performed by using Polyethylenimine (Cat #23966) from Polysciences. PEI (1ug/µl) was dissolved in %100 absolute EtOH to make a stock solution. In this method, firstly, cells were seeded in 6-well or 12-well plates one day before the transfection at 40% confluency. The next day plates at ~%80-90 confluency were used for transfection. For 12-well 125 µl or for 6 well 250 µl of PEI/DNA mixtures were prepared at 2:1 ratio (w/w), respectively, and mixed gently by tapping. During the incubation of this mix at room temperature for 15 min, a mixture of medium with 375 µl or 750 µl, 2% fetal bovine serum (FBS) in DMEM medium was prepared, respectively. The DNA: PEI mixture was mixed with this serum containing medium to reach the final volume of 500 µl or 750 µl of transfection medium,

respectively. The old medium on cells was replaced with the freshly prepared transfection mixture. Next day the transfection mixture was washed away completely.

3.3.3.5.2Transfection By The Electroporation Method

Transfection of plasmid DNA into mouse embryonic and macrophage cell lines was performed by using NEON Electroporation System from Invitrogen. Firstly, the suitable voltage, pulse width and number for each used cell lines were determined by using 24 well optimization protocols from NEON system itself which includes varying voltage, pulse width and number. The manufacturer's recommendation was also used to get an idea about cell lines' requirements. The condition was like table below:

The cell type	Pulse Voltage (V)	Pulse width (ms)	Pulse Number	Cell Density (cells/ml)	The amount of DNA	Tip Type	The amount of DNA	Tip Type	
MEFs	1050	20	2	$4.5x10^5$	2 µg	10 µl	4 µg	100 µl	DMEM
RAW 264.7	1680	20	1	$3.5x10^6$	2 µg (siRNA: 100 nmol)	10 µl	4 µg	100 µl	RPMI

Table 3. 5 The electroporation conditions optimized for different cell types.

Firstly, cells were seeded in 96 mm plate one day before transfection so that the confluency was ~%70-80 on transfection day. Next day cells were collected into a tube and washed with PBS at 500 rpm for 4 minutes. After that, The cell pellet was dissolved in R buffer so that the volume was 10 µl R buffer for each well for 10 µl tip and 100 µl

R buffer for each well for 100 µl tip then followed by the manufacturer's recommendations. The added volume of DNA into R buffer for each well was not exceeding %10 percent of total volume R buffer for each well.

3.3.3.6 Treatment of Cells

Cells were firstly plated to corresponding plates according to the experiment type. One day after seeding, the mediums were removed and the treatments were done in complete mediums. Treatment medium including chemicals such as thapsigargin, palmitate, palmitoleic acids, LPS, ATP analogs etc. were prepared freshly from stocks aliquot before. Complete mediums containing same amount of solvent were prepared as an control samples such as water, EtOH or DMSO. The parameters for chemicals were listed on table next page:

The name of chemicals	The amount of chemicals (Molarity)	The solvent used for treatments	The used solvent for dissolving	Incubation time	The used chemicals for control samples
Thapsigargin (Tg)	300 uM	Complete medium	DMSO	4 hours	DMSO
Palmitate	1000 uM	Only medium containing % 5 fatty acid free BSA and heating to 55-60^{o}C for 15 minutes	EtOH	9 hours	EtOH and only medium containing % 3 fatty acid free BSA
Palmitoleic acid	1000 uM	Only medium containing % 5 fatty acid free BSA	In liquid form	9 hours	only medium containing % 3 fatty acid free BSA
NaPP1	10 uM	DMSO	DMSO	6 hrs. 2 hrs. before Tg Treatment and also 4 hrs. during Tg treatment	DMSO
LPS	40 ng/ml	DNA/RNAase free water	Complete media	2 hrs. before PAL or PAO treatment	ddH_2O

Table 3. 6 The different treatment conditions in cell

3.3.3.7 PERK siRNA Treatment In Macrophages

Transient transfection by electroporation was performed with 100 nmol of siRNA like explained in section 3.3.3.5.2 under the conditions in Table 3.4. After transfection, the cells were incubated for 24 hours without change of complete media and then proceed to further step.

3.3.4 Total Protein Extraction From Cultured Cells

Cells in wells or dishes were put on ice for 5 minutes with the addition of corresponding and sufficient amount of lysis buffer (RIPA or Phospho-Lysis Buffer) on the cells and then scraped with the tip of 1000 ml pipette tip by collecting in eppendorf tubes that are kept on ice. Thereafter, lyzed cells were centrifuged at 14.000 g for 10 minutes at + 4^{o}C and supernatants are collected that are kept on ice. After that, 5X SDS added to samples by making 1X SDS concentration in total volume. After the vortex of mixture, the samples were boiled at 90^{o} C for 5 minutes, vortex and loaded on to SDS-page protein gels.

3.3.5 Western Blot

In first step, concentrations of proteins were calculated by using Bradford Assay. All samples were measured at 595 nm wavelength in spectrophotometer. Meanwhile, the standard curve were calculated with varying concentrations of already known protein concentration of bovine serum albumin (BSA) and used as a reference for calculation of proteins with unknown concentrations. The calculation was done by putting the absorbance values in equation.

After quantification of protein concentrations of samples, all samples were prepared for loading into gel by addition of 5X SDS Loading Dye so that the loading buffer would be 1X of total volume of samples.80 to 100 μg of proteins were loaded into gel relied on the type of experiments. Afterward, the combination of sample and loading buffer were heated at 90^{o}C for 15 minutes before loading into gel.

In this case, BIO RAD Mini Tans Blot protein electrophoresis system was used for running the sample on gels with the help of the method called Tris-glycine SDS-Polyacrylamide Gel Electrophoresis and transferring the protein samples onto membrane. Gel concentrations for Tris-glycine SDS-Polyacrylamide Gel were chosen depending on the size of the interested protein but generally %10 for running gel and %5 for resolving gel were used. The samples were run on gel at 80V voltage for ~30 minutes (until they enter into running gel) and then at 120 V for ~90 minutes until the color of loading dye disappear. After running, proteins were transferred onto Thermo Scientific PVDF Transfer membranes with wet transfer protocol but before that, PVDF membrane was activated inside methanol for 15 seconds. Transfer Buffer was prepared 1X from 5X stocks with %20 methanol in ddH_2O. After all materials were soaked into transfer buffer, wet transfer sandwich were prepared including 1 sponge,1 whatman filter paper, gel, membrane,1 whatman filter paper and 1 sponge ,respectively. Transfer was done for 120 minutes at 95 V voltages. During transfer, western blot tank was either kept in cold room and also the ice pocket supplied with system was put inside tank.

After transfer was end, membranes were neutralized in TBS-T for 5 minutes and then immersed into blocking solution with % 3 milk powder or % 5 BSA in 1X TBS-Tween

for 1 hrs. at RT or o/night at $+4^0$C on a shaker .After that, primary antibodies were prepared in same blocking solution used previous step while membranes were washed in TBT-T and then incubated for 1 hrs. at RT or o/night at $+4^0$C with corresponding dilutions on a shaker. Thereby, membranes were washed in 1X TBS-T four times for 5, 15, 5, 5 minutes at RT on a shaker. Afterward, horseradish peroxidase (HRP) conjugated antibodies; anti mouse or anti rabbit were used as secondary antibodies depending on used primary antibodies. After incubation for 1 hrs, at RT, they were washed in TBS-T four times for 5, 15, 5, 5 minutes on a shaker; again. Detection were performed using chemiluminescent detection kits such as ECL + and ECL Prime + (Amersham, UK) according to manufacturer's recommendations and the intensity of expected signal on membrane. In the end, X-ray films were exposed to the emitted chemiluminescent light from the reaction of HRP and developed in X-ray developer. Exposure time was determined relied on the detection reagent, the specific antibody used against the protein of interest and also the expected signal intensity of interested protein.

3.3.6 Total RNA Extraction From Cultured Cells

RNA from cell lines were extracted by using Ambion Trizol Reagent (Cat#15596, Invitrogen, Grand Island, NY, USA) according to manufacturer's protocol. In the end, RNA was dissolved in 50 µl DNA/RNAase free water per 1 ml of Trizol reagent.

3.3.7 First Strand c-DNA Synthesis

First strand cDNAs were synthesized by using Fermentas RevertAid cDNA synthesis Kit (GMBH Fermentas, Germany). The manufacturer's instructions were followed. 0.5

ug RNA was used for cDNA synthesis. The oligo $(dT)_{18}$ primer was added into RNA since it primed cDNA synthesis from mRNA with poly (A) tails. Then, DNA/RNAase free water was added up to 6 µl. After that, the sample was mixed gently, centrifuged and incubated at 65^{o}C for 5 minutes. Thereafter, it was chilled on ice and spinned down (optional step on manufacturer's instructions if The RNA template is GC rich or contain secondary structures).Subsequent to addition of 2 µl reaction buffer, 1 µl dNTP mix,0.5 µl RNAase inhibitor,0.5 µl Revert aid M-Mul V Reverse Transcriptase (200u/µl) and DNA/RNAase free water up to 10 µl , samples were mixed gently and centrifuged. Afterwards, they were incubated 60 min at 42^{o}C followed by heat activation at 70^{o}C for 5 minutes.

3.3.8 Expression Analysis Of A Gene By Quantative RT-PCR

3.3.8.1 Determination Of Primer Efficiency For Q-PCR Primers

The primers used in q-PCR were taken from published articles or the groups who had already have annealing temperature and cycle optimizations for primers. That's why the optimization protocol for cycles and melting temperature were not performed but efficiencies for the primers were calculated before the actual expression analysis by making serial dilution of cDNA pool forming by mixing all samples. The primer sequences and some parameters were shown on the table on next page:

The name of Primer (For mouse)	Forward	Reverse	T_m	The size of Product (bp)	The Reference Article and Groups	The primer efficiencies
TNFalpha	CATCTTCTCAAA ATTCGAGTGACA A	TGGGAGTAGA CAAGGTACAA CCC	58-60	175	Stig S. Jakobsen, A. Larsen2, M. Stoltenberg, J.M. Bruun3, K. Soballe (2007). Effects of As-Cast and Wrought Cobalt-Chrome-Molybdenum and Titanium-Aluminium-Vanadium Alloys on Cytokine Gene Expression And Proteın Secretion In J774a.1 Macrophages. *European Cells and Materials* Vol. 14.pages 45-55.	2,06
B actin	TTCGTTGCCGGTC CACACCC	GCTTTGCACAT GCCGGAGCC	59	90	Primer blast http://www.ncbi.nlm.nih.gov/ tools/primerblast/primertool. cgi?ctg_time=1344076728&j ob_key=JSID_01_156810_1 30.14.18.128_9002	2,1
IL6	GAGGATACCAC TCCCAACAGACC	AAGTGCATCA TCGTTGTTCAT ACA	58–60	141	Bing Sun, Nan Qi, Tao Shang, Hui Wu, Tingting Deng, and Daishu Han (2010). Sertoli Cell-Initiated Testicular Innate Immune Response through Toll-Like Receptor-3 Activation Is Negatively Regulated by Tyro3, Axl, and Mer Receptors. *Endocrinology*, June 2010, 151(6):2886–2897.	2,10
iNOS	CAGCTGGGCTGT ACAAACCTT	CATTGGAAGT GAAGCGTTTC G	58–60	95	Eun-Mi Park, MD, PhD; Sunghee Cho, PhD; Kelly Frys, BS; Gianfranco Racchumi, BS; Ping Zhou, PhD; Josef Anrather, DVM; Costantino Iadecola, MD (2004). Interaction Between Inducible Nitric Oxide Synthase and Poly(ADP-ribose) Polymerase in Focal Ischemic Brain Injury. *Stroke.*;35:2896-2901	1,95

Table 3. 7 A list of q-PCR primers used: q-PCR conditions and primer efficiencies.

3.3.8.2 Expression analysis of genes by quantative RT-PCR (q-PCR)

Quantitative PCR analysis was performed by using Inceptra Cycler 9660. DyNAmo HS Syber Green q-PCR kit from Finnzymes was used for q-PCR experiments followed by manufacturer's protocol. The amount of 2x DyNAmo master mix was changed into 7 ul instead of 10 ul. The reactions were prepared in 20 ul total volume containing 1 ul cDNA sample. The reactions started with initial denaturation step at 95^{o}C for10 minutes. Then, 40 cycles of amplification reaction was done at 95^{o} 30 seconds, at 60^{o}C 30 seconds, at 72^{o}C 30 seconds with final extension at 72^{o}C 5 minutes. After that, melting temperature step was followed at 95^{o}C 20 seconds ended with one more step for annealing and extension time to make sure all samples were double stranded in case they were run on agarose gel for further steps. Expression levels of the genes were calculated depending on the Ct value of the amplification of the interested gene and reference gene (β actin or 18S) and efficiencies of primer used. Relative quantification was statistically performed with the help of formula (Primer efficiency)$^{-\Delta\Delta Ct}$ where ΔΔCt means ΔCt (sample)- ΔCt (calibrator) and was the Ct of the target gene subtracted from the *C*T of the housekeeping gene and Ct (threshold cycle) was the intersection between an amplification curve and a threshold line. All experiments were performed in duplicates of each sample.

4. RESULTS

4.1 Generation of the Gatekeeper Mutations of PERK

PERK is also known as the eukaryotic translation initiation factor 2 alpha kinase 3 (Eif2ak3), PEK, PKR-like endoplasmic reticulum kinase; pancreatic eIF2-alpha kinase. It is one of the four mammalian serine-threonine kinases that phosphorylate eIF2α. PERK's main function is to regulate translation initiation. There are no other known isoforms of PERK and it is conserved between species such as human, chimpanzee, dog, cow, rat, chicken, zebra fish, fruit fly, and C.elegans.

PERK's NCBI gene ID number is 13666. PERK is located on chromosome 6, NC_000072.6 and mapped to the region of 6 C1; 6 with the neighboring Immunoglobulin kappa constant (Igkc) gene at upstream and forkhead box I3 (Foxi3) at downstream.

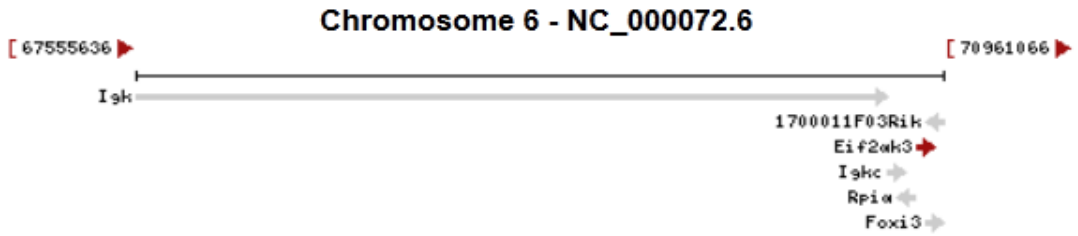

Figure 4. 1 Genomic context of PERK gene in mus musculus

PERK gene is sequestered between Immunoglobulin kappa constant (Igkc) gene and forkhead box I3 (Foxi3) on chromosome 6.

Figure 4. 2 Genomic region and transcripts of PERK

The genomic region containing the PERK transcript

Figure 4. 3 Domain structure of PERK

PERK has two distinct domains: the ER luminal domain in the N' terminal, carrying a signal peptide sensitive to molecular chaperones, and the kinase domain near its C' terminal, residing in the cytoplasmic side of the ER membrane.

There is no identified crystal structure for PERK. However, the crystal structure of the homologous eIF2α protein kinase, GCN2, was resolved by Padyana et al. in 2005. This structure was used for guidance in identification of the correct gatekeeping amino acid in the PERK ATP binding pocket. Furthermore, since the ATP binding pockets of kinases are highly conserved and there are crystal structures and gatekeeper residues identified for some of them, these were also aligned against PERK's ATP binding pocket. These alignments were made with the help of clustalW2 and PyMol software and the results can are shown below.

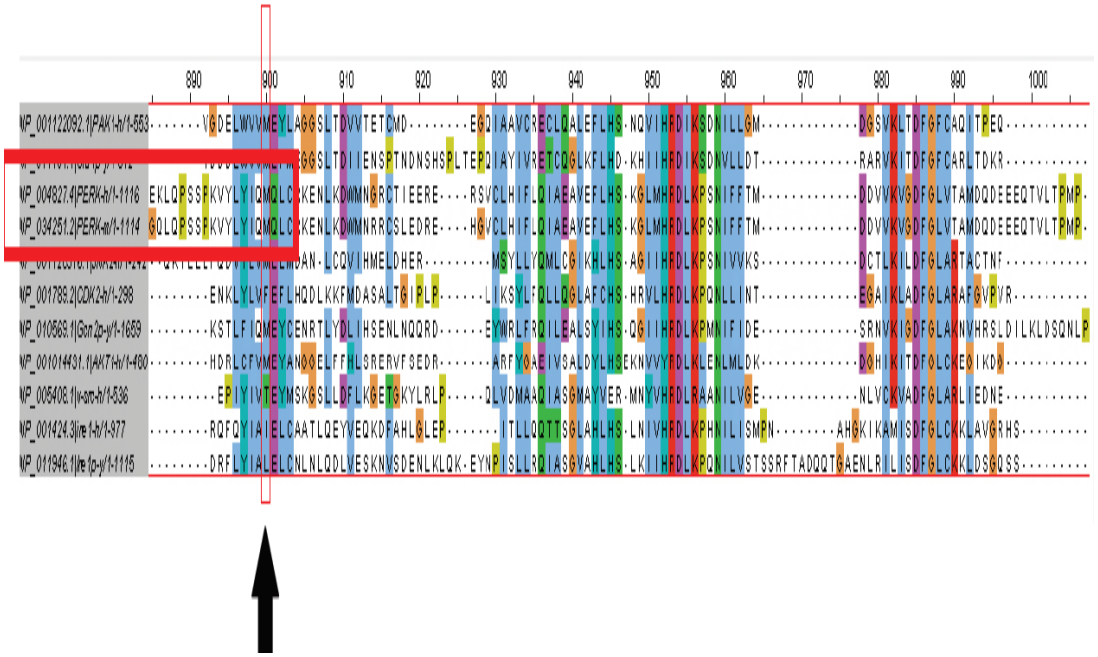

Figure 4. 4 Multiple sequence alignments of several kinases whose ATP binding pocket and the gatekeeper residue in these pockets have been identified (human PAK-1, yeast Cla4p, human JNK2, human CDK2) with yeast and human Ire1 and mouse and human PERK by using Clustal W2.

PERK sequence was aligned with other kinases using Clustal W2. Red vertical rectangle depicted by a thick black arrow represents the potential gatekeeper residues in all of the aligned kinases that can potentially interact with ATP. In PERK, two potential sites were identified: Methionine at 888th amino acid site and glutamine at 889th amino acid site.

After this alignment, two potential gatekeeper residues were identified for mutagenesis: Methionine (M) at 888th amino acids or Glutamine (Q) at 889th amino acids. Then, 3D predicted structure of the kinase domain of PERK was created by Swiss Model program to visualize these potential gatekeeper residues. The results are shown below:

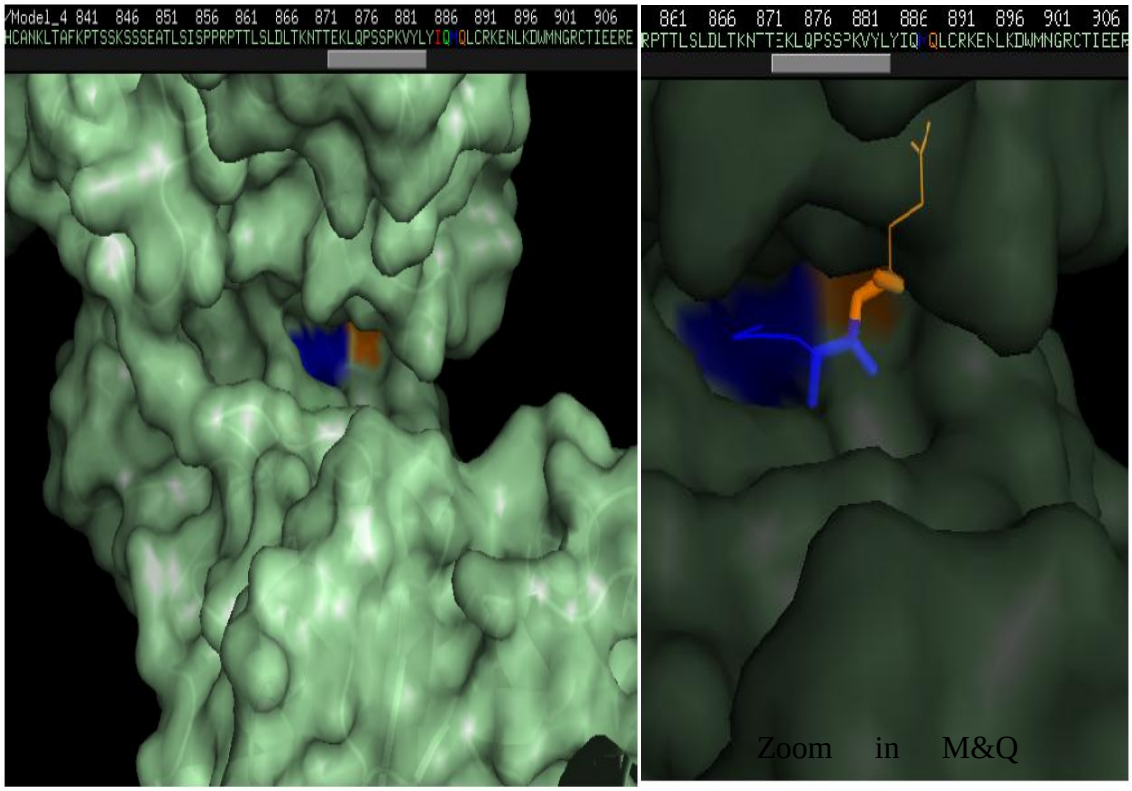

Figure 4. 5 Predicted 3D structure of a PERK fragment from 586 to 1077 by Swiss Model.

Methionine (M) at 888th amino acid site is blue and Glutamic Acid (Q) at 889th amino acid site is orange.

Based on our modeling the methionine and glutamic acid, exposed to surface, seemed like good candidates with which ATP could interact in the ATP binding cavity. For further confirmation , PERK was aligned with the other kinases such as GCN2 or TgCDPK1 whose crystal structures were resolved in complex with ATP or 1NM-PP1 (ATP analog) (at 2.00 Å resolution (PDBID:1ZY5); Padyaneet.al., 2005; and http://www.rcsb.org/pdb/explore/explore.do?structureId=1ZY5) in complex with ATP or 1NM-PP1 (ATP analog).

Figure 4. 6 The hypothetical 3D model of PERK aligned in PyMoL15 with GCN2 (in 2.00 Å resolution (PDBI ID: 1ZY5) and Padyana et al., 2005 and http://www.rcsb.org/pdb/explore/explore.do?structureId=1ZY5).

Light pink represent GCN2 and red represents PERK. DARK blue shows methionine site that hypothetically interacts with ATP (shown in light blue).

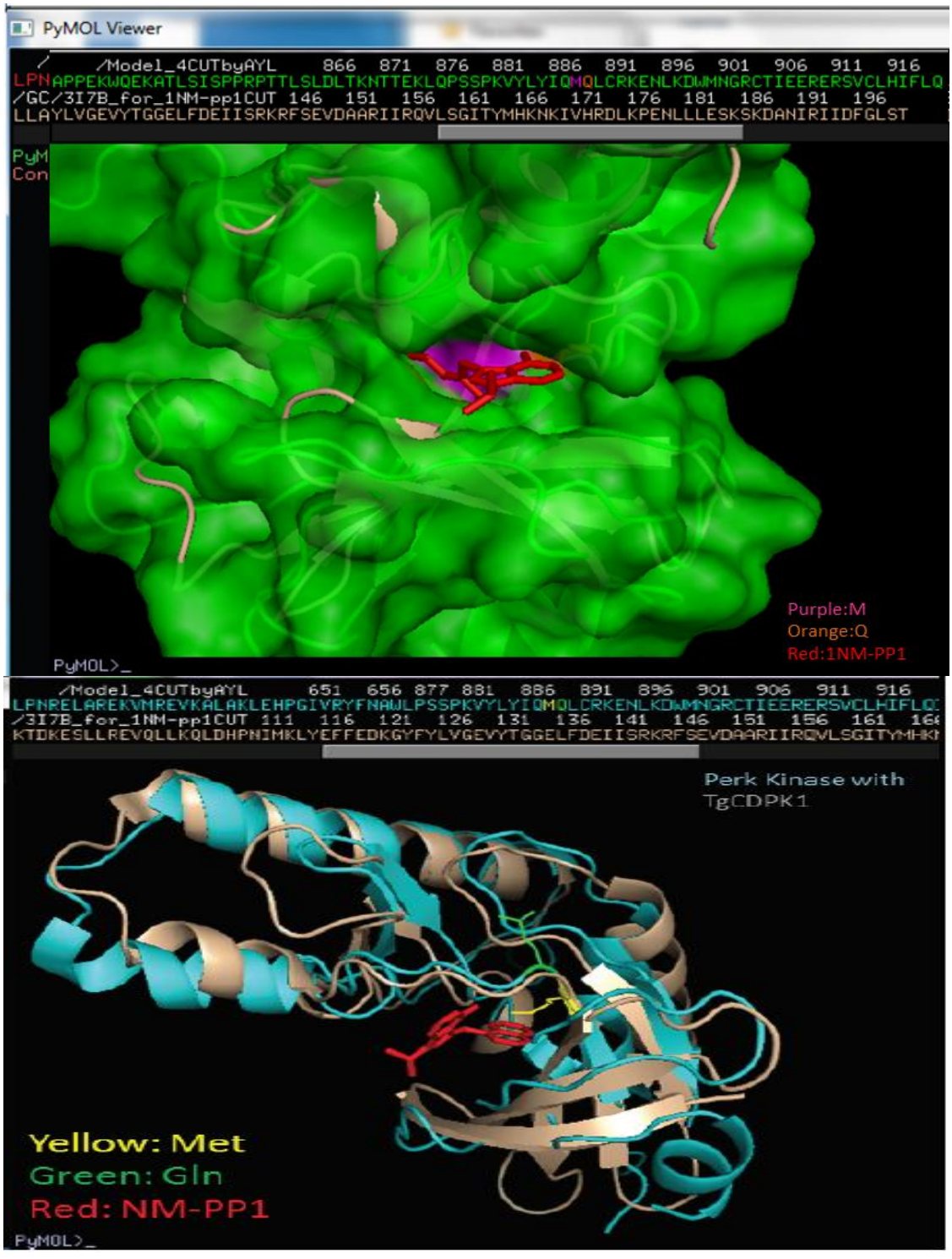

Figure 4. 7 The hypothetical 3D model of PERK in PyMol 15 with TgCDPK1 in a complex with 1NM-PP1 complex (in 2.04 Å resolution (PDB ID: 3I79) and Kayode et al., 2010 and http://www.rcsb.org/pdb/explore/explore.do?structureId=3I79).

Grey represents TgCDPKI and light blue represents PERK. Yellow and Green show methionine and glutamine site, respectively, which can potentially interact with 1NM-PP1 shown red.

According to these results, the potential gatekeeper sites to mutate appeared to be the methionine or glutamine in 888th and 889th amino acids, respectively. The PERK fragments from the wild type and PERK mutants (M888A, M888G, Q888A and Q889G were visualized with 1NM-PP1 complex in order to observe the interaction points between them. The results are shown below:

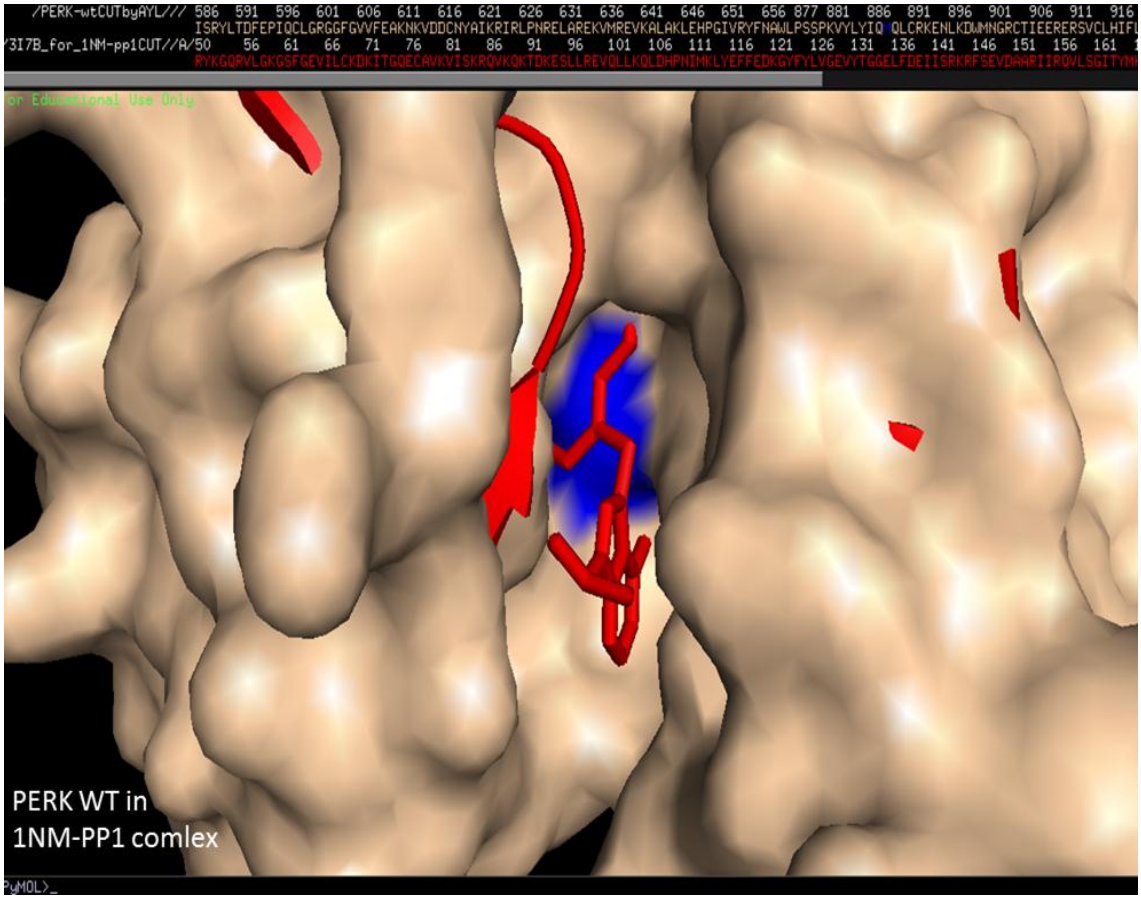

Figure 4. 8 PERK WT in complex with 1NM-PP1

Blue is representative of potential interaction site with 1NM-PP1 shown in red**.**

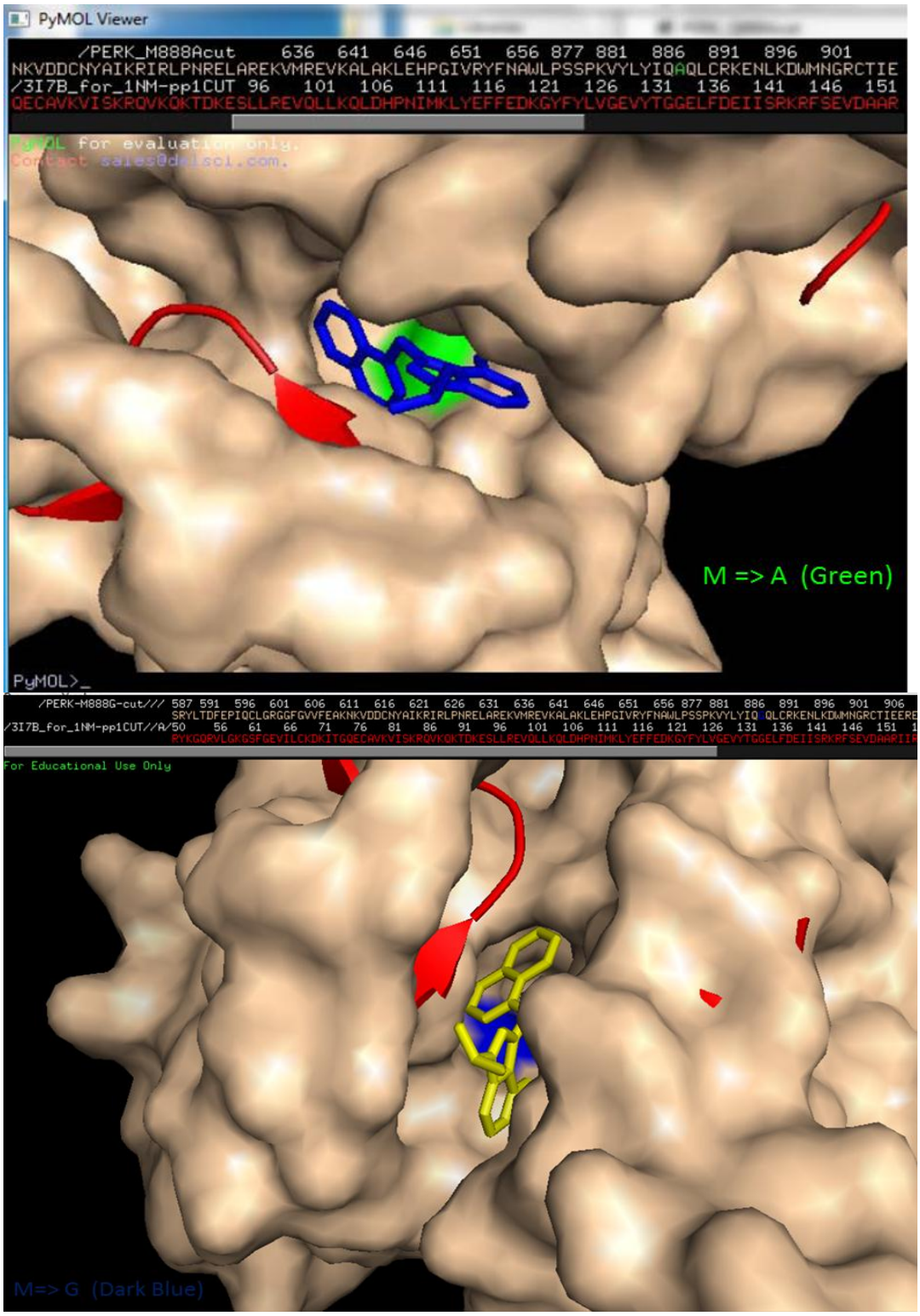

Figure 4. 9 PERK M888G in complex with 1NM-PP1

In first graph, blue represent 1NM-PP1 and green depicts the alanine site mutated from methionine at the 888th amino acid in PERK. In the second graph, yellow represents 1NM-PP1 and blue shows the glycine site mutated from methionine at 889th amino acid site in PERK.

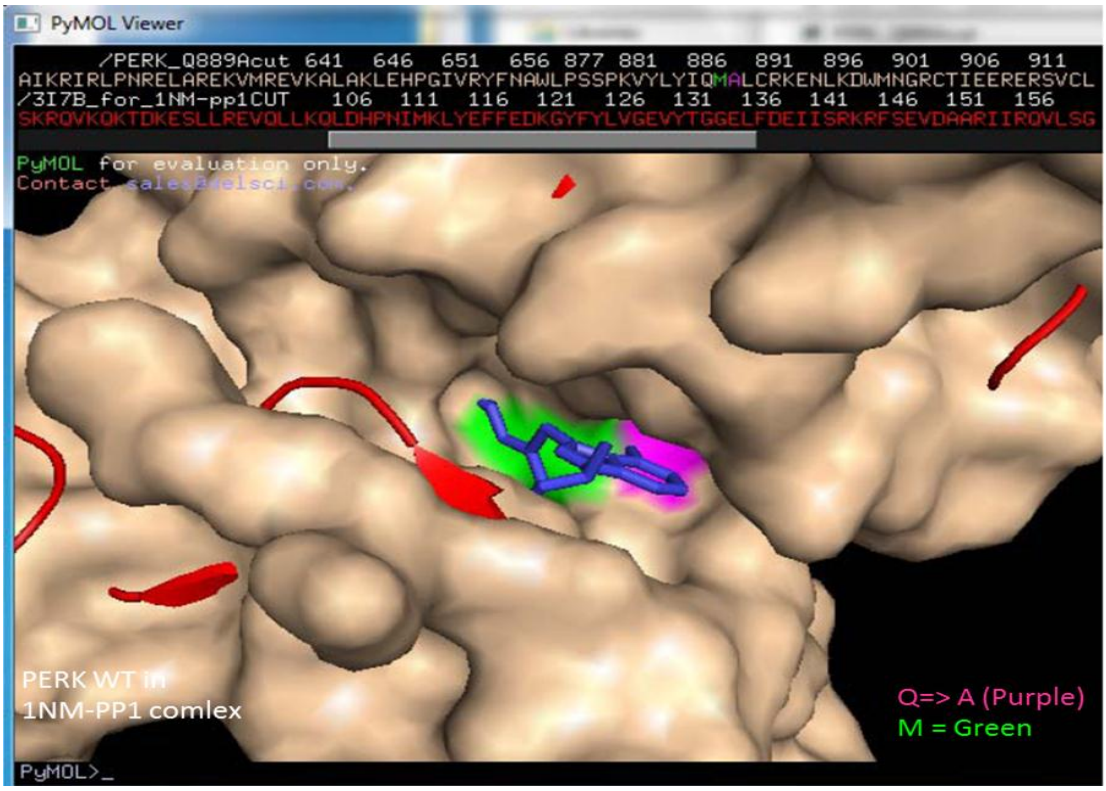

Figure 4. 10 PERK Q889A in complex with 1NM-PP1

Blue represents 1NM-PP1 and purple shows the alanine site mutated from glutamine at the 889th amino acid in PERK.

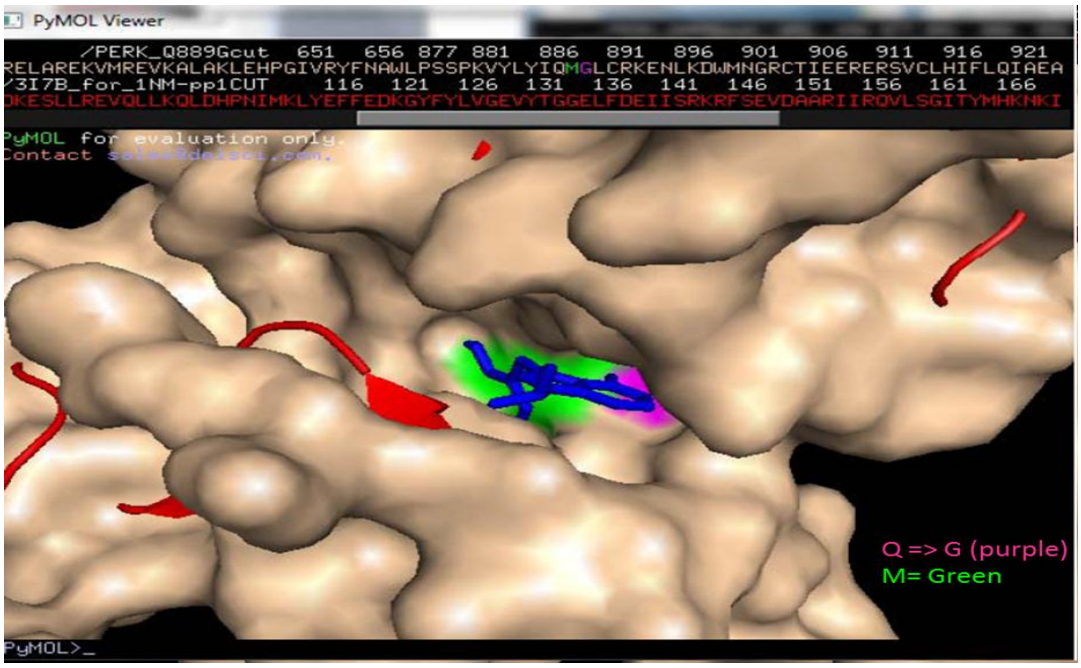

Figure 4. 11 PERK Q889G in complex with 1NM-PP1

Blue represents 1NM-PP1 and purple depicts the glycine site mutated from glutamine at 889th amino acid site in PERK**.**

Figure 4.8 – 11 show the alignment of the hypothetical 3D structures of PERK WT, M888A and M889G in a complex with 1NM-PP1. The ATP analog 1NM-PP1 does not fit the WT ATP binding cavity. The best fit occurs between the gatekeeper mutation site at the methionine in 888th amino acid and not glutamine in the 889th amino acid site. Therefore, methionine 888 site was converted into two different small amino acids, alanine and glycine, to create the enlarged ATP pocket for PERK.

4.2 Molecular Cloning and Site Directed Mutagenesis For mPERK

Plasmid 21814: PERK 1: PERK.WT.9E10.pCDNA, deposited by David Ron, was obtained from Add Gene. The PERK cDNA were inserted between the EcoR1 (on 5'site) and Xho1 (on 3' site) and tagged with C-terminal myc (9E10) epitope tag. The PERK cDNA also included a small part of its own 5'UTR, but not the 3'UTR. The open reading frame (ORF) of PERK started approximately 200 base pairs (bp) after EcoR1 restriction site. The insert size was 3577bp (including the 5' UTR region) while the vector backbone was 4756 bp. The map of plasmid can be seen below:

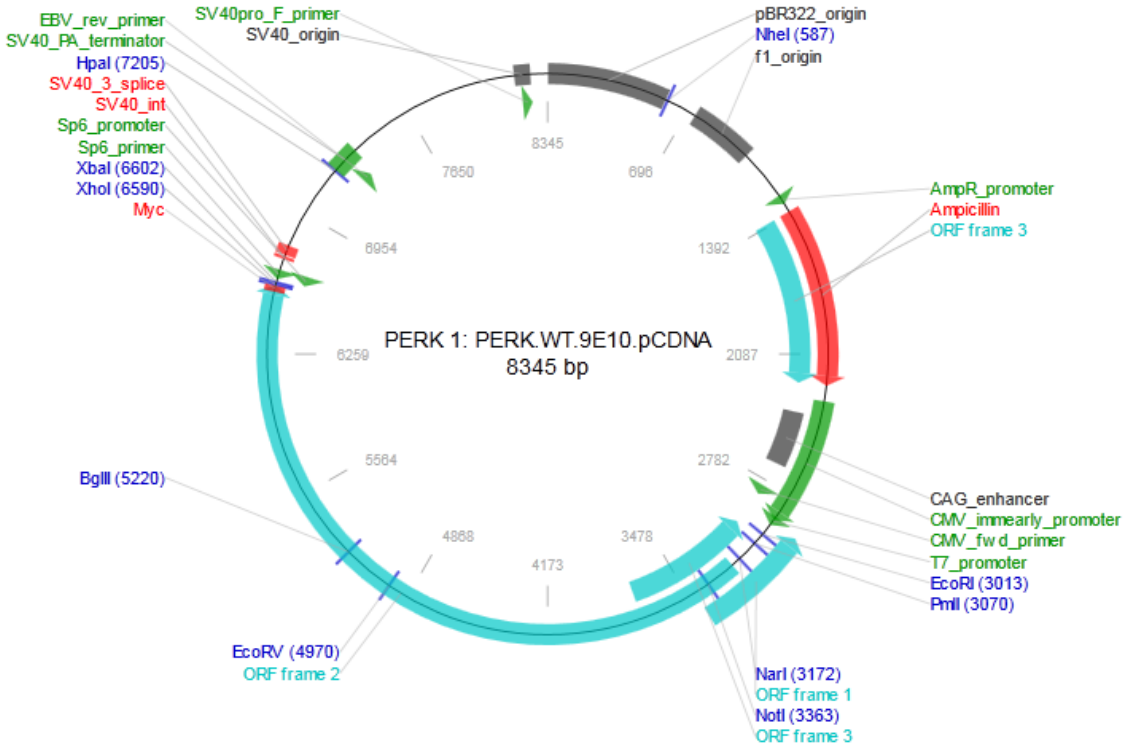

Figure 4. 12 The map of PERK plasmid bought from Add Gene.

The PERK cDNA was inserted between the EcoRI and Xho1 sites and was epitope tagged with c-myc at the c terminal. The plasmid number 21814 was purchased from Add Gene.

After restriction digest and gel confirmation of the size of the insert and the plasmid, site directed mutagenesis PCR was performed using the PERK cDNA as the template. Following the mutagenesis protocol, the mutations were confirmed via sequencing. The sequencing results also confirmed that there were no additional mutations that could alter the protein's function (figure 4.13, 4.14).

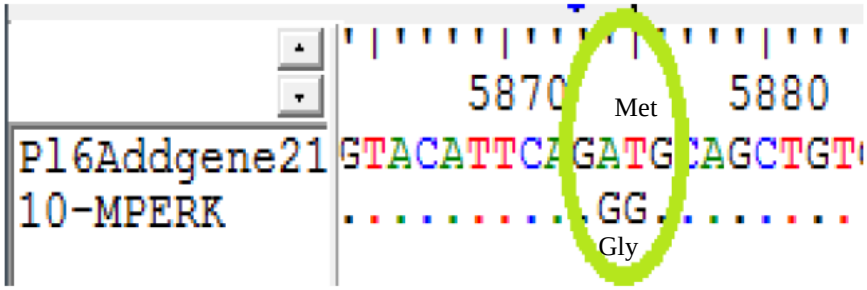

Figure 4. 13 The sequencing results for mPERK M888G mutation.

According to sequencing results, Methionine at 888th amino acid site representing ATG was successfully converted into glycine representing GGG without any unexpected mutations at any site.

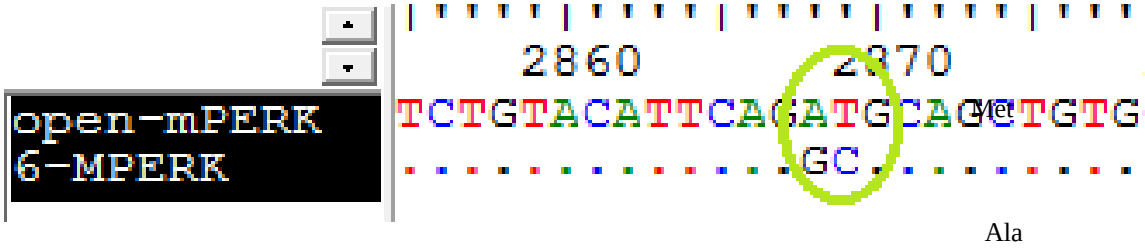

Figure 4. 14 The sequencing results for mPERK M888A mutation.

According to sequencing results, Methionine at 888th amino acid site representing ATG was successfully converted into alanine representing GCG without additional mutations at any site.

Because the vector backbone did not contain a gene encoding a selection marker (drug resistance) the PERK mutants were next sub cloned into appropriate mammalian expression vectors with a puromycin resistance gene. Two cloning primers were designed, one of each ending with am EcoR1 and Xho1 restriction enzymes. The cloning strategy at first excluded the 5' UTR region of PERK. The insert was cloned into FLAG-epitope and neomycin-resistance gene containing pcDNA5F plasmids (derived from Invitrogen pcDNA 3.1). The insert was also cloned into pBABEPuro (Addgene, Plasmid # 1764) using restriction digest and ligation strategy. The puromycin

resistant PERK plasmids were used to create stable cell lines from the PERK$^{-/-}$ mouse fibroblast since this cell lines is already resistant to neomycin.

4.3 Expression of Wild Type and Analog Sensitive Kinase Allele Mutant (ASKA) of PERK in Mammalian Cells

There are only a few known substrates of the UPR kinases other than themselves. In addition to auto phosphorylation, PERK phosphorylates the "eukaryotic initiation factor 2 alpha" (eiF2a) and Nrf2 (Harding et al., 1999; Shiet al., 1998). A major goal in this study was to create the ASKA PERK mutant that could later be used to identify novel PERK substrates. Therefore, after cloning and successful mutagenesis of the PERK gatekeeper residues in the ATP binding cavity, the cellular expression of these new constructs was investigated. First, the expression was observed in transiently transfected HEK293A cells, since this cell lines could be easily transfected with Polyethylanimine. The c-myc tagged PERK wild type (WT) and the PERK mutants PERK-M888A and -M888G protein expression levels were evaluated in Western blots. Importantly, the PERK WT and mutants in c-myc containing original vectors also included part of PERK's UTR.

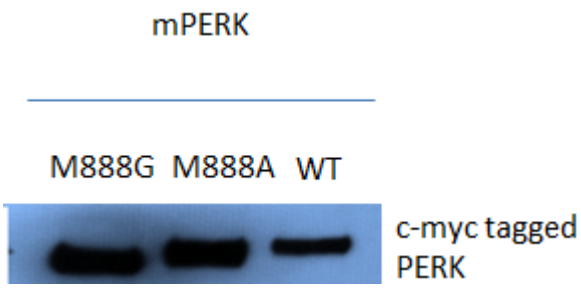

Figure 4. 15 PERK expression in HEK293 cells.

Western Blot lysates from HEK cell lines transfected with 2 µg of mutant and wild type of mPERK plasmid DNA are detected by c-myc antibody.

As seen in figure 4.12, mouse PERK (mPERK) is expressed at significantly higher levels. As a result mPERK was used in subsequent cell culture experiments.

Next, I determined whether the PERK gatekeeper mutants could be inhibited with NaPP1 and is suitable for downstream chemical-genetic applications. The PERK$^{-/-}$ mouse embryonic fibroblast cells (MEFs, a generous gift of Prof. Dr. Gokhan Hotamisligil (Harvard University), were transfected with the plasmids containing mPERK-WT, PERK-M888A and PERK-M888G. 4 hours post-electroporation the cells were treated with NaPP1 for an additional 20 hours. After a total of 24 hours post-electroporation, the cells were treated with 300 nM thapsigargin, an inhibitor of SERCA pumps and an ER stress inducer, for 4 more hours. The cells were flash frozen in liquid nitrogen or directly lyzed in phospholysis buffer for analysis of PERK autophosphorylation by Western Blot. The results are shown in figures 4.16-17.

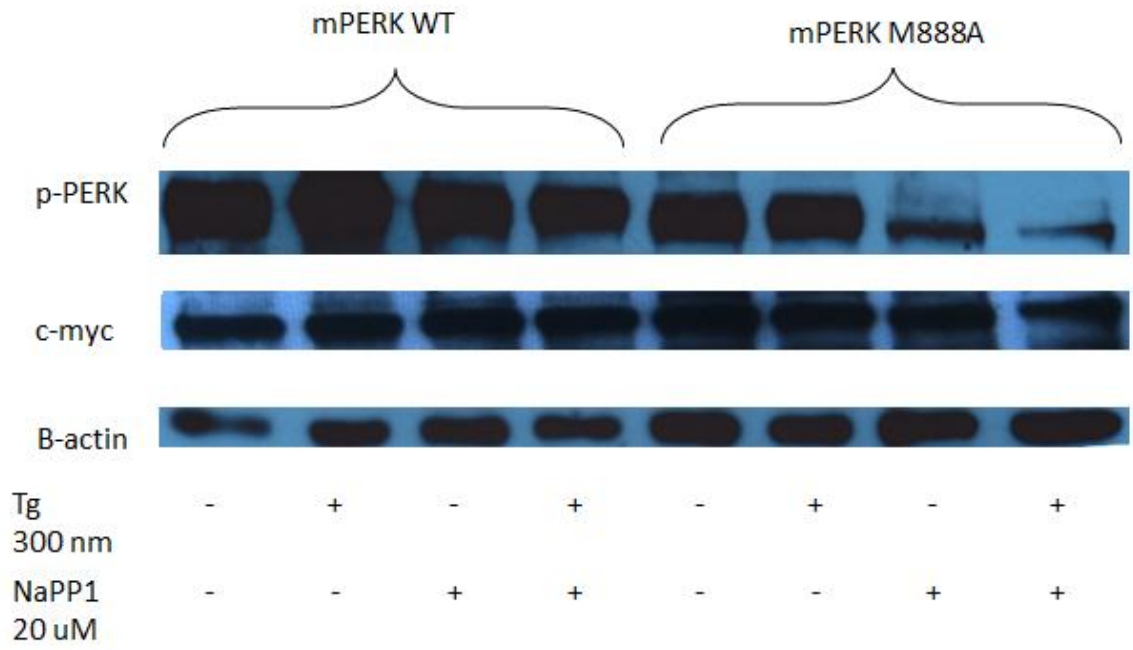

Figure 4. 16 NaPP1 inhibits ASKA mutant (M888A) mPERK but not wild type mPERK expressed in PERK$^{-/-}$ MEFs.

Western Blot analysis of cell lysates from PERK $^{-/-}$ MEFs that were transfected with 4µg of mutant or wild type of mPERK plasmid DNA. Then, the cells were treated with NaPP1, an ATP analog inhibitor 4 hours after transfection and incubated overnight. Afterwards, cells were treated with 300nM thapsigargin (Tg) for 4 hours. PERK phosphorylation, c-myc and b-actin expression were detected by Western blots using specific antibodies against these proteins. c-myc expression represents the expression level for recombinant PERK proteins and β actin was used as a loading control**.**

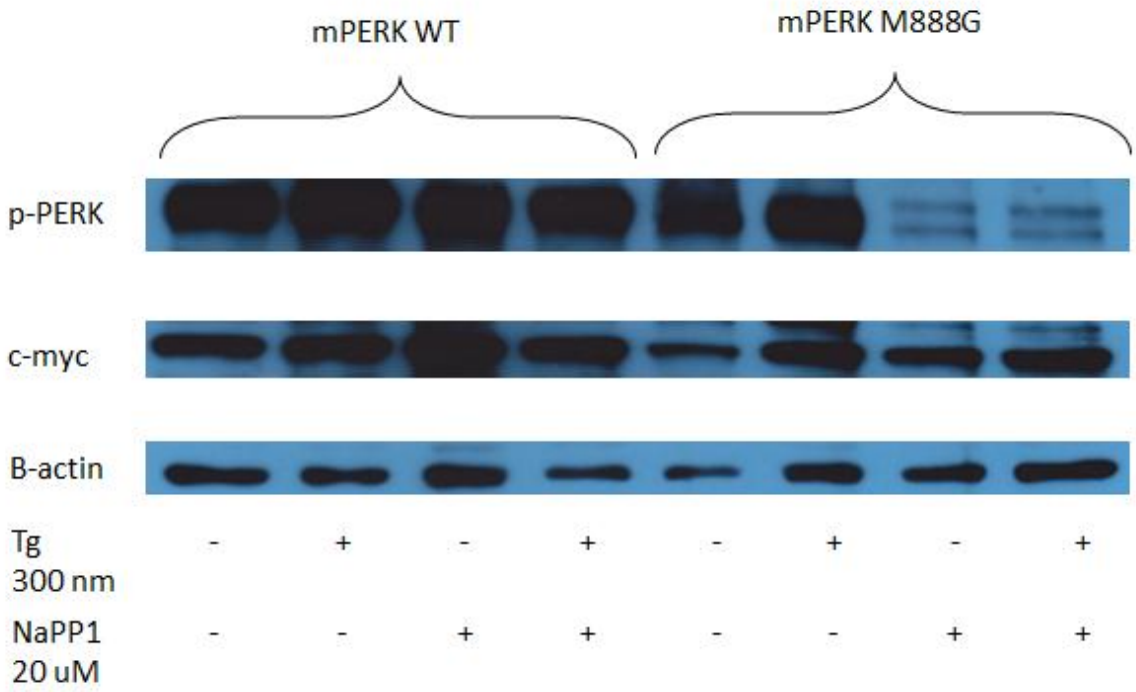

Figure 4. 17 NaPP1 inhibits ASKA mutant (M888G) of mPERK but not wild type mPERK expressed in PERK$^{-/-}$MEFs.

Western Blot analysis of cell lysates from PERK $^{-/-}$ MEFs that were transfected with 4µg of mutant or wild type of mPERK plasmid DNA. Then, the cells were treated with NaPP1, an ATP analog inhibitor 4 hours after transfection and incubated overnight. Afterwards, cells were treated with 300nM thapsigargin (Tg) for 4 hours. PERK phosphorylation, c-myc and b-actin expression were detected by Western blots using specific antibodies against these proteins. c-,myc expression represents the expression level for recombinant PERK proteins and β actin was used as a loading control.

According to the western blot results, the overexpression of PERK-WT or the mutants in the PERK$^{-/-}$ MEF cell lines lead to their auto-phosphorylation, but the kinase activity was less in mPERK_M888G when compared to mPERK_M888A. In mutant PERK (M888G and M888A) expressing MEFs, PERK phosphorylation was almost completely abolished upon NaPP1 treatment at the baseline and also during thapsigargin treatment in cells. On the other hand, there was no reduction in the phosphor transfer activity of the wild type mPERK with NaPP1 treatment (Figure 4.16, 4.17).

4.4 The Knock down of PERK Expression in Macrophages By siRNA

In order to observe the direct contribution of PERK to lipotoxic ER stress-associated inflammation, the siRNA-mediated silencing of PERK expression was attempting testing various different siRNAs specifically designed against mPERK sequence in stressed macrophages. Only one of the tested mPERK siRNAs could effectively reduce PERK phosphorylation in stressed macrophages.

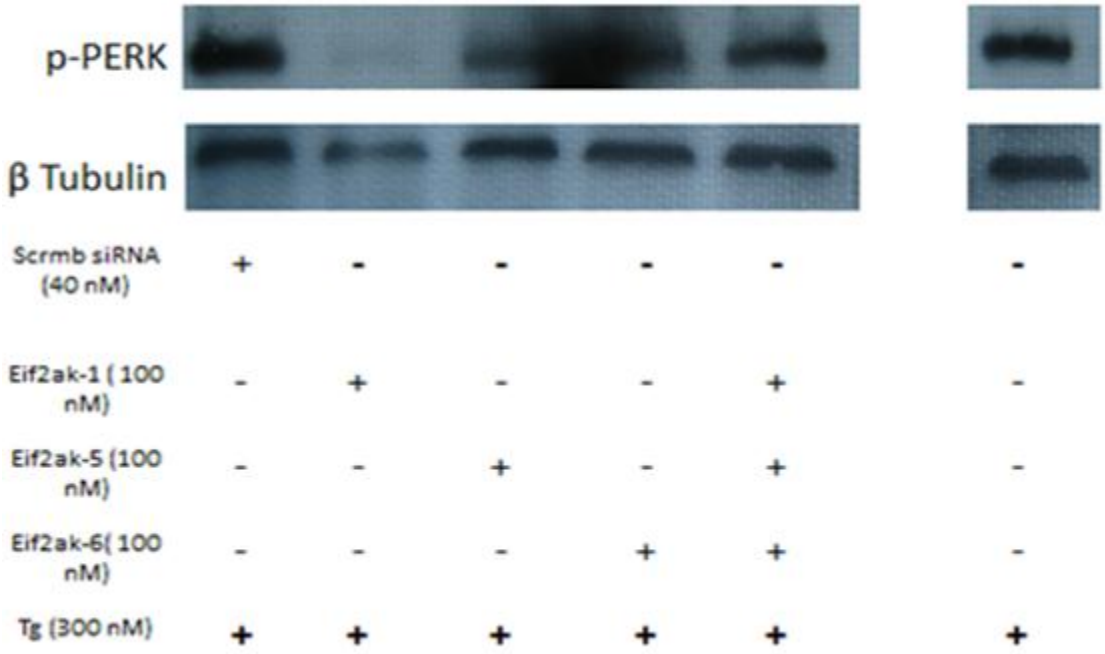

Figure 4. 18 siRNA mediated silencing of mPERK in macrophages.

The Raw 264.7 cell lines transfected with siRNA and thapsigargin is administrated 4 hours later. Western blot protein lysates were detected with p-PERK antibody and β tubulin as an equal control.

As seen figure 4.18, treatment with a specific siRNA for PERK (EIF2AK3_1 from Qiagen) leads to significant reduction in the phosphorylated PERK levels induced by thapsigargin.

4.5 The Loss of Function of PERK Activity during Lipid Induced ER Stress and Inflammation in Macrophages

After confirming the successful reduction in the expression levels of PERK protein with specific siRNA (EIF2AK3_1 from Qiagen), I examined its impact on palmitate alone and palmitate induced ER stress and inflammation in macrophages, in previously described experimental conditions[18, 32, 158]. In addition to stimulating ER stress with palmitate, I also used palmitate together with lipopolysaccharide (LPS) as a prerequisite to the activation of the inflammasome and an inducer of pro-inflammatory response[14].

Figure 4. 19 siRNA mediated silencing of mPERK expression under lipotoxic ER stress conditions

Raw 264.7 cell lines transfected with 100 nM of siRNA were treated with only PAL or LPS combined PAL after overnight incubation. Western blot protein lysates were detected with p-PERK antibody and β tubulin as an equal control.

In these experiments, I observed phosphorylation of PERK is increased by palmitate treatment further when the cells are pre-stimulated with lipopolysaccharide (LPS).

Earlier studies showed that the phosphorylation of IRE1 and its downstream target JNK are not affected in PERK knockout adipocytes (Jiao P. et al., 2011). Here, I also examined IRE1 expression and phosphorylation in my experimental conditions with transient silencing of PERK using specific siRNA. As seen in Figure 4.20, the suppression of PERK levels in macrophages did not alter JNK phosphorylation but may have had an effect on IRE1, though in the protein levels in the last two lanes may have been less in this specific experiment. Hence, I also examined IRE-1 induced XBP1 splicing under the same experimental conditions by semi-quantative PCR was investigated and saw no reduction induced by PERK siRNA treatment (Figure 4.21).

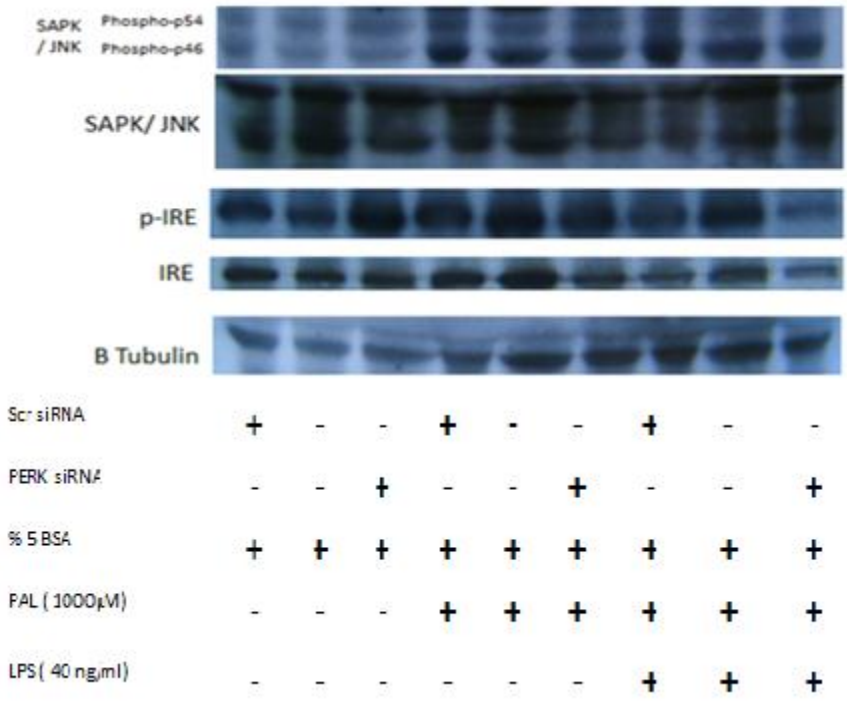

Figure 4. 20 Phosphorylation of IRE1 and JNK in macrophages treated with PERK siRNA.

100 nM of PERK siRNA and scrambled siRNA was electroporated into macrophages. 24 hours later, the cells were pre-stimulated with 40 ng/ml of lipopolysaccharide (LPS) for 2 hours. After this, the cells were incubated 1000 µM palmitate (PA) dissolved in % 5 fatty acid free bovine serum albumin (BSA) in complete RPMI media for an additional 9 hours. Phosphorylated forms and total JNK and IRE1 were detected using specific antibodies against these proteins in western blots.

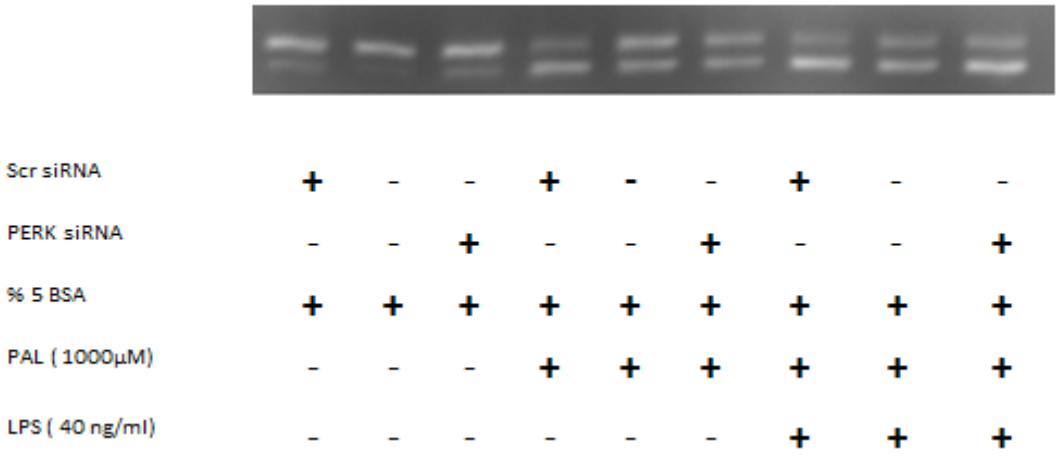

Figure 4. 21 The changes in spliced and unspliced XBP-1 by semi quantative PCR in the absence of PERK

The semi quantative PCR products done with use of XBP1 primers were loaded into % 3 agarose gel and run for 1 hour. Higher band represents unspliced XBP-1 and lower band represents spliced XBP1 (lacking 26 bp).

As seen in figure 4.21, there is no reduction in spliced XBP-1 levels induced by palmitate or palmitate and LPS in macrophages treated with PERK siRNA compared to scrambled RNA treated or untreated macrophages.

Experimental induction of UPR via free cholesterol or high amounts of free fatty acids has been shown to increase the expression of pro-inflammatory molecules such as Il-8, Il-6, MCP-1 and TNFalpha and iNOS[82, 149]. In 2011, Jiao and colleagues also showed that TNFalpha expression is increased, but not IL6, in the PERK knock out adipocytes[66]. To gain insight into the role of PERK in lipid induced inflammation in macrophages, PERK expression was silenced by PERK-specific siRNA treatment in macrophages, the cells were stimulated with palmitate or palmitate and LPS, and the mRNA levels of TNFalpha and iNOS were detected with q-PCR.

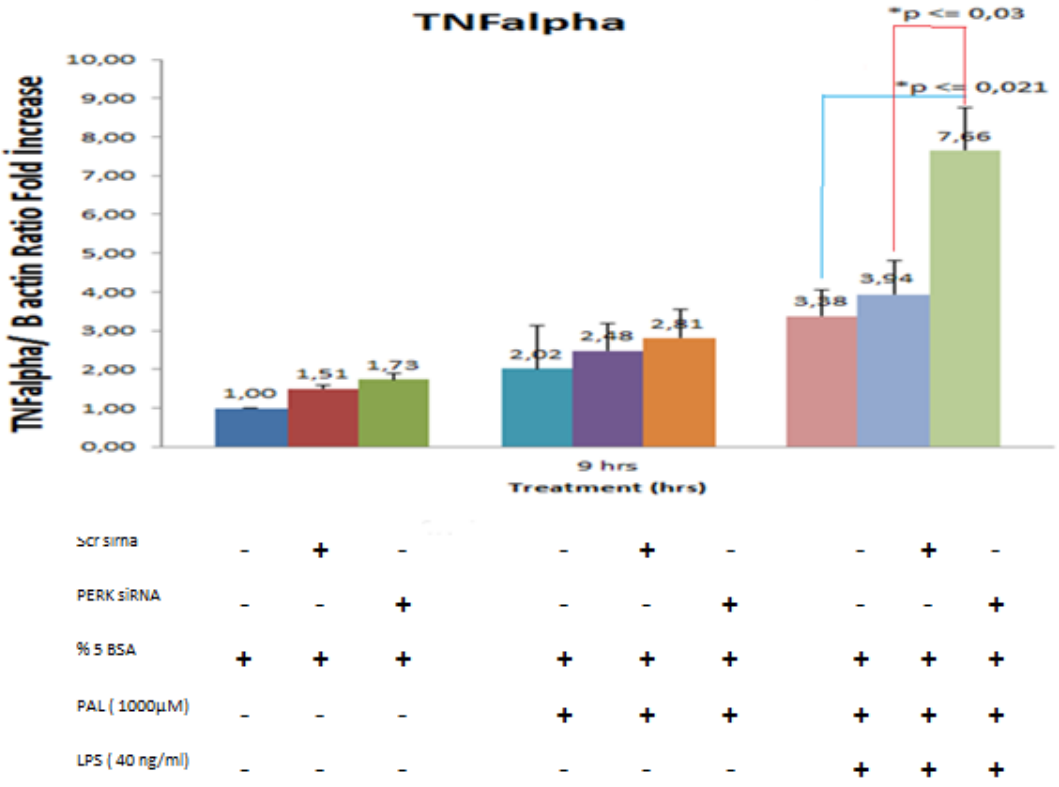
TNFalpha
*p <= 0,03
*p <= 0,021
TNFalpha/ B actin Ratio Fold Increase
10,00
9,00
8,00
7,00
6,00
5,00
4,00
3,00
2,00
1,00
0,00
1,00
1,51
1,73
2,02
2,48
2,81
3,38
3,94
7,66
9 hrs
Treatment (hrs)
Scr sirna - + - - + - - + -
PERK siRNA - - + - - + - - +
% 5 BSA + + + + + + + + +
PAL (1000µM) - - - + + + + + +
LPS (40 ng/ml) - - - - - - + + +

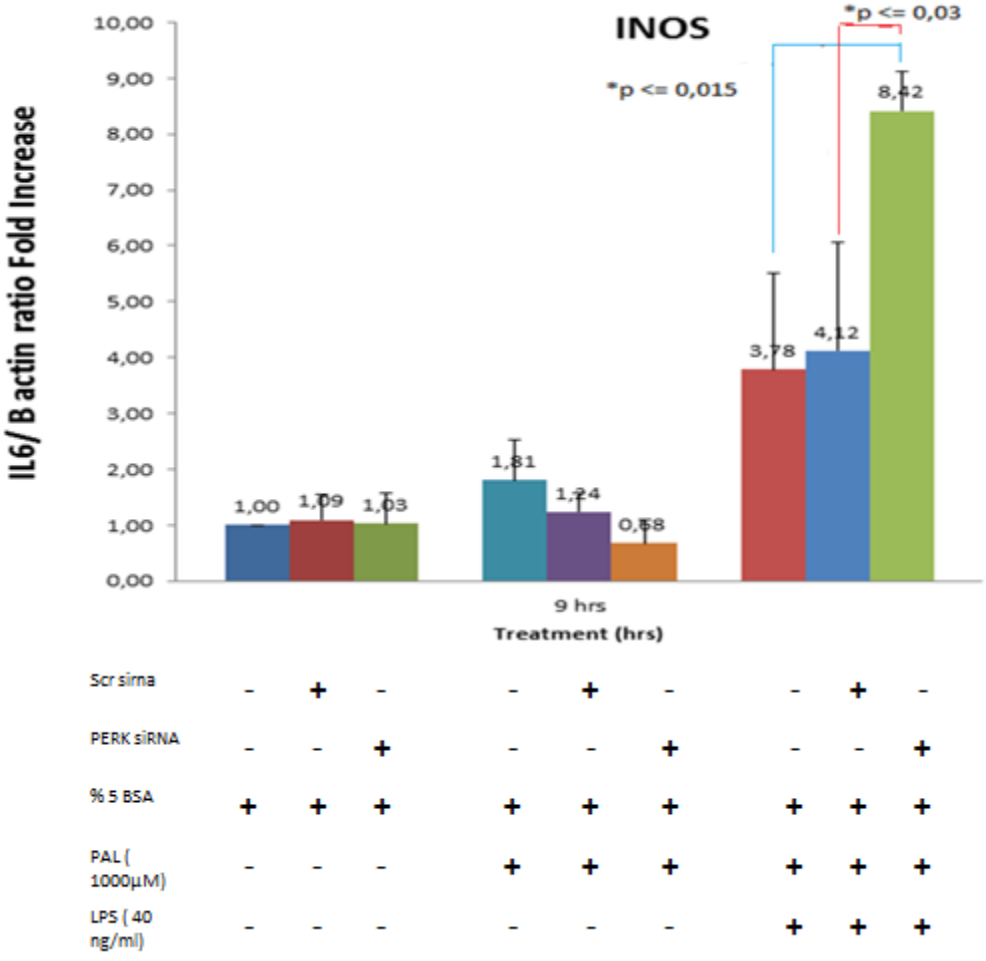
INOS
*p <= 0,03
*p <= 0,015
IL6/ B actin ratio Fold Increase
10,00
9,00
8,00
7,00
6,00
5,00
4,00
3,00
2,00
1,00
0,00
1,00
1,09
1,03
1,81
1,24
0,68
3,78
4,12
8,42
9 hrs
Treatment (hrs)
Scr sirna - + - - + - - + -
PERK siRNA - - + - - + - - +
% 5 BSA + + + + + + + + +
PAL (1000µM) - - - + + + + + +
LPS (40 ng/ml) - - - - - - + + +

Figure 4. 22 The changes in lipid-induced cytokine expression in the absence of PERK

Reduction of PERK levels was achieved by transfection of PERK-specific siRNA to macrophages. The cells were treated with only LPS or LPS combined PAL TNFalpha and iNOS expression was determined by qPCR. The values depicted in the graphs represent the mean of three experiments and the standard deviations (SD) were shown on the bars. Student T-test was performed to determine significance (* P <0.05).

These results imply that suppression of PERK activity leads to further induction of iNOS and TNFalpha upon stressing macrophages with palmitate and LPS pre-stimulation.

4.6 Palmitate-LPS Induced Inflammation and Its Reduction with Palmitoleic Acid

Saturated fatty acid (such as palmitate) or cholesterol administration to cells is known to lead to ER stress and cytotoxicity[18, 32, 158]. On the other hand, unsaturated fatty acids particularly palmitoleate, can significantly alleviate ER stress under palmitate or cholesterol induced ER stress[176, 177 and 178]. Additionally, lipopolysaccharide stimulates the pro-inflammatory responses in macrophages[14]. When used together, LPS and PA, induce marked ER stress and inflammation in macrophages. In this part of my thesis studies, I attempted to reduce lipid-induced ER stress and associated inflammation by treating macrophages with palmitoleate.

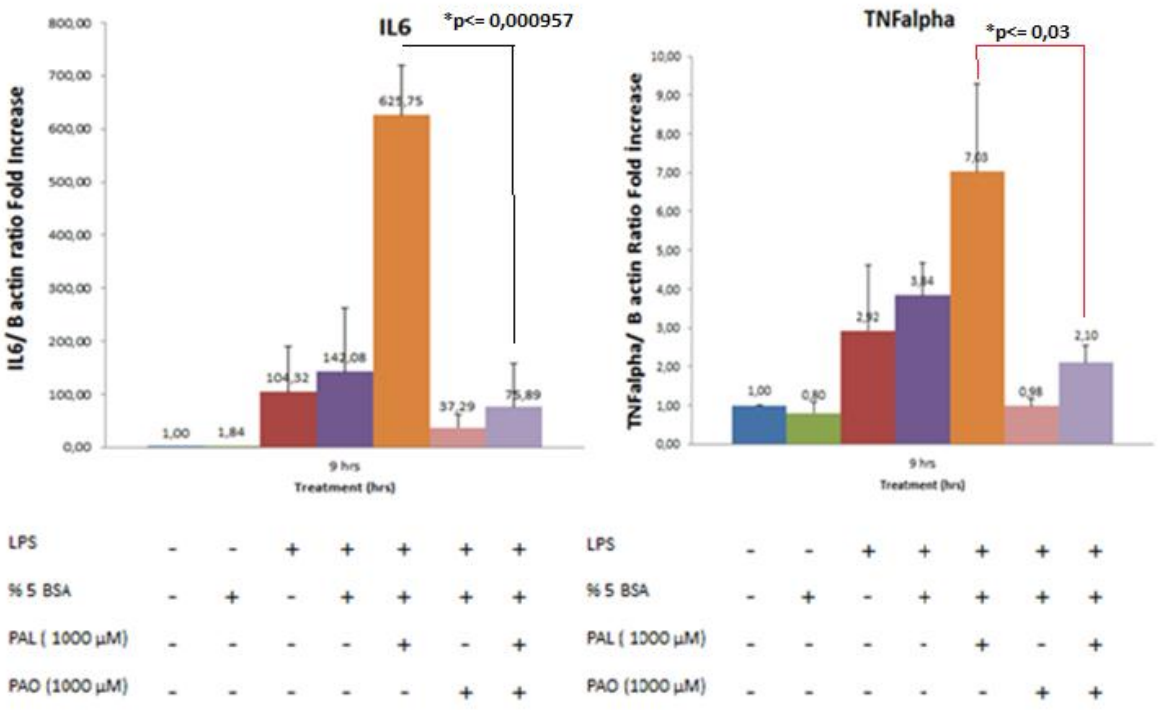

Figure 4. 23 Reduction of lipotoxic ER stress-associated inflammation in macrophages by palmitoleic acid treatment

Macrophages were treated with 1000 µM of palmitate and 40 ng/ml of LPS (pre-stimulation) and the expression of TNFalpha and IL6 were determined by q-PCR. The values represent means valued from three different experiments. Standard deviations (SD) is shown and student T-test was performed for significance (* P <0.05).

As seen in figure 4.23, LPS or LPS with palmitate stimulated inflammation, which was blocked by palmitoleate treatment. Unexpectedly, an unsaturated fatty acid, palmitoleate significantly masked the effect of LPS on inflammation; it's mechanism worthy of further investigation.

6. DISCUSSION AND CONCLUSION

The main focus of my thesis study was the characterization of PERK in the context of lipid induced inflammation in macrophages. For this purpose, two experimental tools, a specific siRNA against PERK and an ATP analog sensitized mutant of PERK were created to block PERK's activity without affecting the two other UPR pathways.

6.1 **Creating An ATP Analog Sensitive Mutant Of PERK For Chemical Genetic Approaches**

Chemical genetics approach can be coupled to the discovery of novel kinase targets that could be developed into future therapeutics. The chemical-genetic strategy can also be used to modulate the activities protein kinases during signal transduction events[13]. This strategy, a semisynthetic reaction scheme, requires the use of labeled or detectable bulky ATP analogs for thio-phosphorylation, followed by alkylation of this bond, which generates a semisynthetic epitope on the modified substrates that can be recognized by a monoclonal, anti-thiophosphate specific antibody[2]. In this thesis, I adopted this chemical-genetic approach to create a PERK mutant that could be modulated by bulky ATP analogs and inhibitors.

PERK[136] is an important kinase that phosphorylates eukaryotic initiation factor 2 alpha leading to global translation arrest during unresolved ER stress[51, 52]. ER stress can be the result of many signals such as glucose deprivation, aberrant calcium regulation, viral infection and hypoxia[70, 128]. In addition to autophosphorylating itself, PERK has two other known substrates, Nrf2[27] and eIF2α[52]. In this thesis, I attempted to generate PERK

mutant that can be monospecifically activated or inhibited via bulky ATP analogs. This mutant can also be coupled to identify the full range of PERK substrates during lipid-induced stress.

In the beginning of my thesis, I identified the potential mutagenic sites for the gatekeeper residue of PERK (M888A and M88G) that would allow the fitting of a bulky ATP analog into the ATP binding cavity of PERK (Figure 4.4-4.11). A significant observation during this study was that these mutations conserved the kinase activity of PERK (Figure 4.16 and 4.17). Furthermore, I observed the mutant PERK's activity, but not wild type PERK activity, could be controlled by a cell permeable bulky ATP analog such as NaPP1[2] (Figure 4-15-17). This result demonstrated the specificity of the created mutation for accepting the bulky ATP inhibitor. In future studies, PERK kinase assay using the bulky ATP analog (N6benzylATPgammaS) can be coupled to proteomics for the identification of novel PERK substrates during lipotoxic stress.

6.2 Characterization Of PERK's Role In Lipid-Induced Inflammation

Previous studies showed that ER stress may be linked to inflammation through various mechanisms including activation of JNK by IRE-1, NF-κB through PERK and IRE1[28, 62], the production of ROS, the generation of nitric oxide that activates Nrf2/Keap complex and phosphorylation of Nrf2 by PERK[27, 42]. ER stress through these and other mechanisms can lead to induction of pro-inflammatory genes such as TNF alpha, IL6, IL1-B and IL18. The excess of lipids or their metabolites impact both the metabolic and immune functions through mechanisms not clearly understood[81, 175]. In recent studies, saturated fatty acids such as palmitate, but not unsaturated ones, were shown to induce ER stress and inflammatory response in human islets[179], β cells[4], mouse 3T3-L1 cells

and rat primary pre-adipocytes[46] and liver cells[158]. Since metabolic stress generated by lipids can cause the activation of all three arms of UPR, the individual contribution of the PERK arm to inflammation is not clear. To evaluate the specific contribution of PERK to lipid-induced inflammation I identified specific siRNA sequences that can block PERK's activity upon transfection into macrophages. Using this tool, the expression of PERK was silenced in macrophages during lipid induced ER stress and the changes in the expression of some cytokines' levels, including TNF alpha and iNOS, were analyzed (Figure 4.22). The outcomes of these studies showed that the expression of PERK has a direct effect on expression of proinflammatory cytokines such as TNF alpha and iNOS induced by saturated fatty acids in macrophages. In 2011, Jiao and et al. had unexpectedly observed an increase of TNF alpha levels and the phosphorylation of JNK in PERK-deficient adipocytes[66]. However, PERK-deficient adipocytes exhibited a converse reduction in IL6 production in the same conditions. The increase in cytokines may be due to an induction in IKKβ, since Jiao et al. also observed the increased phosphorylation of IKKβ with FFAs in the same cells. Based on these results, PERK dampens IKKβ activity which is associated with TNFalpha increase. It appears that the absence of PERK worsens inflammation but the changes in other pro-inflammatory cytokines need to be examined for a generalized view. In this thesis study, I showed that PERK can directly suppress inflammation, particularly iNOS levels.

Furthermore, I examined whether the absence of PERK activates the other arms of UPR, in particularly IRE1 that has been shown to be involved in inflammation[57, 58]. A published work showed that IRE1's phosphorylation is not increased by the absence of PERK, at least in adipocytes[66]. There was no further increase in either the phosphorylation of IRE-1 and JNK or the splicing of XBP-1 upon silencing of PERK

with siRNA, demonstrating the induction of cytokine production and iNOS levels are independent of counter-up regulation of the IRE-1 arm (Figure 4.20 and 4.21).

6.3 **Reduction of lipid induced ER-stress and inflammation by palmitoleate**

Previous studies showed that saturated free fatty acids can induce lipoapoptosis via ER stress[158]. Moreover, it has been showed that mutated conductance regulator Cl-channel (CFTR) resulting in cystic fibrosis induced ER stress and inflammation but this also was increased by chronic bacterial infection[180]. Several agonists of Toll-like receptor (TLR) 2,4 and 5 might stimulate XBP-1 splicing demonstrating that activation of TLR by pathogens might have an synergistic interaction with ER stress followed by enhancing the secretion of pro inflammatory cytokines[94, 180]. The outcome of my thesis studies support this notion, since I observed there was significant increase in the pro-inflammatory output in combined LPS and palmitate treatment when compared to LPS or palmitate alone (Figure 4-23). Meanwhile unsaturated fatty acids such as palmitoleate can significantly reduce acute ER stress stimulated by the excess of saturated fatty acids or cholesterol[32, 176, 177 and 178]. One possibility for this protection may be due to monounsaturated fatty acids ability to promote adaptive mechanisms such as storing the excess fatty acids as triglyceride[81, 176]. In fact, it has been observed that ER stress is stimulated in cells and mice through the genetic inhibition of conversion of saturated acids to monounsaturated acids[181, 182]. Studies recently demonstrated that palmitoleate is able to reduce the potential destructive effects of saturated fatty acids, such as insulin resistance, in vivo[183, 184]. In this thesis study, I observed that palmitoleate can completely block lipid-induced ER stress and inflammation in macrophages. Unexpectedly, I also observed that palmitoleate can prevent LPS-induced and combined

LPS and lipid induced inflammation. These results show that the protective mechanisms of this promising, palmitoleate involve prevention of lipid induced inflammation. Palmitoleate may become a potent anti-inflammatory and metabolic enhancing therapeutic targeting obesity and related disorders such as insulin resistance, diabetes and atherosclerosis.

Lipid induced macrophage inflammation plays an important role in the pathogenesis of metabolic diseases. Previous studies conducted in obese mouse models detected the cross-talk between adipocytes and macrophages in adipose tissues leads to local and systemic insulin resistance through the activation of Jun N-terminal kinase (JNK), inhibitor of κB kinase (IKKβ) via secretion of free fatty acids and pro-inflammatory cytokines such as TNFalpa, IL6 and IL1β [144, 185]. Furthermore, other studies showed that Kupffer cells, a major bone-derived macrophage cell type in liver induce insulin resistance in the neighboring hepatocytes through the secretion of inflammatory cytokines[5, 130]. Also, in atherosclerosis, macrophages recruited to the lesions play a central role in the maladaptive and non-resolving inflammatory response leading to plaque progression and rupture[97]. Taken together, lipid induced macrophage inflammation is very important in the regulation of metabolism, so the studies about the elucidation of molecular mechanism of this type of inflammation offer promise for the discovery of new therapeutics against metabolic and inflammatory diseases.

In conclusion, the experimental tools created in this thesis study lead to important observations that deepens our understanding of PERK's role in inflammatory and metabolic diseases. The results of my thesis study demonstrate for the first time a direct role of PERK in lipid-induced inflammation in macrophages. Furthermore, the

chemical-genetic mutant of PERK that was created in this study can become a useful tool to identify the full spectrum of PERK substrates in lipid-induced stress in future studies and guide the development of novel and specific new therapeutics against metabolic and inflammatory diseases

7. FUTURE PERSPECTIVES

First, this thesis study identified two mutants of PERK suitable for the chemical-genetics approach, which allows the temporal and specific control of the mutant of PERK activity when combined with permeable bulky ATP analogs or inhibitors. The expression of this mutant of PERK in macrophages leads to its spontaneous activation and a gain of function for PERK, which can be inhibited by NaPP1 addition to cells. Second, I identified specific siRNA species that can reduce PERK expression in macrophages. Using these siRNAs, I studied the loss of function for PERK in lipid induced inflammation. These complementary experimental strategies can be used to understand the direct role of PERK in lipid induced inflammation. The outcome of my studies showed that PERK has a direct role in pro-inflammatory response. These studies should be supported by experiments for additional pro- inflammatory cytokines such as MCP1, anti-inflammatory cytokines such as IL10 and also inflammasome related cytokines such as IL18 and IL1β. Additionally, I only used the mouse macrophage cell line RAW 264.7 in this study. Similar experiments should be carried out in mouse primary bone-marrow derived macrophages and human macrophages.

Unexpectedly and interestingly, I also observed that palmitoleate can mitigate LPS alone-induced or combined LPS and lipid treatment-induced inflammation. All together, the data presented in this thesis study supports the direct role of PERK and the promising effects of palmitoleic acid on inflammation, further studies are needed to understand their precise molecular mechanisms of action. In the future, ATP-analog sensitized mutant of PERK, in a kinase reaction with a different ATP analog N6-ATPgammaS to thiophosphorylate its substrates, should be coupled with proteomics to

identify full spectrum of PERK's substrates. In this study, we optimized the usage of bulky ATP analog inhibitor NaPP1 by the ASKA mutant of PERK, but PERK kinase assay optimization using the N6-ATPgammaS need to be carried out. After identification of potential substrates of PERK, they need to be validated in further kinase assay and biological experiments. Moreover, transgenic expression of this mutant of PERK in mice and chemical ablation by NaPP1 can become a useful tool in studying the direct contribution of PERK to metabolic disease pathogenesis.

8. References

1. Adesnik M., Lande M., Martin T., Sabatini D.D. (1976) Retention of mRNA on the endoplasmic reticulum membranes after in vivo disassembly of polysomes by an inhibitor of initiation. *J Cell Biol* 71:307–313.

2. Allen JJ., Li M., Brinkworth CS., Paulson JL., Wang D., Hübner A., Chou WH., Davis RJ., Burlingame AL., Messing RO, Katayama CD., Hedrick SM, Shokat K.M. (2007). A semisynthetic epitope for kinase substrates. *Nat Methods*.Jun; 4(6): 511-6.

3. Arkan M.C., Hevener AL., Greten FR., Maeda S., Li Z. (2005). IKK-β links inflammation to obesity induced insulin resistance. *Nat. Med.* 11:191–98.

4. Back S.H., Kaufman R.J. (2012) Endoplasmic Reticulum stress and Type 2 Diabetes. *Annu. Rev. Biochem*. 81:16.1–16.27

5. Baltzis D., Qu L.K., Papadopoulou S., Blais JD., Bell JC. (2004). Resistance to vesicular stomatitis virus infection requires a functional cross talk between the eukaryotic translation initiation factor 2α kinases PERK and PKR. *J. Virol*. 78:12747–61.

6. Banko M.R, Allen J.J., Schaffer B.E. , Wilker E.W., Tsou P., White J.L., Ville´n J., Wang B., Kim S.R., Sakamoto K., Gygi S.P., Cantley L.C., Yaffe M.B., Shokat K.M., and Brunet A. (2011). Chemical Genetic Screen for AMPKa2 Substrates Uncovers a Network of Proteins Involved in Mitosis. *Molecular Cell* 44, 878–892.

7. Bennett MR. (1999). Apoptosis of vascular smooth muscle cells in vascular remodeling and atherosclerotic plaque rupture. *Cardiovasc Res*.; 41:361–368.

8. Bernales S., McDonald K.L., Walter P. (2006). Autophagy counterbalances endoplasmic reticulum expansion during the unfolded protein response. *PLoS Biol* 4:e423.

9. Berridge MJ. (2002). The endoplasmic reticulum: a multifunctional signaling organelle. *Cell Calcium* 32:235–249.

10. Bertolotti, A., Zhang, Y., Hendershot, L.M., Harding, H.P., and Ron, D. (2000). Dynamic interaction of BiP and ER stress transducers in the unfolded-protein response. *Nat. Cell Biol*. 2, 326–332.

11. Bishop, A.C. *et al.* (1998). Design of allele-specific inhibitors to probe protein kinase signaling. *Curr. Biol.* 8, 257–266

12. Bishop, A.C. *et al.* (2000). A chemical switch for inhibitor-sensitive alleles of any protein kinase. *Nature* 407, 395–401.

13. Bishop, A.C. *et al.* (2001). Magic bullets for protein kinases. *Trends Cell .Biol.* 11, 167–172.

14. Blais DR., Vascotto SG., Griffith M., Altosaar I. (2005). LBP and CD14 secreted in tears by the lacrimal glands modulate the LPS response of corneal epithelial cells. *Invest Ophthalmol Vis Sci*.;46(11):4235-44

15. Bluher, M., M. D. Michael, O. D. Peroni, K. Ueki, N. Carter, B. B. Kahn, and C. R. Kahn. (2002). Adipose tissue selective insulin receptor knockout protects against obesity and obesity-related glucose intolerance. *Dev. Cell.* 3: 25–38.

16. Boden G. (2009). Endoplasmic Reticulum Stress: Another Link between Obesity and Insulin Resistance/ Inflamamtion.*Diabetes* 58:518-19.

17. Boden, G., Song, W., Duan, X., Cheung, P., Kresge, K., Barrero, C., and Merali, S. (2011). Infusion of glucose and lipids at physiological rates causes acute endoplasmic reticulum stress in rat liver. *Obesity (Silver Spring)* 19, 1366– 1373.

18. Borradaile, N.M., Han, X., Harp, J.D., Gale, S.E., Ory, D.S., and Schaffer, J.E. (2006). Disruption of endoplasmic reticulum structure and integrity in lipotoxic cell death. *J. Lipid Res.* 47, 2726–2737.

19. Cabibbo A, Pagani M, Fabbri M, Rocchi M, Farmery MR, Bulleid NJ, Sitia R (2000). ERO1-L, a human protein that favors disulfide bond formation in the endoplasmic reticulum. *J Biol Chem* 275: 4827–4833.

20. Calfon, M., Zeng, H., Urano, F., Till, J.H., Hubbard, S.R., Harding, H.P., Clark, S.G., and Ron, D. (2002). IRE1 couples endoplasmic reticulum load to secretory capacity by processing the XBP-1 mRNA. *Nature* 415, 92–96.

21. Carroll, A.S. *et al.* (2001). Chemical inhibition of the Pho85 cyclin dependent kinase reveals a role in the environmental stress response. *Proc. Natl. Acad. Sci. U. S. A.* 98, 12578–12583.

22. Causton, H.C. *et al.* (2001). Remodeling of yeast genome expression in response to environmental changes. *Mol. Biol. Cell* 12, 323–337.

23. Chen, X., Shen, J., and Prywes, R. (2002). The luminal domain of ATF6 senses endoplasmic reticulum (ER) stress and causes translocation of ATF6 from the ER to the Golgi. *J. Biol. Chem.* 277, 13045–13052.

24. Chen X., Ye H., Kuruvilla R., Ramanan N., Scangos K.W., Zhang C., Johnson N.N., England P.M., Shokat K.M., Ginty D.D. (2005). A Chemical-Genetic Approach to Studying Neurotrophin Signaling. *Neuron*, Vol. 46, 13–21.

25. Cnop, M. et al. (2007). Selective inhibition of eukaryotic translation initiation factor 2a dephosphorylation potentiates fatty acid-induced endoplasmic reticulum stress and causes pancreatic b-cell dysfunction and apoptosis. *J. Biol. Chem*. 282, 3989–3997.

26. Cox JS, Shamu CE, Walter P (1993). Transcriptional induction of genes encoding endoplasmic reticulum resident proteins requires a trans membrane protein kinase. *Cell* 73:1197–1206.

27. Cullinan, S.B., and Diehl, J.A. (2006). Coordination of ER and oxidative stress signaling: the PERK/Nrf2 signaling pathway. Int. J. Biochem. Cell Biol. 38, 317–332.

28. Deng, J., Lu, P.D., Zhang, Y., Scheuner, D., Kaufman, R.J., Sonenberg, N., Harding, H.P., and Ron, D. (2004). Translational repression mediates activation of nuclear factor kappa β by phosphorylated translation initiation factor 2. *Mol. Cell. Biol*. 24, 10161–10168.

29. Diakogiannak E., Welters H., Morgan N.G., (2008). Differential regulation of the endoplasmic reticulum stress response in pancreatic b-cells exposed to long-chain saturated and monounsaturated fatty acids. *Journal of Endocrinology,* 197, 553–563.

30. Ellgaard L., Helenius A. (2003). Quality control in the endoplasmic reticulum. *Nat Rev Mol Cell Biol* 4:181–191.

31. Engin F., Hotamisligil G.S. (2010). Restoring endoplasmic reticulum function by chemical chaperones: an emerging therapeutic approach for metabolic diseases. *Diabetes, Obesity and Metabolism* 12 (Suppl. 2): 108–115.

32. Erbay, E., Babaev, V.R., Mayers, J.R., Makowski, L., Charles, K.N., Snitow, M.E., Fazio, S., Wiest, M.M., Watkins, S.M., Linton, M.F., et al. (2009). Reducing endoplasmic reticulum stress through a macrophage lipid chaperone alleviates atherosclerosis. *Nat. Med*. 15, 1383–1391.

33. Farese Jr. R.V., Walther T.C. (2009) Lipid Droplets Finally Get a Little R-E-S-P-E-C-T. *Cell*. November 25; 139(5): 855–860.

34. Feng, B., Yao, P. M., Li, Y., Devlin, C. M., Zhang, D., Harding, H. P., Sweeney, M., Rong, J. X., Kuriakose, G., Fisher, E. A., Marks, A. R., Ron, D., and Tabas, I. (2003) The endoplasmic reticulum is the site of cholesterol-induced cytotoxicity in macrophages. *Nat. Cell Biol*. 5, 781–792.

35. Fonseca SG., Burcin M., Gromada J., Urano F. (2009). Endoplasmic reticulum stress in beta-cells and development of diabetes. *Curr Opin Pharmacol* 9:763–770.

36. Fonseca, S.G. et al. (2010). Wolfram syndrome 1 gene negatively regulates ER stress signaling in rodent and human cells. *J. Clin. Invest*. 120, 744–755

37. Fu, S., Yang, L., Li, P., Hofmann, O., Dicker, L., Hide, W., Lin, X., Watkins, S.M., Ivanov, A.R., and Hotamisligil, G.S. (2011). Aberrant lipid metabolism disrupts calcium homeostasis causing liver endoplasmic reticulum stress in obesity. *Nature* 473, 528–531.

38. Fu, S., Watkins, S.M., and Hotamisligil, G.S. (2012). The Role of Endoplasmic Reticulum in Hepatic Lipid Homeostasis and Stress Signaling. *Cell Metabolism*, 623-634.

39. Fujita E., Kouroku Y., Isoai A., Kumagai H., Misutani A., Matsuda C., Hayashi YK., Momoi T. (2007). Two endoplasmic reticulum-associated degradation (ERAD) systems for the novel variant of the mutant dysferlin: Ubiquitin/proteasome ERAD (I) and autophagy/lysosome ERAD (II). *Hum Mol Genet* 16:618–629.

40. Glass CK., Witztum JL. (2001). Atherosclerosis. The road ahead. *Cell*.104: 503–516.

41. Gerrity RG. (1991). Transition of blood-borne monocytes into foam cells in fatty lesions. *Am J Pathol*.; 103:181–190.

42. Gotoh, T., and Mori, M. (2006). Nitric oxide and endoplasmic reticulum stress. *Arterioscler. Thromb. Vasc.* Biol. 26, 1439–1446.

43. Gregor MF., Yang L., Fabbrini E. et al. (2009). Endoplasmic reticulum stress is reduced in tissues of obese subjects after weight loss. *Diabetes*; 58: 693–700.

44. Gross, E., Sevier, C. S., Heldman, N., Vitu, E., Bentzur, M., Kaiser, C. A., Thorpe, C., and Fass, D. (2006). Generating disulfides enzymatically: Reaction products and electron acceptors of the endoplasmic reticulum thiol oxidase Ero1p. *Proc. Natl. Acad. Sci. U.S.A.* 103, 299–304.

45. Gu, F. et al. (2004). Protein-tyrosine phosphatase 1B potentiates IRE1 signaling during endoplasmic reticulum stress. *J. Biol. Chem*. 279, 49689–49693.

46. Guo W., Wong S., Xie W., Lei T., and Luo Z. (2007). Palmitate modulates intracellular signaling, induces endoplasmic reticulum stress, and causes apoptosis in

mouse 3T3-L1 and rat primary preadipocytes. *American Journal of Physiology*, vol. 293, no. 2, pp. E576–E586,

47. Gurzov, E.N. and Eizirik, D.L. (2011). Bcl-2 proteins in diabetes: mitochondrial pathways of b-cell death and dysfunction. *Trends Cell Biol*. 21, 424–431.

48. Hapala I., Marza E., Ferreira T. (2011). Is fat so bad? Modulation of endoplasmic reticulum stress by lipid droplet formation. *Biol. Cell* 103, 271–285.

49. Haynes, C.M., Titus, E.A., and Cooper, A.A. (2004). Degradation of misfolded proteins prevents ER-derived oxidative stress and cell death. *Mol. Cell* 15, 767–776.

50. Harding H. P. and Ron D. (2002). Endoplasmic reticulum stress and the development of diabetes: a review. *Diabetes*, vol. 51, no. 3, pp. S455–S461.

51. Harding H.P, Zhang Y, Ron D. (1999). Protein translation and folding are coupled by an endoplasmic-reticulum-resident kinase. *Nature* 397: 271–274.

52. Harding H.P., Zhang Y., Bertolotti A., Zeng H., and Ron D. (2000). Perk Is Essential for Translational Regulation and Cell Survival during the Unfolded Protein Response. *Molecular Cell*, Vol. 5, 897–904.

53. Hollien, J. and Weissman, J.S. (2006). Decay of endoplasmic reticulum-localized mRNAs during the unfolded protein response. *Science* 313, 104–107.

54. Hong M., Luo S., Baumeister P., Huang JM., Gogia RK., Li M., Lee AS. (2004). Underglycosylation of ATF6 as a novel sensing mechanism for activation of the unfolded protein response. *J Biol Chem* 279:11354–11363.

55. Hotamisligil, G.S., Shargill, N.S., and Spiegelman, B.M. (1993). Adipose expression of tumor necrosis factor-alpha: direct role in obesity-linked insulin resistance. *Science* 259, 87–91.

56. Hotamisligil, G.S. (2006). Inflammation and metabolic disorders. *Nature* 444, 860–867.

57. Hotamisligil GS. (2008a).Inflammation and endoplasmic reticulum stress in obesity and diabetes. *International journal of Obesity* 32:52-54.

58. Hotamisligil GS. (2008b) Endoplasmic Reticulum stress and inflammatory basis of metabolic disease. *Cell* 140, 900–917.

59. Hotamisligil G.S. (2010). Endoplasmic reticulum stress and atherosclerosis. *Nature Medicine* Volume 16 Number 4

60. Hotamisligil, G. S. & Erbay, E. (2008). Nutrient sensing and inflammation in metabolic diseases. *Nature Rev. Immunol*. 8, 923–934

61. Høyer-Hansen M., Bastholm L., Szyniarowski P., Campanella M., Szabadkai G., Farkas T., Bianchi K., Fehrenbacher N., Elling F., Rizzuto R., Mathiasen IS., Jaattela M. (2007). Control of macro autophagy by calcium, calmodulin dependent kinase kinase-beta, and bcl-2. *Mol Cell* 25:193–205.

62. Hu P., Han Z., Couvillon A., Kaufman R., Exton J. (2006). Autocrine tumor necrosis factor alpha links endoplasmic reticulum stress to the membrane death receptor pathway through IRE1a-mediated NF-kB activation and down-regulation of TRAF2 expression. *Mol Cell Biol*. 26:3071–3084.

63. Ihle, J.N. (2000). The challenges of translating knockout phenotypes into gene function. *Cell* 102,131-134.

64. Jäger R., Mathieu J.M., Bertran, Gorman A.M., Vandenabeele P., and Samali A. (2012). The unfolded Protein Response at the crossroads of cellular life and death during endoplasmic reticulum stress. *Biol. Cell*; 104, 259–270.

65. Jiang HY., Wek SA., McGrath BC., Lu D., Hai T., Harding HP., Wang X., Ron D., Cavener DR., Wek RC. (2004). Activating transcription factor 3 is integral to the eukaryotic initiation factor 2 kinase stress response. *Mol Cell Biol* 24:1365–1377.

66. Jiao P., Ma J., Feng B., Zhang H., Alan Diehl J. et al. (2011). FFA-induced adipocyte inflammation and insulin resistance: involvement of ER stress and IKKbeta pathways. *Obesity (Silver Spring)* 19: 483–491.

67. Johar D., Roth JC., Bay GH., Walker JN., Kroczak TJ., Los M., (2004). Inflammatory response, reactive oxygen species, programmed (necrotic-like and apoptotic) cell death and cancer. *Rocz Akad Med Bialymst*. 49:31-9.

68. Kahn SE., Hull RL., Utzschneider KM. (2006). Mechanisms linking obesity to insulin resistance and type 2 diabetes. *Nature* 444:840–46.

69. Kamimoto T., Shoji S., Hidvegi T., Mizushima N., Umebayashi K., Perlmutter DH., Yoshimori T. (2006). Intracellular inclusions containing mutant alpha1-antitrypsin Z are propagated in the absence of autophagic activity. *J Biol Chem* 281:4467–4476.

70. Kaufman RJ., Scheuner D., Schroder M., Shen X., Lee K., Liu CY., Arnold SM. (2002). The unfolded protein response in nutrient sensing and differentiation. N*at Rev Mol Cell Biol* 3:411–421.

71. Kars M., Yang L., Gregor M.F, Mohammed BS., Pietka TA., Finck BN., Patterson BW., Horton JD., Mittendorfer B., Hotamisligil GS., Klein S. (2010). Tauroursodeoxycholic Acid may improve liver and muscle but not adipose tissue insulin sensitivity in obese men and women. *Diabetes*; 59(8):1899-905.

72. Kayode K.O., Larson E.T., Keyloun K.R., Castaneda L.J., DeRocher A.E., Inampudi K.K., Kim J.E., Arakaki T.L., Murphy R.C., Zhang L., Napuli AJ., Maly D.J., Verlinde C., Buckner F.S., Parsons M., Hol W.GJ., Merritt E.A. , Van Voorhis W.C. (2009). Toxoplasma gondii calcium-dependent protein kinase 1 is a target for selective kinase inhibitors, *Nature Structural & Molecular Biology* 17,602–607.

73. Kebache S., Cardin E., Nguyen DT., Chevet E., Larose L. (2004). Nck-1 antagonizes the endoplasmic reticulum stress-induced inhibition of translation. *J Biol Chem* 279:9662–9671.

74. Kevan Shokat and Mark Velleca (2002). Novel chemical genetics approaches to the discovery of signal transduction inhibitors. *Drug Discov Today*.Aug 15; 7(16):872-9.

75. Kharroubi, I., Ladriere, L., Cardozo, A.K., Dogusan, Z., Cnop, M., and Eizirik, D.L. (2004). Free fatty acids and cytokines induce pancreatic beta-cell apoptosis by

different mechanisms: role of nuclear factor kappa β and endoplasmic reticulum stress. *Endocrinology* 145, 5087–5096.

76. Kim M.K., Kim H.S., Lee IK., and Park K.G. (2012). Endoplasmic Reticulum Stress and Insulin Biosynthesis: A Review. *Experimental Diabetes Research*, vol. 2012, Article ID 509437, 7 pages.

77. Kouroku Y., Fujita E., Tanida I., Ueno T., Isoai A., Kumagai H., Ogawa S., Kaufman RJ., Kominami E., Momoi T. (2007). ER stress (PERK/eIF2alpha phosphorylation) mediates the polyglutamine-induced LC3 conversion, an essential step for autophagy formation. *Cell Death Differ* 14: 230–239.

78. Kozutsumi Y., Segal M., Normington K., Gething MJ., Sambrook J. (1988). The presence of misfolded proteins in the endoplasmic reticulum signals the induction of glucose regulated proteins. *Nature* 332:462–464.

79. Kulp, M. S., Frickel, E. M., Ellgaard, L., and Weissman, J. S. (2006). Domain architecture of protein –disulfide isomerase facilitates its dual role as an oxidase and an isomarase in Ero1p- mediated disulfide formation. *J. Biol.Chem.* 281, 876–884.

80. Ladrie `re, L. et al. (2010). Enhanced signaling downstream of ribonucleic acid-activated protein kinase-like endoplasmic reticulum kinase potentiates lipotoxic

endoplasmic reticulum stress in human islets. *J. Clin. Endocrinol. Metab*. 95, 1442–1449.

81. Lee K., Tirasophon W., Shen X., Michalak M., Prywes R., Okada T., Yoshida H., Mori K., Kaufman RJ. (2002). IRE1-mediated unconventional mRNA splicing and S2p-mediated ATF6 cleavage merge to regulate XBP1 in signaling the unfolded protein response. *Genes Dev* 16:452–466.

82. Li, Y., Schwabe, R.F., DeVries-Seimon, T., Yao, P.M., Gerbod-Giannone, M.C., Tall, A.R., Davis, R.J., Flavell, R., Brenner, D.A., and Tabas, I. (2005). Free cholesterol-loaded macrophages are an abundant source of tumor necrosis factor-alpha and interleukin-6: model of NF-kappaB- and map kinase-dependent inflammation in advanced atherosclerosis. *J. Biol. Chem*. 280, 21763–2177.

83. Libby P. (2000). Changing concepts of atherogenesis. *J Intern Med*.; 247: 349–358.

84. Libby P. (2002). Inflammation in atherosclerosis. *Nature*.420:868–874.

85. Libby P., Clinton SK. (1993). The role of macrophages in atherogenesis. *Curr Opin Lipidol*. 4:355–363.

86. Lilley BN, Ploegh HL 2004 A membrane protein required for dislocation of misfolded proteins from the ER. *Nature* 429:834–840

87. Lilley BN., Ploegh HL. (2005) Multiprotein complexes that link dis- location, ubiquitination, and extraction of misfolded proteins from the endoplasmic reticulum membrane. *Proc Natl Acad Sci* USA 102:14296–14301.

88. Liu, Y. *et al.* (1998). Engineering Src family protein kinases with unnatural nucleotide specificity. *Chem. Biol.* 5, 91–101.

89. Lusis AJ. (2000). Atherosclerosis. *Nature*.;407:233–241.

90. Ma Y., Brewer JW., Diehl JA., Hendershot LM. (2002). Two distinct stress signaling pathways converge upon the CHOP promoter during the mammalian unfolded protein response. *J Mol Biol* 318: 1351–1365.

91. Makowski, L., Boord, J.B., Maeda, K., Babaev, V.R., Uysal, K.T., Morgan, M.A., Parker, R.A., Suttles, J., Fazio, S., Hotamisligil, G.S., et al. (2001). Lack of macrophage fatty-acid-binding protein aP2 protects mice deficient in apolipoprotein E against atherosclerosis. *Nat. Med.* 7, 699–705.

92. Malhotra JD., Kaufman RJ. (2007). The endoplasmic reticulum and the unfolded protein response. *Semin Cell Dev Biol* 18:716–731.

93. Martin, S., and R. G. Parton. (2005). Caveolin, cholesterol, and lipid bodies. *Semin. Cell Dev. Biol*. 16: 163–174.

94. Martinon, F. et al. (2010) TLR activation of the transcription factor XBP1 regulates innate immune responses in macrophages. *Nat. Immunol*. 11, 411–418.

95. Maxfield, F.R., and Tabas, I. (2005). Role of cholesterol and lipid organization in disease. *Nature* 438, 612–621.

96. Meer, G. et al. (2008). Membrane lipids: where they are and how they behave. *Nat. Rev. Mol. Cell Biol*. 9, 112–124.

97. Moore K.J. and Tabas I. (2011). Macrophages in the pathogenesis of atherosclerosis. *Cell* 145.

98. Mori K, Ma W, Gething MJ, Sambrook J (1993).A trans membrane protein with a cdc2+/CDC28-related kinase activity is required for signaling from the ER to the nucleus. *Cell* 74:743–756.

99. Mori K., Ogawa N., KawaharaT., Yanagi H., Yura T. (1998). Palindrome with spacer of one nucleotide is characteristic of the cis-acting unfolded protein response element in Saccharomyces cerevisiae. *J Biol Chem* 273:9912–9920.

100. Mori K., Sant A., Kohno K., Normington K., Gething MJ., Sambrook JF. (1992). A 22 bp cis-acting element is necessary and sufficient for the induction of the yeast KAR2 (BiP) gene by unfolded proteins. *EMBO J* 11:2583–2593.

101. Myoishi M., Hao H., Minamino T., Watanabe K., Nishihira K., Hatakeyama K., Asada Y., Okada K., Ishibashi-Ueda H., Gabbiani G., Bochaton-Piallat ML., Mochizuki N., Kitakaze M. (2007). Increased endoplasmic reticulum stress in atherosclerotic plaques associated with acute coronary syndrome. *Circulation*. 116:1226–1233.

102. Nadanaka S., Okada T., Yoshida H., Mori K. (2007) Role of disulfide bridges formed in the luminal domain of ATF6 in sensing endoplasmic reticulum stress. *Mol Cell Biol* 27:1027–1043.

103. Nagasawa K., Higashi T., Hosokawa N., Kaufman RJ., Nagata K. (2007). Simultaneous induction of the four subunits of the TRAP complex by ER stress accelerates ER degradation. *EMBO Rep* 8:483– 489

104. Nakamura, T., Furuhashi, M., Li, P., Cao, H., Tuncman, G., Sonenberg, N., Gorgun, C.Z., and Hotamisligil, G.S. (2010). Double-stranded RNA-dependent protein kinase links pathogen sensing with stress and metabolic homeostasis. *Cell* 140, 338–348.

105. Naidoo N. (2009). ER and aging-protein folding and the ER stress response. *Ageing Res Rev* 8:150–159.

106. Nguyen DT., Kebache S., Fazel A., Wong HN., Jenna S., Emadali A., Lee EH., Bergeron JJM., Kaufman RJ., Larose L., Chevet E. (2004). Nck-dependent activation of extracellular signal regulated kinase-1 and regulation of cell survival during endoplasmic reticulum stress. *Mol Biol Cell* 15: 4248–4260.

107. Nikawa, J. and S. Yamashita. (1992). *IRE1* encodes a putative protein kinase containing a membrane-spanning domain and is required for inositol prototrophy in *Saccharomyces cerevisiae. Mol. Microbiol.* **6:** 1441–1446.

108. Novoa I., Zeng H., Harding HP., Ron D. (2001). Feedback inhibition of the unfolded protein response by GADD34-mediated dephosphorylation of eIF2alpha. *J Cell Biol* 153:1011–1022.

109. Ozcan U., Yilmaz E., Ozcan L. et al. (2006). Chemical chaperones reduce ER stress and restore glucose homeostasis in a mouse model of type 2 diabetes. *Science*; 313: 1137–1140.

110. Ozcan, U. et al. (2004). Endoplasmic reticulum stress links obesity, insulin action, and type 2 diabetes. *Science* 306, 457–461

111. Ogata M., Hino SI., Saito A., Morikawa K., Kondo S., Kanemoto S., Murakami T., Taniguchi M., Tanii I., Yoshinaga K., Shiosaka S., Hammarback JA., Urano F., Imaizumi K. (2006). Autophagy is activated for cell survival after endoplasmic reticulum stress. *Mol Cell Biol* 26:9220–9231.

112. Padyana AK., Qiu H., Roll-Mecak A., Hinnebusch AG., Burley SK. (2005). Structural basis for auto inhibition and mutational activation of eukaryotic initiation factor 2alpha protein kinase GCN2. *J Biol Chem*. 12;280(32):29289-99.

113. Pagani M., Fabbri M., Benedetti C., Fassio A., Pilati S., Bulleid NJ., Cabibbo A., Sitia R. (2000). Endoplasmic reticulum oxidoreductin 1-l (ERO1-L), a human gene induced in the course of the unfolded protein response. *J Biol Chem* 275:23685–23692.

114. Papa FR., Zhang C., Shokat K., Walter P. (2003). Bypassing a kinase activity with an ATP-competitive drug. *Science* 302:1533–1537.

115. Patil, C., and Walter, P. (2001). Intracellular signaling from the endoplasmic reticulum to the nucleus: the unfolded protein response in yeast and mammals. *Curr. Opin. Cell Biol.* 13, 349–355.

116. Pfaffenbach, K.T., Nivala, A.M., Reese, L., Ellis, F., Wang, D., Wei, Y., and Pagliassotti, M.J. (2010). Rapamycin inhibits postprandial-mediated X-box- binding protein-1 splicing in rat liver. *J. Nutr.* 140, 879–884.

117. Ploegh HL. (2007). A lipid-based model for the creation of an escape hatch from the endoplasmic reticulum. *Nature* 448:435–438

118. Pilon M., Romisch K., Quach D., Schekman R. (1998). Sec61p serves multiple roles in secretory precursor binding and translocation into the endoplasmic reticulum membrane. *Mol Biol Cell* 9:3455–3473.

119. Pirot P., Ortis F., Cnop M., Ma Y., Hendershot LM., Eizirik DL., Cardozo AK. (2007). Transcriptional regulation of the endoplasmic reticulum stress gene chop in pancreatic insulin-producing cells. *Diabetes* 56:1069–1077.

120. Qi X., Hosoi T., Okuma Y., Kaneko M., Nomura Y. (2004). Sodium 4-phenylbutyrate protects against cerebral ischemic injury. *Mol Pharmacol*; 66: 899–908.

121. Rader, D.J. & Daugherty, A. (2008).Translating molecular discoveries into new therapies for atherosclerosis.*Nature* 451, 904–913.

122. Rao RV., Bredesen DE. (2004). Misfolded proteins, endoplasmic reticulum stress and neurodegeneration. *Curr Opin Cell Biol* 16:653–662. (a).

123. Rao, R.V., Ellerby, H.M., and Bredesen, D.E. (2004). Coupling endoplasmic reticulum stress to the cell death program. *Cell Death Differ.* 11, 372–380. (b).

124. Rhodes, C.J. (2004). Processing of the insulin molecule. In Diabetes Mellitus, D. LeRoith, S.I. Taylor, and J.M. Olefsky, eds. (Philadelphia, PA: Lippincott Williams & Wilkins), pp. 27–50.

125. Rhodes, C.J., Shoelson, S., and Halban, P.A. (2005). Insulin Biosynthesis, Processing, and Chemistry. In Joslin's Diabetes Mellitus, C.R. Kahn, G.C. Weir, G.L. King, A.M. Jacobson, A.C. Moses, and R.J. Smith, eds. (Boston: Joslin Diabetes Center), pp. 65–82.

126. Ribeiro, C.M. and Boucher, R.C. (2010) Role of endoplasmic reticulum stress in cystic fibrosis-related airway inflammatory responses. *Proc. Am. Thorac. Soc*. 7, 387–394.

127. Robenek, H., O. Hofnagel, I. Buers, M. J. Robenek, D. Troyer, and N. J. Severs. (2006). Adipophilin-enriched domains in the ER membrane are sites of lipid droplet biogenesis. J. Cell Sci. 119: 4215–4224.

128. Ron D. (2002). Translational control in the endoplasmic reticulum stress response. *J Clin Invest* 110:1383–1388.

129. Ron, D., and Walter, P. (2007). Signal integration in the endoplasmic reticulum unfolded protein response. Nat. Rev. Mol. Cell Biol. 8, 519–529.

130. Schenk S., Saberi M., Olefsky JM. (2008). Insulin sensitivity: modulation by nutrients and inflammation. *J. Clin. Investig.* 118:2992–3002.

131. Seimon TA., Liao X., Magallon J., Moore KJ., Witztum JL., Tsimikas S., Golenbock DT., Webb NR., Tabas I. (2010). Atherogenic lipids and lipoproteins trigger CD36-TLR2-dependent apoptosis in macrophages undergoing endoplasmic reticulum stress. *Cell Metabolism* 12, 467–482.

132. Sevier, C. S., and Kaiser, C. A. (2002). Formation and transfer of disulphide bonds in living cells. *Nat. Rev. Mol. Cell Biol.* 3,836–847.

133. Shamu CE., Walter P. (1996). Oligomerization and phosphorylation of the Ire1p kinase during intracellular signaling from the endoplasmic reticulum to the nucleus. *EMBO J* 15:3028–3039.

134. Shen, J., Chen, X., Hendershot, L., and Prywes, R. (2002). ER stress regulation of ATF6 localization by dissociation of BiP/GRP78 binding and unmasking of Golgi localization signals. *Dev. Cell* 3, 99–111.

135. Shen X., Ellis RE., Lee K., Liu CY., Yang K., Solomon A., Yoshida H., Morimoto R., Kurnit DM., Mori K, Kaufman RJ. (2001). Complementary signaling pathways regulate the unfolded protein response and are required for C. elegans development. *Cell* 107:893–903.

136. Shi Y., Vattem KM., Sood R., An J., Liang J., Stramm L., Wek RC. (1998). Identification and characterization of pancreatic eukaryotic initiation factor 2 alpha-subunit kinase, PEK, involved in translational control. *Mol Cell Biol* 18:7499–7509.

137. Shi Y., An J., Liang J., Hayes SE., Sandusky GE., Stramm LE., Yang NN. (1999). Characterization of a mutant pancreatic eif-2alpha kinase, PEK, and co-localization with somatostatin in islet delta cells. *J Biol Chem* 274:5723–5730.

138. Shoelson, S.E., Lee, J., and Goldfine, A.B. (2006). Inflammation and insulin resistance. *J. Clin. Invest.* 116, 1793–1801.

139. Sriburi, R., Jackowski, S., Mori, K. & Brewer, J.W. (2004). XBP1: a link between the unfolded protein response, lipid biosynthesis, and biogenesis of the endoplasmic reticulum *J. Cell Biol*. 167, 35–41.

140. Szegezdi E., Logue SE., Gorman AM., Samali A. (2006). Mediators of endoplasmic reticulum stress-induced apoptosis. *EMBO Rep* 7:880–885.

141. Tabas, I. and Ron, D. (2011). Integrating the mechanisms of apoptosis induced by endoplasmic reticulum stress. *Nat. Cell Biol*. 13, 184–190.

142. Tabas I., Williams KJ., Boren J. (2007).Subendothelial lipoprotein retention as the initiating process in atherosclerosis: update and therapeutic implications. *Circulation*. 116:1832–1844.

143. Tabas I. (2005). Consequences and therapeutic implications of macrophage apoptosis in atherosclerosis: the importance of lesion stage and phagocytic efficiency. *Arterioscler Thromb Vasc Biol*.; 25:2255–2264.

144. Tajiri Y., Mimura K., Umeda F. (2005). High-sensitivity C-reactive protein in Japanese patients with type 2 diabetes. *Obes. Res.* 13:1810–16.

145. Tirasophon W., Welihinda AA., Kaufman RJ. (1998). A stress response pathway from the endoplasmic reticulum to the nucleus requires a novel bifunctional protein kinase/endoribonuclease (IRE1p) in mammalian cells. *Genes Dev* 12:1812–1824.

146. Tuncman, G., Hirosumi, J., Solinas, G., Chang, L., Karin, M., and Hotamisligil, G.S. (2006). Functional in vivo interactions between JNK1 and JNK2 isoforms in obesity and insulin resistance. *Proc. Natl. Acad. Sci*. USA 103, 10741–10746.

147. Uehara, T., Nakamura, T., Yao, D., Shi, Z.Q., Gu, Z., Ma, Y., Masliah, E., Nomura, Y., and Lipton, S.A. (2006). S-nitrosylated protein-disulphide isomerase links protein misfolding to neurodegeneration. *Nature* 441, 513–517.

148. Ultanir S.K., Hertz N.T., Li G., Ge W.P., Burlingame A.L., Pleasure S.J., Shokat K., Jan L.Y. Jan Y.N. (2012). Chemical Genetic Identification of NDR1/2 Kinase Substrates AAK1 and Rabin8 Uncovers Their Roles in Dendrite Arborization and Spine Development. *Neuron* Vol. 73, Issue 6, pp. 1127-1142.

149. Urano F., Wang X., Bertolotti A., Zhang Y., Chung P., Harding HP., Ron D. (2000). Coupling of stress in the ER to activation of JNK protein kinases by transmembrane protein kinase IRE1. *Science* 287:664–666.

150. Vallerie, S.N., Furuhashi, M., Fucho, R., and Hotamisligil, G.S. (2008). A predominant role for parenchymal c-Jun amino terminal kinase (JNK) in the regulation of systemic insulin sensitivity. *PLoS ONE* 3, e3151.

151. van Huizen R., Martindale JL., Gorospe M., Holbrook NJ. (2003). P58IPK, a novel endoplasmic reticulum stress-inducible protein and potential negative regulator of eIF2alpha signaling. *J Biol Chem* 278:15558– 15564.

152. Vecchi, C., Montosi, G., Zhang, K., Lamberti, I., Duncan, S.A., Kaufman, R.J., and Pietrangelo, A. (2009). ER stress controls iron metabolism through induction of hepcidin. *Science* 325, 877–880.

153. Vilatoba M., Eckstein C., Bilbao G. et al. (2005) .Sodium 4-phenylbutyrate protects against liver ischemia reperfusion injury by inhibition of endoplasmic reticulum-stress mediated apoptosis. *Surgery*; 138: 342–351

154. Virmani R., Burke AP., Kolodgie FD., Farb A. (2002).Vulnerable plaque: the pathology of unstable coronary lesions. *J Interv Cardiol*.; 15:439–446.

155. Wahlman J., DeMartino GN., Skach WR., Bulleid NJ., Brodsky JL., Johnson AE. (2007). Real-time fluorescence detection of ERAD substrate retro translocation in a mammalian in vitro system. *Cell* 129: 943–955.

156. Wang XZ., Harding HP., Zhang Y., Jolicoeur EM., Kuroda M., Ron D. (1998). Cloning of mammalian IRE1 reveals diversity in the ER stress responses. *EMBO J* 17:5708–5717.

157. Wang H., Shimizu E., Tang YP., Cho M., Kyin M., Zuo W., Robinson DA., Alaimo PJ., Zhang C., Morimoto H., Zhuo M., Feng R., Shokat KM., Tsien JZ. (2003). Inducible protein knockout reveals temporal requirement of CaMKII reactivation for memory consolidation in the brain. *Proc Natl Acad Sci USA* 100: 4287–4292.

158. Wei, Y., Wang, D., Topczewski, F., and Pagliassotti, M.J. (2006). Saturated fatty acids induce endoplasmic reticulum stress and apoptosis independently of ceramide in liver cells. Am. J. *Physiol. Endocrinol. Metab*. 291, E275–E281.

159. Weiss A., Schlessinger J. (1998). Switching signals on or off by receptor dimerization. *Cell* 94:277–280.

160. Weiss, E.L. et al. (2000). Chemical genetic analysis of the budding-yeast p21-activated kinase Cla4p. *Nat. Cell Biol*. 2, 677–685.

161. Welihinda AA., Kaufman RJ. (1996). The unfolded protein response pathway in Saccharomyces cerevisiae. Oligomerization and trans- phosphorylation of Ire1p (Ern1p) are required for kinase activation. *J Biol Chem* 271:18181–18187.

162. Williams KJ., Tabas I. (1995). The response-to-retention hypothesis of early atherogenesis. *Arterioscler Thromb Vasc Biol*.; 15:551–561.

163. Witucki, L.A. *et al.* (2002). Mutant tyrosine kinases with unnatural nucleotide specificity retain the structure and phospho-acceptor specificity of the wild-type enzyme. *Chem. Biol.* 9, 25–33.

164. Wolins, N. E., D. L. Brasaemle, and P. E. Bickel. (2006). A proposedmodel of fat packaging by exchangeable lipid droplet proteins.*FEBS Lett.* 580: 5484–5491.

165. Xie Q.W., Kashiwabara Y., Nathan C. (1994). Role of transcription factor NF-κB/Rel in induction of nitric oxide synthase. *J. Biol. Chem***.,** 269 pp. 4705–4708.

166. Yamazaki, H., Hiramatsu, N., Hayakawa, K., Tagawa, Y., Okamura, M., Ogata, R., Huang, T., Nakajima, S., Yao, J., Paton, A.W., et al. (2009). Activation of the Akt-NF-kappaB pathway by subtilase cytotoxin through the ATF6 branch of the unfolded protein response. *J. Immunol.* 183, 1480–1487.

167. Yan W., Frank CL., Korth MJ., Sopher BL., Novoa I., Ron D., Katze MG. (2002). Control of PERK eIF2alpha kinase activity by the endoplasmic reticulum stress-induced molecular chaperone p58ipk. *Proc Natl Acad Sci* USA 99:15920–15925.

168. Ye Y., Shibata Y., Yun C., Ron D., Rapoport TA. (2004). A membrane protein complex mediates retro-translocation from the ER lumen into the cytosol. *Nature* 429:841–847.

169. Yoneda, T. et al. (2001). Activation of caspase-12, an endoplasmic reticulum (ER) resident caspase, through tumor necrosis factor receptor-associated factor-2-dependent mechanism in response to the ER stress. *J. Biol. Chem*. 276, 13935–13940

170. Yorimitsu T., Nair U., Yang Z., Klionsky DJ. (2006). Endoplasmic reticulum stress triggers autophagy. *J Biol Chem* 281:30299–30304.

171. Yoshida H., Matsui T., Yamamoto A., Okada T., Mori K. (2001). XBP1mRNAis induced by ATF6 and spliced by IRE1 in response to ER stress to produce a highly active transcription factor. *Cell* 107:881–891.

172. Yusta B., Baggio LL., Estall JL., Koehler JA., Holland DP., Li H., Pipeleers D., Ling Z., Drucker DJ. (2006). GLP-1 receptor activation improves β cell function and survival following induction of endoplasmic reticulum stress. *Cell Metab* 4:391–406.

173. Zhang, K., Shen, X., Wu, J., Sakaki, K., Saunders, T., Rutkowski, D.T., Back, S.H., and Kaufman, R.J. (2006a). Endoplasmic reticulum stress activates cleavage of CREBH to induce a systemic inflammatory response. *Cell* 124, 587–599.

174. Zhang, X., Zhang, G., Zhang, H., Karin, M., Bai, H., and Cai, D. (2008). Hypothalamic IKKbeta/NF-kappaB and ER stress link over nutrition to energy imbalance and obesity. *Cell* 135, 61–73.

175. Zhou, J., Lhotak, S., Hilditch, B.A. & Austin, R.C. (2005). Activation of the unfolded protein response occurs at all stages of atherosclerotic lesion development in apolipoprotein E-deficient mice.*Circulation* 111, 1814–1821.

176. Listenberger, L.L., Han, X., Lewis, S.E., Cases, S., Farese, R.V., Jr., Ory, D.S., and Schaffer, J.E. (2003). Triglyceride accumulation protects against fatty acid-induced lipotoxicity. *Proc. Natl. Acad. Sci*. USA 100, 3077–3082.

177. Pineau, L., Colas, J., Dupont, S., Beney, L., Fleurat-Lessard, P., Berjeaud, J.-M., Berge` s, T., and Ferreira, T. (2009). Lipid-induced ER stress: synergistic effects of sterols and saturated fatty acids. *Traffic* 10, 673–690.

178. Peng, G., Li, L., Liu, Y., Pu, J., Zhang, S., Yu, J., Zhao, J., and Liu, P. (2011). Oleate blocks palmitate-induced abnormal lipid distribution, endoplasmic reticulum

expansion and stress, and insulin resistance in skeletal muscle. *Endocrinology* 152, 2206–2218.

179. Igoillo-Esteve, M. et al. (2010) Palmitate induces a pro-inflammatory response in human pancreatic islets that mimics CCL2 expression by beta cells in type 2 diabetes. *Diabetologia* 53, 1395–1405.

180. Ribeiro, C.M. and Boucher, R.C. (2010) Role of endoplasmic reticulum stress in cystic fibrosis-related airway inflammatory responses. *Proc. Am. Thorac. Soc*. 7, 387–394.

181. Green, C.D., and Olson, L.K. (2011). Modulation of palmitate-induced endoplasmic reticulum stress and apoptosis in pancreatic b-cells by stearoyl-CoA desaturase and Elovl6. *Am. J. Physiol. Endocrinol. Metab*. 300, E640–E649.

182. Flowers, M.T., Keller, M.P., Choi, Y., Lan, H., Kendziorski, C., Ntambi, J.M., and Attie, A.D. (2008). Liver gene expression analysis reveals endoplasmic reticulum stress and metabolic dysfunction in SCD1-deficient mice fed a very low-fat diet. *Physiol. Genomics* 33, 361–372.

183. Cao, H., Gerhold, K., Mayers, J.R., Wiest, M.M., Watkins, S.M., and Hotamisligil, G.S. (2008). Identification of a lipokine, a lipid hormone linking adipose tissue to systemic metabolism. *Cell* 134, 933–944.

184. Riquelme, C.A., Magida, J.A., Harrison, B.C., Wall, C.E., Marr, T.G., Secor, S.M., and Leinwand, L.A. (2011). Fatty acids identified in the Burmese python promote beneficial cardiac growth. Science 334, 528–531.

185. Olefsky, J.M., and Glass, C.K. (2010). Macrophages, inflammation, and insulin resistance. Annu. Rev. Physiol. 72, 219–246.